# "ROLE OF SONOELASTOGRAPHY IN DIFFERENTIATING BENIGN FROM MALIGNANT CERVICAL LYMPH NODES AND CORRELATING WITH PATHOLOGY"


**By**

**Dr. E. VINEELA**


**DISSERTATION SUBMITTED TO SRI DEVARAJ URS ACADEMY OF HIGHER EDUCATION AND RESEARCH, KOLAR, KARNATAKA**

**In partial fulfilment of the requirements for the degree of**

**DOCTOR OF MEDICINE**
**IN**
**RADIODIAGNOSIS**

**Under the Guidance of**

**Dr. ANIL KUMAR SAKALECHA, M.D.,**
**PROFESSOR OF RADIODIAGNOSIS**

**&**

**Co-Guidance of**

**Dr. T. N. SURESH, M.D., DNB,**
**PROFESSOR OF PATHOLOGY**


**DEPARTMENT OF RADIODIAGNOSIS,**
**SRI DEVARAJ URS MEDICAL COLLEGE,**
**TAMAKA, KOLAR – 563 101.**


**MAY 2021**

**SRI DEVARAJ URS ACADEMY OF HIGHER EDUCATION AND RESEARCH, TAMAKA, KOLAR, KARNATAKA**

## DECLARATION BY THE CANDIDATE

I hereby declare that this dissertation entitled "**ROLE OF SONOELASTOGRAPHY IN DIFFERENTIATING BENIGN FROM MALIGNANT CERVICAL LYMPH NODES AND CORRELATING WITH PATHOLOGY"** is a bonafide and genuine research work carried out by me under the guidance of **Dr. ANIL KUMAR SAKALECHA**, Professor, Department of Radiodiagnosis, Sri Devaraj Urs Medical College, Kolar, and co-guidance of **Dr. T. N. SURESH**, Professor, Department of Pathology, Sri Devaraj Urs Medical College, Kolar, in partial fulfilment of University regulation for the award "**M.D. DEGREE IN RADIODIAGNOSIS**", the examination to be held in May 2021 by SDUAHER. This has not been submitted by me previously for the award of any degree or diploma from the university or any other university.

**Dr. E. VINEELA,**
Postgraduate in Radiodiagnosis,
Sri Devaraj Urs Medical College,
Tamaka, Kolar.

Date:

Place: Kolar.

**SRI DEVARAJ URS ACADEMY OF HIGHER EDUCATION**

**AND RESEARCH, TAMAKA, KOLAR, KARNATAKA**

## CERTIFICATE BY THE GUIDE

This is to certify that the dissertation entitled **"ROLE OF SONOELASTOGRAPHY IN DIFFERENTIATING BENIGN FROM MALIGNANT CERVICAL LYMPH NODES AND CORRELATING WITH PATHOLOGY"** is a bonafide research work done by **Dr. E. VINEELA,** under my direct guidance and supervision at Sri Devaraj Urs Medical College, Kolar**,** in partial fulfilment of the requirement for the degree of "**M.D. IN RADIODIAGNOSIS"**.

**Dr. ANIL KUMAR SAKALECHA, M.D.,**

Professor,

Department of Radiodiagnosis,

Sri Devaraj Urs Medical College,

Tamaka, Kolar.

Date:

Place: Kolar.

**SRI DEVARAJ URS ACADEMY OF HIGHER EDUCATION**

**AND RESEARCH TAMAKA, KOLAR, KARNATAKA**

## CERTIFICATE BY THE HEAD OF DEPARTMENT

This is to certify that the dissertation entitled **"ROLE OF SONOELASTOGRAPHY IN DIFFERENTIATING BENIGN FROM MALIGNANT CERVICAL LYMPH NODES AND CORRELATING WITH PATHOLOGY"** is a bonafide research work done by **Dr. E. VINEELA,** under direct guidance and supervision of **Dr. ANIL KUMAR SAKALECHA**, Professor, Department of Radiodiagnosis at Sri Devaraj Urs Medical College, Kolar**,** in partial fulfilment of the requirement for the degree of "**M.D. IN RADIODIAGNOSIS"**.

**Dr. N. RACHEGOWDA, M.D., DMRD,**

Professor & HOD,

Department of Radiodiagnosis,

Sri Devaraj Urs Medical College,

Tamaka, Kolar.

Date:

Place: Kolar.

**SRI DEVARAJ URS ACADEMY OF HIGHER EDUCATION AND RESEARCH, TAMAKA, KOLAR, KARNATAKA**

## CERTIFICATE BY THE CO- GUIDE

This is to certify that the dissertation entitled **"ROLE OF SONOELASTOGRAPHY IN DIFFERENTIATING BENIGN FROM MALIGNANT CERVICAL LYMPH NODES AND CORRELATING WITH PATHOLOGY"** is a bonafide research work done by **Dr. E. VINEELA,** under my co-guidance and supervision at Sri Devaraj Urs Medical College, Kolar**,** in partial fulfilment of the requirement for the degree of "**M.D. IN RADIODIAGNOSIS"**.

**Dr. T. N. SURESH, M.D., DNB,**
Professor,
Department of Pathology,
Sri Devaraj Urs Medical College,
Tamaka, Kolar.

Date:

Place: Kolar.

**SRI DEVARAJ URS ACADEMY OF HIGHER EDUCATION AND RESEARCH TAMAKA, KOLAR, KARNATAKA**

## ENDORSEMENT BY THE HEAD OF THE DEPARTMENT AND PRINCIPAL

This is to certify that the dissertation entitled **"ROLE OF SONOELASTOGRAPHY IN DIFFERENTIATING BENIGN FROM MALIGNANT CERVICAL LYMPH NODES AND CORRELATING WITH PATHOLOGY"** is a bonafide research work done by **Dr. E. VINEELA** under the direct guidance and supervision of **Dr. ANIL KUMAR SAKALECHA,** Professor, Department of Radiodiagnosis, Sri Devaraj Urs Medical College, Kolar, in partial fulfilment of University regulation for the award "**M.D. DEGREE IN RADIODIAGNOSIS**"**.**

**Dr. N. RACHEGOWDA**,
Professor & HOD,
Department of Radiodiagnosis,
Sri Devaraj Urs Medical College,
Tamaka, Kolar.

Date:
Place: Kolar.

**Dr. P. N. SREERAMULU,**
Principal,
Sri Devaraj Urs Medical College,
Tamaka, Kolar.

Date:
Place: Kolar.

**SRI DEVARAJ URS ACADEMY OF HIGHER EDUCATION AND RESEARCH, TAMAKA, KOLAR, KARNATAKA**

# ETHICAL COMMITTEE CERTIFICATE

This is to certify that the Ethical committee of Sri Devaraj Urs Medical College, Tamaka, Kolar has unanimously approved

**Dr. E. VINEELA,**

***Post-Graduate student in the subject of***

*RADIODIAGNOSIS at Sri Devaraj Urs Medical College, Kolar*

***to take up the Dissertation work entitled***

**"ROLE OF SONOELASTOGRAPHY IN DIFFERENTIATING BENIGN FROM MALIGNANT CERVICAL LYMPH NODES AND CORRELATING WITH PATHOLOGY"**

*to be submitted to the*

**SRI DEVARAJ URS ACADEMY OF HIGHER EDUCATION AND RESEARCH, TAMAKA, KOLAR, KARNATAKA.**

**Member Secretary,**

Sri Devaraj Urs Medical College,

Kolar – 563 101.

**SRI DEVARAJ URS ACADEMY OF HIGHER EDUCATION**

**AND RESEARCH, TAMAKA, KOLAR, KARNATAKA**

## COPY RIGHT

I hereby declare that Sri Devaraj Urs Academy of Higher Education and Research, Kolar, Karnataka shall have the rights to preserve, use and disseminate this dissertation/thesis in print or electronic format for academic/research purpose.

**Dr. E. VINEELA**

Date:

Place: Kolar.

Sri Devaraj Urs Academy of Higher Education and Research

Certificate of Plagiarism Check for Dissertation

| | |
|---|---|
| **Author Name** | Dr. E. VINEELA |
| **Course of Study** | MD RADIODIAGNOSIS |
| **Name of Major Supervisor** | Dr. ANIL KUMAR SAKALECHA |
| **Department** | RADIODIAGNOSIS |
| **Acceptable Maximum Limit** | 10% |
| **Submitted By** | librarian@sduu.ac.in |
| **Paper Title** | ROLE OF SONOELASTOGRAPHY IN DIFFERENTIATING BENIGN FROM MALIGNANT CERVICAL LYMPH NODES AND CORRELATING WITH PATHOLOGY |
| **Similarity** | 7% |
| **Paper ID** | 187616 |
| **Submission Date** | 2020-11-26 15:01:42 |

Signature of Student

Signature of Major Advisor

Professor
Dept. of Radio-Diagnosis
R.L.J. Hospital & Reaserch Centre
Tamaka, Kolar-563 101

Head of the Department

Prof. & HOD,
Dept. of Radio Diagnosis,
R.L.J. Hospital & Research Centre,
Tamaka, KOLAR-563 101.

University Librarian

Director Of Post Graduate Studies

Director
P.G. STUDIES
Sri Devaraj Urs Medical College
Tamaka, KOLAR-563 101

# ACKNOWLEDGEMENT

*I owe my debt and gratitude to my parents* ***Dr. E. UMAPATHI REDDY*** *and* ***Smt. R. UMA*** *for their moral support and constant encouragement during the course of the study.*

*With humble gratitude and great respect, I would like to thank my teacher, mentor and guide,* ***Dr. ANIL KUMAR SAKALECHA****, Professor, Department of Radiodiagnosis, Sri Devaraj Urs Medical College and Research Institute, Kolar, for his able guidance, constant encouragement, immense help and valuable advices which went a long way in moulding and enabling me to complete this work successfully.*

*I have great pleasure in expressing my deep sense of gratitude to* ***Dr. N. RACHEGOWDA,*** *Professor and Head, Department of Radiodiagnosis, Sri Devaraj Urs Medical College and Research Institute, Kolar, without his initiative and constant encouragement this study would not have been possible.*

*I would like to express my sincere thanks to* ***Dr. T. N. SURESH,*** *Professor, Department of Pathology, Sri Devaraj Urs Medical College for his valuable support, guidance and encouragement throughout the study.*

*I would like to thank* ***Dr. NABAKUMAR SINGH****, Associate professor, and* ***Dr. RAJESWARI****,* ***Dr. SHIVAPRASAD G SAVAGAVE and Dr. BUKKE RAVINDRA NAIK****, Assistant professors, Department of Radiodiagnosis, Sri Devaraj Urs Medical College and Research Institute, Kolar, for their constant support and encouragement during the study period.*

*I would also like to thank* ***Dr. ASHWATHNARAYANA SWAMY, Dr. VARUN. S, Dr. GAURAV YADAV, Dr. GOWTHAMI. M, Dr. MADHUKAR. M, Dr. DARSHAN. A. V, Dr. RAHUL DEEP. G, Dr. GNANA SWAROOP RAO POLADI*** *and all my teachers of Department of Radio diagnosis, Sri Devaraj Urs Medical College, Kolar for their support.*

*I would like to express my sincere thanks to my seniors* ***Dr. Parameshwar Keerthi, Dr. Essaki Rajulu, Dr. Anshul Singh, Dr. Athira. P. M and Dr. Hithishini,*** *my fellow postgraduates****, Dr. Amrutha Ranganath, Dr. Thati Sai Soumya****,* ***Dr. Divya Teja Patil, Dr. Sahana N Gowda*** *and* ***Dr. Sushmitha Prasad*** *and all other postgraduates for having rendered all their co-operation and help to me during my study.*

*I am extremely grateful to the patients and their families who volunteered to this study, without them this study would just be a dream.*

*My sincere thanks to* ***Mrs. Hamsa, Mrs. Naseeba, Mr. Sunil*** *and* ***Mrs. Shobha,*** *along with rest of the computer operators.*

*I am also thankful to staff nurse **Mrs. Radha, Mrs. Munivenkatamma** and other **technicians** of Department of Radiodiagnosis, R.L Jalappa Hospital & Research Centre, Tamaka, Kolar for their help.*

*Last but not least I would be failing in my duty if I do not express my gratefulness to the **Almighty,** who helped me to successfully complete this study.*

**Dr. E. VINEELA**

# LIST OF ABBREVIATIONS

AJCC – American Joint Committee on Cancer

ARFI – Acoustic Radiation Force Impulse

BF – Blood Flow

BV – Blood Volume

CDI – Colour Doppler Imaging

CECT – Contrast Enhanced Computed Tomography

CMV – Cytomegalovirus

CNS – Central Nervous System

CT – Computed Tomography

CTP – Computed Tomography Perfusion

DRESS syndrome – Drug Reaction with Eosinophilia and Systemic Symptoms

DCU – Deep Cortical Unit

EBV – Epstein Barr Virus

FDG-PET – 18-Fluorodeoxyglucose Positron Emission Tomography

FNAC – Fine Needle Aspiration Cytology

HIV – Human Immunodeficiency Virus

HPV – Human Papilloma Virus

HSV – Herpes Simplex Virus

HU – Hounsfield Unit

IJV – Internal Jugular Vein

LN – Lymph Node

MALT – Mucosa-Associated Lymphoid Tissue

| | |
|---|---|
| MRI | – Magnetic Resonance Imaging |
| MTT | – Mean Transit Time |
| MUO | – Metastasis from Unknown Origin |
| NBI | – Narrow Band Imaging |
| NPV | – Negative Predictive Value |
| PI | – Pulsatility Index |
| PPV | – Positive Predictive Value |
| RI | – Resistive Index |
| ROI | – Region of Interest |
| SCC | – Squamous Cell Carcinoma |
| SI | – Signal Intensity |
| S/L ratio | – Short/ Long axis ratio |
| SLE | – Systemic Lupus Erythematosus |
| STIR | – Short T1 Inversion Recovery |
| SWE | – Shear Wave Elastography |
| UICC | – Union for International Cancer Control |
| USG | – Ultrasonography |
| VTI | – Virtual Touch Tissue Imaging |

# ABSTRACT

**Background**: Cervical lymphadenopathy can be secondary to numerous etiologies. Combined use of ultrasonography and elastography improves diagnostic efficacy in differentiating benign from malignant cervical lymph nodes, thereby helping in treatment planning and reducing unnecessary fine needle aspiration cytology/ biopsy.

**Aims and Objectives**: To perform B-mode ultrasonography, color Doppler imaging and elastography of the cervical lymph nodes, to correlate B-mode ultrasonography, color Doppler imaging, and elastography findings with pathological findings and to calculate sensitivity, specificity and diagnostic accuracy of ultrasonography and elastography.

**Material and Methods**: A prospective observational study was conducted over a period of eighteen months on 78 patients with clinically enlarged cervical lymph nodes who were referred to our department for ultrasonography. Patients first underwent ultrasonography (B-mode and color Doppler imaging) followed by elastography. Lymph node morphology on B-mode was assessed based on short axis diameter, short-to-long axis ratio, fatty hilum, echogenicity and margin. Vascularity of lymph node on colour Doppler imaging was divided into three patterns. On elastography, lymph nodes were defined based on elastography pattern and strain index.

**Results**: Out of 78 cases, there were total of 43 females and 35 males. There was no significant difference between gender distribution among benign and malignant cervical lymph nodes. Among all ultrasonography parameters, fatty hilum was found to have highest diagnostic accuracy (73%), followed by vascularity pattern (70%). Combined use of all ultrasonography parameters yielded better sensitivity (90%), specificity (88%) and diagnostic accuracy (89%) than individual parameters. Five scale elastography pattern had 83% sensitivity, 97% specificity and 89% diagnostic accuracy. In the current study, use of strain index cut-off of 2 showed sensitivity of 93%, specificity of 96% and diagnostic accuracy of 94%. Elastography pattern and strain index together had sensitivity of 93%, specificity of 94% and diagnostic accuracy of 94%. Together ultrasonography and elastography achieved sensitivity of 96%, specificity of 94% and diagnostic accuracy of 95%.

**Conclusion**: Elastography can be a useful adjunct to ultrasonography and plays a major role in accurate diagnosis of cervical lymphadenopathy. Elastography pattern and cut-off strain index of 2 can effectively differentiate benign from malignant cervical lymph nodes.

**Keywords**: Cervical lymph nodes, elastography, elastography pattern, strain index, ultrasonography, colour Doppler imaging.

# TABLE OF CONTENTS

# LIST OF TABLES

# LIST OF FIGURES

# INTRODUCTION

Cervical lymphadenopathy can manifest secondary to benign or malignant etiology. Hence, its evaluation will give a clue to underlying cause and help in treatment planning. Ultrasonography (USG) is usually the first preferred imaging modality. Various criteria are defined on B-mode ultrasonography and color Doppler imaging (CDI) for lymph node evaluation. There is however considerable overlap in diagnostic criteria on B-mode ultrasonography and CDI for differentiating benign and malignant cervical lymph nodes [1,2.]

Elastography can help in characterizing lymph nodes based on the stiffness of tissues (malignant tissues are harder than benign). Strain elastography measures the relative stiffness of the lymph node with respect to adjacent normal tissue in response to externally applied manual force[3].

Cervical lymph nodes and adjacent normal structures are color coded representing varying degree of tissue hardness. Elastography pattern is described based on proportion of blue or hard area on elastograms[4]. Strain index (muscle-to-lymph node strain ratio) is a semi-quantitative measure based on elasticity of the target lymph node with respect to surrounding neck muscles[5]. The probability of malignancy increases as the strain index increases[3].

Elastography can increase the accuracy of ultrasonography in diagnosis of cervical lymphadenopathy[3]. It can also aid in selecting cervical lymph nodes for fine

needle aspiration cytology (FNAC) which is required for accurate diagnosis and treatment[5].

The purpose of this study was to determine whether sonoelastography is an effective tool in differentiating benign from malignant cervical lymph nodes.

# AIMS AND OBJECTIVES

The aims and objectives of the study were:

1. To perform B-mode ultrasonography, colour Doppler imaging, and elastography of the cervical lymph nodes.
2. To correlate B-mode ultrasonography, colour Doppler imaging, and elastography findings with pathological findings.
3. To calculate sensitivity, specificity and diagnostic accuracy of ultrasonography and elastography.

# REVIEW OF LITERATURE

## EMBRYOLOGY OF LYMPHATIC SYSTEM AND LYMPH NODES

Lymph nodes are essential component of the lymphatic system and adaptive immune system. They are located throughout the body in relation to lymphatic vessels. Lymphatic system development starts approximately at 5$^{th}$ week of intrauterine gestation. Lymph nodes develop from lymphatic sacs. Different theories exist regarding lymphatic system development. One school of thought is that, there is budding of endothelial cells from veins into lymph sacs. Another theory suggested that lymph sacs develop from mesenchyme followed by budding of endothelial cells into lymph sacs. The first theory is widely recognized and is supported by subsequent studies[6].

Lymph sacs develop adjacent to blood vessels. Hence, lymph nodes and lymphatic system which evolve from lymph sacs are closely related to the vascular system. They form a functional anastomosis between lymph vessels and blood vessels[7].

Developing fetus has six major groups of lymph sacs. Jugular sacs and iliac sacs are paired, whereas retroperitoneal sac and cisterna chyli are unpaired. Jugular sacs are the first ones to appear adjacent to the junction of anterior cardinal vein and subclavian veins. Bilateral iliac sacs are found around common iliac veins. Retroperitoneal sac lies near the root of mesentery. Cisterna chyli lies in the midline dorsal to the retroperitoneal sac[8].

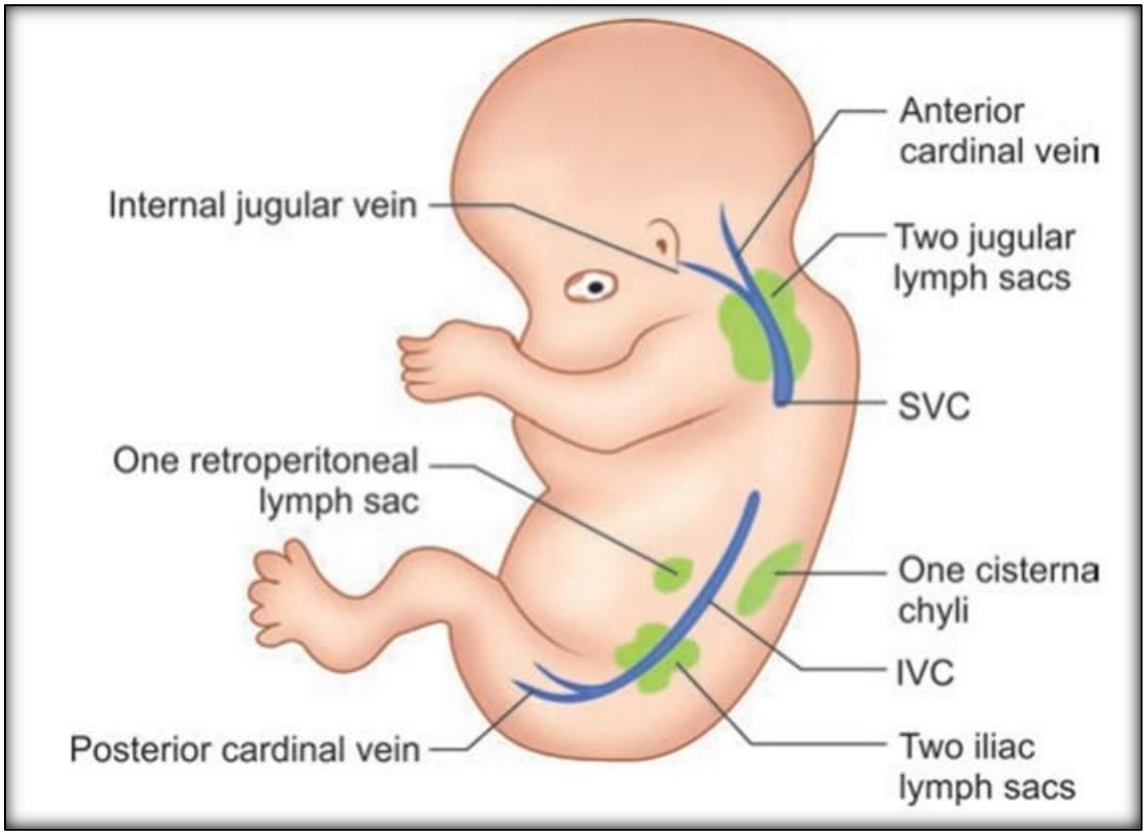


Figure 1: Lymph sacs

All the lymph sacs are interconnected to each other with multiple channels which drain lymph from the head and neck region, limbs and body wall. Jugular sacs and cisterna chyli are joined by two main channels (right and left thoracic channels) and anastomosis forms between these channels. Formation and development of jugular lymph sacs play a crucial role in diagnosing aneuploidy fetuses. Thickening of nuchal translucency on ultrasound between 11 to 14 weeks is seen in approximately 75% of trisomy 21 foetus. Increase in accumulation of tissue fluid between the skin and soft tissues manifests as thickening of nuchal translucency. It tends to resolve beyond 14 weeks of gestation because of development of lymphatic system[9,11].

The thoracic duct develops from the caudal portion of the right channel, the anastomosis between right and left channel, and the cranial portion of the left channel. Cranial portion of the right channel forms right lymphatic duct. Right and left thoracic duct drain lymph into the junction of the internal jugular vein (IJV) and subclavian vein. Eventually, connective tissue and lymphocytes invade all the sacs except the cisterna chyli forming groups of lymph nodes[9].

Transcription factor PROXI upregulates genes of lymphatic vessel and it also downregulates genes of blood vessel, thus making the lineage specific for the lymphatic system. VEGFR3 gene is the receptor for paracrine factor VEGFC and is upregulated by PROXI. VEGFC protein act on endothelial cells and initiate growth of lymphatic vessels[9].

Mesenchymal cells invade into lymph sacs. Lymph nodes are formed from these condensed mesenchymal areas which eventually bulge into the lymphatic vessels. Further development leads to differentiation into cortex and medulla. Early lymph nodes develop around 15 to 17 weeks of intrauterine gestation and late lymph nodes develop around 18 to 24 weeks of intrauterine gestation. Cortico-medullary differentiation becomes apparent at around 25 to 38 weeks[7].

There are two type of lymphocytes, B-cells and T-cells. Embryologically, T-lymphocytes originate from primitive stem cells of mesenchyme of yolk sac. B-cells originate from marrow and lymphatic tissue associated with gut and spleen[10].

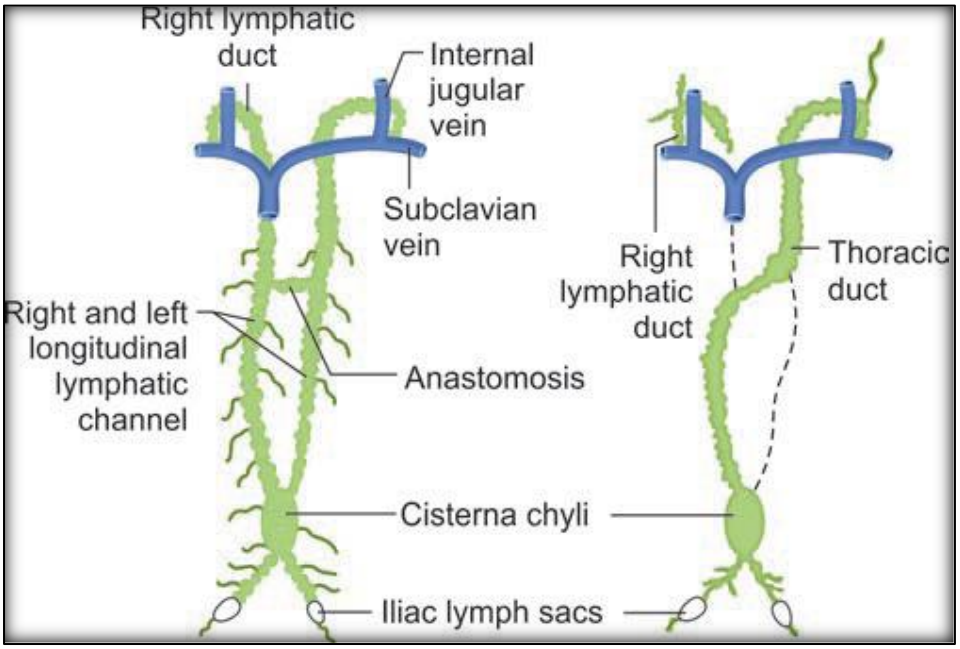


Figure 2: Development of thoracic duct and right lymphatic duct

Lymphopoietic stem cells which are precursors of T lymphocytes migrate to thymus from bone marrow. These lymphopoietic stem cells differentiate in thymus and are ultimately released into circulation. Immature lymphocytes derived from thymus reach lymphoid organs. Thymus is the source of lymphocytes in lymph nodes before birth. After birth mesenchymal cells in lymph nodes modify into lymphocytes. Lymphocytes are not produced in lymph nodule or germinal centers until just before or after birth[10].

## ANATOMY OF LYMPH NODES

Lymphoid tissue is classified into primary and secondary lymphoid organs. Primary lymphoid organs (ex: bone marrow and thymus) are site for de novo synthesis and maturation of lymphocytes. Secondary lymphoid organs (ex: lymph nodes, Peyer's patches, tonsils, spleen, and MALT (mucosa-associated lymphoid tissue)) are responsible for activation of lymphocytes and initiation of immune response[11].

Lymph nodes are part of secondary lymphoid organs. They are located throughout the body along lymphatic vessels. Human body of a young adult has approximately 450-500 lymph nodes predominantly located in abdominopelvic region followed by thorax and head and neck region[11].

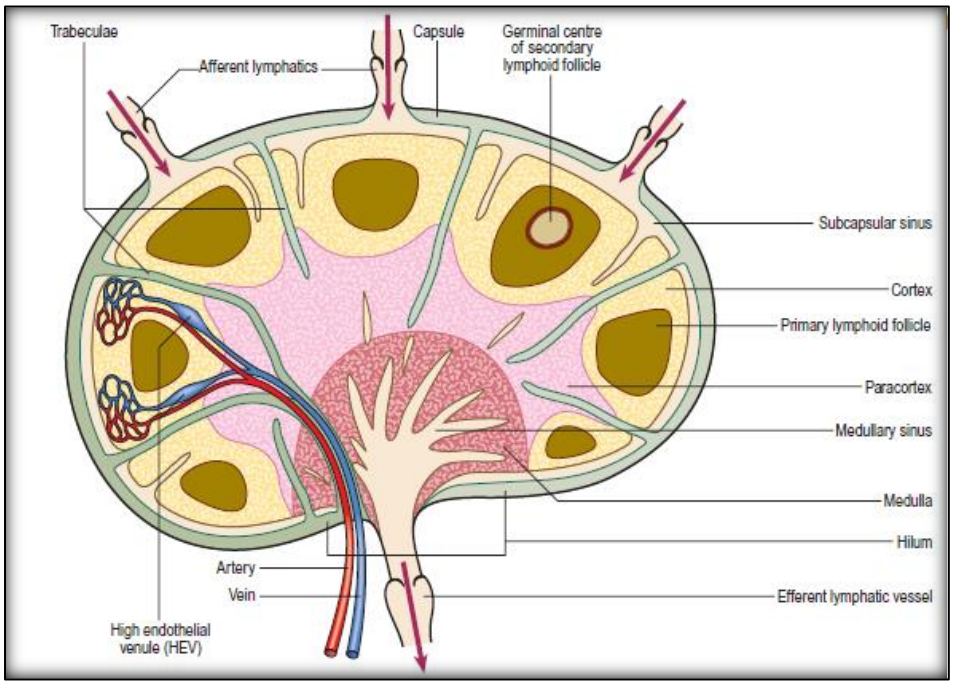


Figure 3: Anatomy of lymph node

Lymph nodes are typically described to have oval or kidney shape with an indentation on one side called as hilum. Efferent lymphatics and blood vessels traverse through hilum, whereas afferent lymphatics enter the capsule around the periphery of the lymph node. Lymph node structure can be divided into various components like capsule, subcapsular sinus, paracortex, cortex, medullary cords, medullary sinuses, and hilum (Figure 3). Lymphoid lobules are present in all lymph nodes and they form basic functional and anatomical unit of the lymph node. Each lymphoid nodule is composed of cortex, paracortex and medulla[12].

Capsule is mainly made of collagen fibers, elastin fibers (predominantly in deeper layers) and few fibroblasts. Capsule extends as trabeculae composed of dense connective tissue radially into lymph node. These trabeculae are interconnected with network of fine fibrils (type III collagen fibrils) forming a dense network in the cortex. This network of collagen fibrils and trabeculae provide attachment for lymphocytes, dendritic cells, macrophages and various other cells[11].

There is a clear space devoid of lymphocytes just below the capsule called subcapsular sinus. Subcapsular sinus is also called as lymph sinus or marginal sinus. It allows transportation of the lymph within the lymph node[13].

The cortex is composed of lymphocytes and numerous lymphatic follicles (or nodules). Each nodule has a peripheral area of lymphocytes surrounding central germinal center (Figure 4). Paracortex (also called deep cortex) is an innermost layer of cortex and is composed of deep cortical unit (DCU). DCU contains T-cells which

interact with the dendritic cells. DCUs can be further subdivided into central and peripheral DCU within each lymphoid lobule[14].

Medulla forms innermost part of lymph node and contains numerous lymphocytes which are arranged in the form of anastomosing cords. Medulla is a source of B-cells, macrophages and plasma cells. It also contains several blood vessels and medullary sinuses (space between medullary cord). Lymph from afferent lymphatics is filtered in medullary sinuses and drained into efferent lymphatics[13, 14].

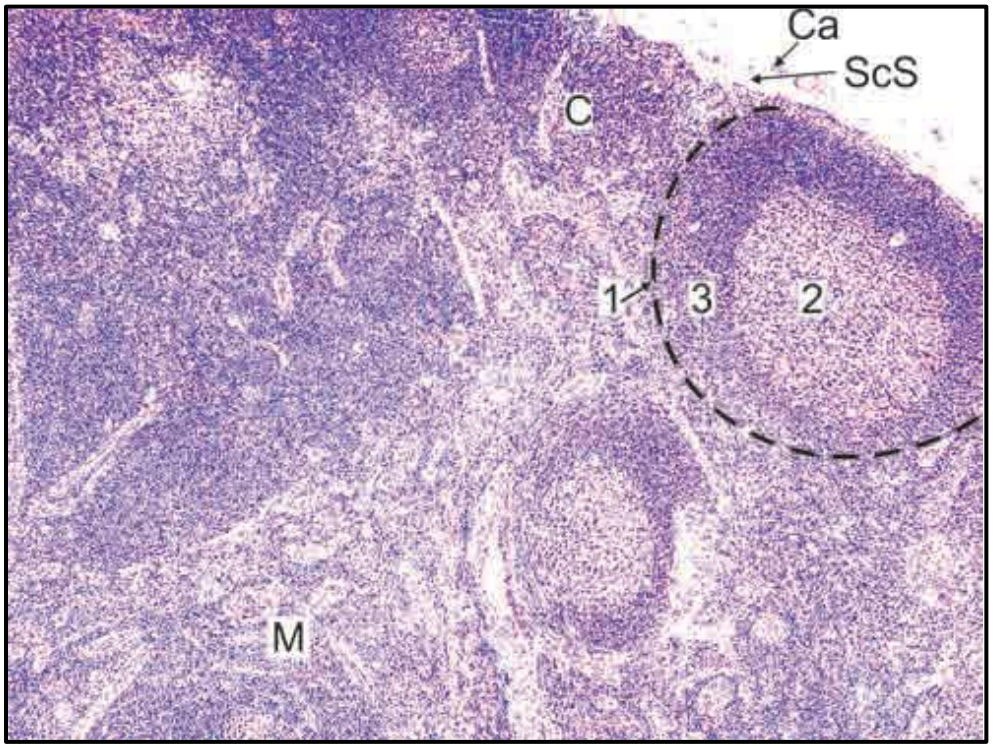


Figure 4: Histology of lymph node

(1. Lymphatic nodule; 2. Germinal center; 3. Zone of dense lymphocytes;

C: Cortex; M: Medulla; Ca: Capsule; ScS: Subcapsular sinus)

## FLOW OF LYMPH AND FUNCTION OF LYMPH NODES

Lymph is composed of tissue fluids, large extracellular molecules and cells. Lymph from interstitial spaces of tissues and organs is drained into lymphatic capillary vessels which eventually join larger lymphatic channels. All organs of human body have lymphatic vessels other than brain, retina, and bone. Lymph nodes are present along these lymphatic vessels[15].

Afferent vessels enter lymph node through hilum. Lymph from afferent lymphatic vessel traverse through subcapsular sinus and continue within the trabecular sinuses and join medullary sinus. All the medullary sinuses of the lymph node drain lymph into efferent lymphatic vessel which exits the lymph node through its hilum. Efferent lymphatics drain lymph into thoracic or lymphatic ducts that subsequently join subclavian veins[13,15].

During the process of circulating and filtering lymph through lymph node, B-cells and T-cells within the node are exposed to antigens present in the lymph. Antigen-presenting cells, dendritic cells, and follicular dendritic cells play a role in activating antigen specific B-cells and T cells. Lymph nodes form an integral part of both adaptive and innate immune system of the body[13].

Apart from being part of immune system, lymphatic system also plays a role in tissue fluid homeostasis, absorption of large molecules and lipids in the digestive systems, transportation of degraded extracellular molecules and cell debris[13].

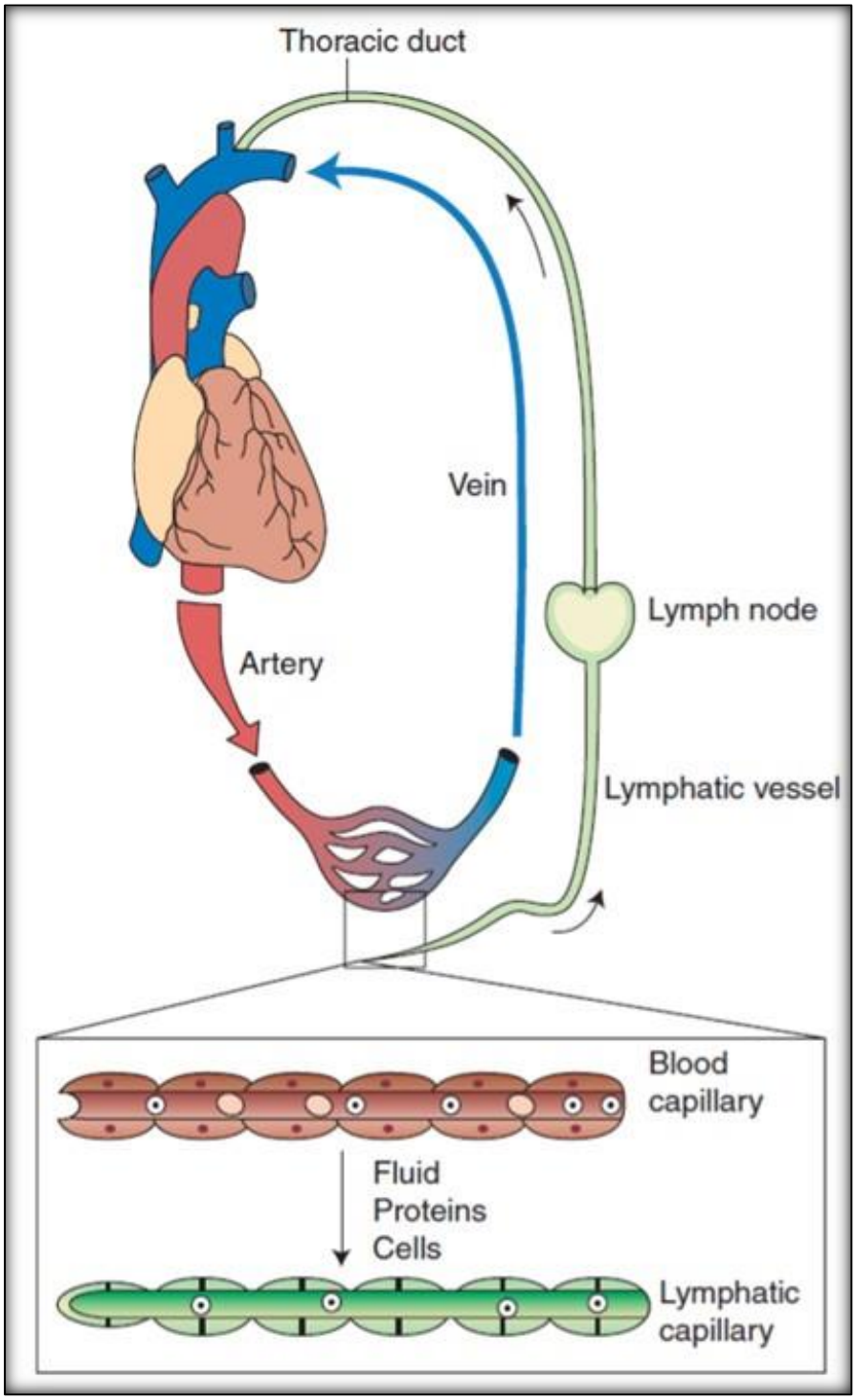


Figure 5: Flow of lymph through lymphatic system

## Classification of head and neck lymph nodes

Head and neck region lymph nodes are broadly classified into superficial and deep group of cervical lymph nodes.

| Superficial lymph nodes | Deep lymph nodes |
|---|---|
| 1. Occipital nodes.<br>2. Mastoid nodes or post-auricular nodes.<br>3. Pre-auricular nodes.<br>4. Superficial parotid nodes.<br>5. Submental nodes<br>6. Submandibular nodes<br>7. Facial nodes - Maxillary, buccinator, and supramandibular lymph nodes.<br>8. Superficial cervical: Anterior superficial cervical and Posterior superficial cervical | 1. Deep parotid<br>2. Deep cervical:<br>Pretracheal, prelaryngeal, infrahyoid, retropharyngeal, jugulo-omohyoid, jugulo-digastric, and supraclavicular nodes. |

Table 1: Classification of head and neck group of lymph nodes[13,16]

## Levels of cervical lymph nodes

**Level I**

Level IA (submental nodes) – Submental nodes are located anteriorly in the midline bounded by anterior belly of digastric muscle on either side, posteriorly by mylohyoid muscle, inferiorly by hyoid bone and superiorly by mandible. These lymph nodes drain lymph from lower lip, anterior mandibular alveolar ridge, floor of the mouth, and anterior 1/3$^{rd}$ of tongue.

Level IB (submandibular nodes) – Located in submandibular triangle bounded by anterior and posterior belly of the digastric muscles on either side, stylohyoid muscle and body of the mandible. Receives lymphatic drainage from submandibular gland, oral cavity and anterior nasal cavity[16].

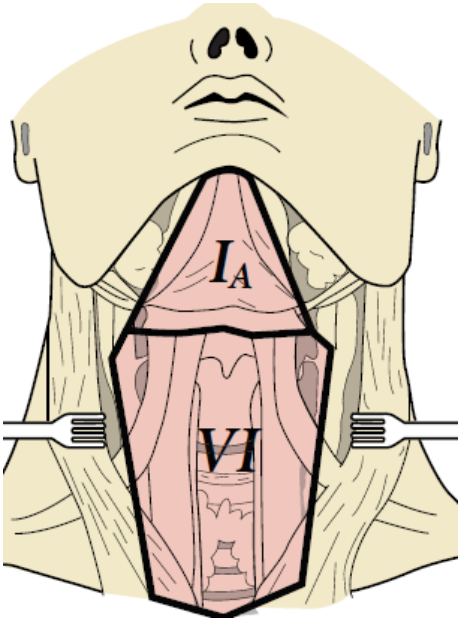


Figure 6: Submental and anterior compartment group of lymph nodes

**Level II (Upper Jugular Group)**

They are found around the upper 1/3rd of the IJV. Extend from the level of skull base upto the level of lower margin of hyoid bone. Stylohyoid muscle and lateral border of the sternohyoid muscle form the antero-medial boundary, and posterior border of sternocleidomastoid muscle forms the postero-lateral boundary[16].

Lymph nodes located in level II are further divided into level IIA (anterior) and IIB (posterior) by spinal accessory nerve. Nasal cavity, nasopharynx, oral cavity, oropharynx, hypopharynx, larynx and parotid glands drain lymph into upper jugular group of lymph nodes[16].

**Level III (Middle Jugular Group)**

These are located along middle third of the IJV between lower margin of the hyoid bone (superior border) and lower margin of the cricoid cartilage (inferior border). Lateral border of the sternohyoid muscle forms the medial boundary and posterior border of the sternocleidomastoid muscle forms the lateral boundary. These lymph nodes drain lymph from nasopharynx, oropharynx, hypopharynx, oral cavity, and larynx[13,16].

**Level IV: Lower Jugular Group**

Lower jugular group of lymph nodes are located along lower 1/3rd of the IJV bounded superiorly by cricoid cartilage and inferiorly by clavicle. Medial and lateral borders are formed by lateral margin of the sternohyoid muscle and posterior margin of the sternocleidomastoid muscle, respectively. This group also includes Virchow

nodes. These lymph nodes drain lymph from larynx, hypopharynx and cervical esophagus[13,17].

**Levels V: Posterior Triangle Group**

Posterior triangle group of lymph nodes are located along transverse cervical artery and spinal accessory nerve (lower half). Superior border is formed by the convergence of the sternocleidomastoid and trapezius muscles at the skull base and the inferior border is formed by clavicle. Medial and lateral boundaries are formed by posterior margin of the sternocleidomastoid muscle and the anterior margin of the trapezius muscle respectively. Level V is divided into VA and VB by horizontal plane along the inferior margin of cricoid cartilage. Sublevel VA drains nasopharynx and oropharynx. Sublevel VB drains thyroid gland[16,17].

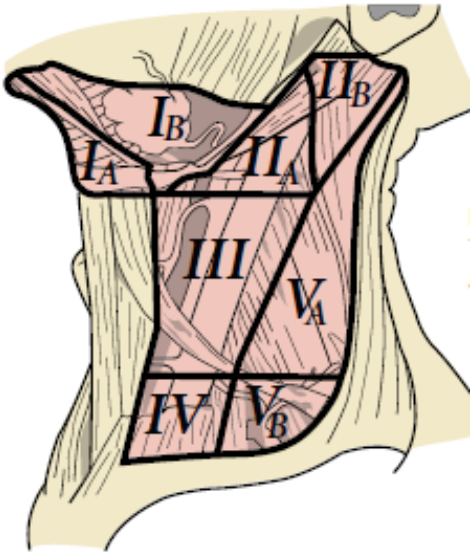


Figure 7: Cervical lymph nodes level

**Level VI: Anterior Compartment Group**

Anterior group of lymph nodes include perithyroid, Delphian (precricoid), pre- and paratracheal nodes, and lymph nodes along recurrent laryngeal nerves.

Common carotid arteries form lateral boundaries, hyoid bone forms superior boundary and suprasternal notch forms inferior boundary. These lymph nodes drain larynx (glottis and subglottis), pyriform sinus, thyroid gland, and cervical esophagus[13,16].

**Supraclavicular group of lymph nodes:**

Supraclavicular group of lymph nodes are bounded superiorly by the lower border of the cricoid cartilage and inferiorly by clavicle. Sternocleidomastoid muscle forms the medial border and trapezius muscle forms the lateral border. They belong to level VA (posterior triangle group)[18].

Virchow node is located near venous confluence of IJV and subclavian vein and it is the most proximal supraclavicular lymph node on left side. Virchow node belongs to group IV.

Breast, lung and upper esophagus drain into right supraclavicular lymph nodes which eventually drain into right lymphatic duct. Left supraclavicular lymph nodes receive lymph from distant organs (kidney, cervix, testis, and pancreas) and they drain into the thoracic duct[18].

## CERVICAL LYMPHADENOPATHY

Cervical lymph nodes can be enlarged in numerous conditions either as a part of generalised lymphadenopathy or as isolated cervical lymphadenopathy. Etiology of cervical lymphadenopathy can be divided into following categories:

### 1. Infective causes:

Infections are the commonest etiology for cervical nodal enlargement, especially in paediatric age group. In most of these cases, infective foci is usually in head and neck region (eg: tonsillitis, pharyngitis) or any other tissue/ organ system. However, cervical lymph node enlargement can present even in cases with no evident primary site of infection. Infective causes of cervical lymph nodal enlargement can be further divided based on infective organism[19].

**A. Viral:**

Viral infections are the frequent etiological factor for cervical lymphadenitis in paediatric age group and result in mildly enlarged cervical lymph nodes on both sides without evidence of periadenitis. Recurrent upper respiratory tract viral infections (influenza virus, parainfluenza virus, adenovirus, etc) predispose to development of acute cervical lymphadenitis. Most common presentation is bilateral enlarged cervical lymph nodes[20].

Chronic cervical lymphadenopathy is usually caused by Epstein Barr virus (EBV), cytomegalovirus (CMV), Human Immunodeficiency Virus (HIV). Patients with HIV usually present with persistent generalized lymphadenopathy rather than

isolated cervical lymphadenopathy. HIV also predisposes patients to opportunistic infections which can also cause cervical lymhpadenopathy[20,21].

**B. Bacterial:**

Bacteria usually cause unilateral cervical lymphadenopathy. Streptococcus is the most common bacteria causing cervical lymphadenitis, especially in children between 1–4 years of age. Bacterial cervical lymphadenitis is often associated with perinodal inflammatory changes and eventually necrosis may develop and result in lymph nodal abscess formation[22].

Lymph nodes are the typical site for extra-pulmonary tubercular infection. Presence of necrosis, adjacent inflammatory changes/soft tissue edema and lymph node matting favour diagnosis of tubercular lymphadenitis. On CT, lymph nodes show peripheral rim enhancement, obliteration of surrounding fat plane with or without evidence of abscess formation. Longstanding cases present with sinus tract extending to the skin surface. Calcification maybe present in chronic or healed cases of tuberculosis[23].

**C. Parasites/protozoa:**

Protozoal infections are secondary to consumption of contaminated water/ unpasteurized milk/meat or from animals. Infection of neck and throat region by protozoa result in cervical lymph nodal enlargement. Organisms like leishmaniasis, toxoplasmosis and microfilaria have predilection for lymphoreticular system and hence result in enlargement of lymph nodes[20].

**D. Fungi:**

Fungal infections (histoplasmosis, coccidioidomycosis, etc) are secondary to inhalation of fungi or direct skin infection. Lung involvement result in reactive enlargement of supraclavicular lymphadenopathy. Isolated cervical lymphadenopathy is rare[20].

| | |
|---|---|
| **VIRAL** | EBV, CMV, HIV, varicella, rubella, measles, HSV II (Herpes Simplex Virus), enterovirus, rhinovirus, parvovirus B19. |
| **BACTERIAL** | Staphylococci, streptococci, tuberculosis, non-tuberculous mycobacteria, brucellosis, bartonella henselae, tularemia, Mycoplasma pneumoniae, yersinia pestis, pasteurella multocida, cervical actinomycosis. |
| **PARASITES/PROTOZOAN** | Toxoplasmosis, trypanosomes, toxocariasis, leishmaniasis, microfilaria. |
| **FUNGAL** | Dermatophytes (tinea), coocidiocomycosis, histoplasmosis, blastomycosis. |

Table 2: Infective causes of cervical lymphadenopathy[20]

## 2. Immunologic:

### A. Granulomatous diseases:

Granulomatous diseases causing cervical lymphadenopathy have predilection for the posterior triangle and jugular chain lymph nodes groups. On imaging, they present either as necrotic lymph nodes or can have homogeneous echotexture in case of chronic granulomatous infiltration[24].

Nearly 33% of patients with sarcoidosis have cervical lymphadenopathy (intraparotid and supraclavicular lymph nodes are commonly involved) depending on stage of sarcoidosis. On imaging, they have homogeneous attenuation without evidence of necrosis and show homogenous enhancement on post-contrast study. In sarcoidosis patients, calcification is a frequent finding in mediastinal lymph nodes but is rarely seen in cervical lymph nodes[24].

### B. Rheumatoid disorders:

Cervical lymphadenopathy, enlargement of major salivary glands and sicca symptoms are most common presentations of rheumatoid disorders in head and neck region. Cervical lymphadenopathy is more common in childhood SLE (systemic lupus erythematosus) occurring in approximately 15% of cases. Lymphoid involvement in rheumatoid arthritis causes generalised lymphadenopathy rather than isolated cervical lymphadenopathy[20,25].

### C. Lymphoproliferative and histiocytic disorders:

Lymphadenopathy in cervical region can be the presenting feature in many patients with histiocytic disorders (Rosai- Dorfman disease, langerhans cell

histiocytosis, hemophagocytic lymphohistiocytosis). Patients with Rosai-Dorfman disease (also known as sinus histiocytosis) present with significant lymphadenopathy, predominantly involving cervical region[20].

Castleman's disease is a benign condition associated with lymph node enlargement in > 80% of patients (mediastinal lymphadenopathy followed by cervical lymphadenopathy). Autoimmune lymphoproliferative syndrome is another lymphoproliferative disease associated with cervical lymphadenopathy[20,26].

Cervical lymphadenopathy is one among the five diagnostic criteria for Kawasaki disease and manifest as unilateral coalescent nodal mass. Kikuchi-Fujimoto disease occurs in young women and presents with cervical lymphadenopathy associated perinodal inflammatory change and intranodal necrosis[20,26].

| | |
|---|---|
| **Granulomatous diseases** | - Sarcoidosis<br>- Common variable immunodeficiency<br>- Hyper-IgM syndrome<br>- Chronic granulomatous disease |
| **Rheumatoid disorders** | - Arthritis<br>- Systemic lupus erythematosus<br>- Dermatomyositis |
| **Lymphoproliferative and histiocytic disorders** | - Rosai-Dorfam disease<br>- Castleman's disease<br>- Autoimmune lymphoproliferative syndrome<br>- Langerhans cell histiocytosis<br>- Hemophagocytic lymphohistiocytosis<br>- Kawasaki syndrome<br>- Kikuci-Fujimoto disease |

Table 3: Immunologic disorders causing cervical lymphadenopathy

## 3. **Metabolic diseases:**

### A. Storage disorders:

Niemann-Pick disease is an autosomal recessive lysosomal storage disease associated with accumulation of sphingomyelin in lysosomes present in the liver, spleen, lymph nodes and brain. Other storage disorders like Gaucher's disease and Tangier disease less frequently involve cervical lymph nodes[20].

### B. Hypersensitivity:

Serum sickness is a Type III hypersensitivity reaction to proteins from animal source. Apart from systemic symptoms, lymphadenopathy is seen predominately near site of injection and head & neck region. Allergic reaction to certain drugs can also result in lymphadenopathy, either as direct cause or secondary to serum sickness. DRESS syndrome (drug reaction with eosinophilia and systemic symptoms) is a special form of the drug-induced systemic reaction associated with lymphadenopathy[20].

| | |
|---|---|
| **Storage disease** | - Niemann-Pick disease<br>- Gaucher's disease<br>- Tangier disease<br>- Amyloidosis |
| **Hypersensitivity** | - Serum sickness<br>- Adverse drug reaction: Antiepileptic drugs, heparin, antituberculosis drugs (isoniazid), allopurinol, antibiotics (cephalosporins), pyrimethamines, hydralazine, etc. |

Table 4: Metabolic disorders causing cervical lymphadenopathy

## 4. Neoplastic diseases:

### A. Lymphoma:

Lymphoma is malignancy of lymphocytes and lymphoblasts manifesting as nodal or extranodal disease. It is the most prevalent head and neck malignancy in paediatric age group (27%). Hodgkin's lymphoma usually manifest as lymph nodal disease, involving either upper cervical or less frequently supraclavicular group of lymph nodes. Extranodal involvement with or without diffuse nodal involvement is a feature of Non-Hodgkin's lymphoma[27].

On ultrasound, lymphomatous lymph nodes appear diffusely hypoechoic with pseudocystic appearance secondary to reduced fat in lymph nodes. Lack of calcifications and necrosis helps in differentiating from tubercular/ metastatic etiology[27].

Four patterns of head and neck lymphoma are described on CT (computed tomography): Type 1: only nodal involvement, type 2: only extranodal involvement, type 3: combination of extranodal and nodal disease, and type 4: multifocal extranodal disease with or without nodal involvement. Non-Hodgkin's lymphoma usually presents as extranodal disease (type 2), followed by combination of extranodal and nodal disease (type 3). Waldeyer's ring, nasal cavity, and paranasal sinuses are the extranodal sites frequently affected in head and neck lymphomas[28].

**B. Metastasis:**

Lymph nodal metastasis in cervical region can either be from a known primary tumor or from clinically unidentified primary or from unknown/ occult primary tumor. Head and neck cancers account for bulk of cervical lymph node metastasis cases. Squamous cell carcinoma (SCC) constitutes majority of these malignant tumors. SCC spreads through lymphatic system hence have high incidence of lymph node metastasis. Rate of metastasis can even give a clue to nature of primary tumor[29].

Cervical lymph node metastasis is a significant prognostic factor for head and neck tumors. 5-year survival rate decreases by 50% in patients with nodal metastasis. Factors affecting prognosis are: size of lymph node, level and site of lymph node and extranodal extension[29].

Malignant tumors can metastasize to either ipsilateral / contralateral or bilateral or midline lymph nodes. Other than thyroid cancer cases, midline cervical lymph nodes are considered as ipsilateral nodes. Bilateral and contralateral lymph nodal involvement indicates poor prognosis and is considered as N2c disease. Metastasis to lymph nodes in lower neck levels, i.e. level IV and level V (supraclavicular area) and metastasis to distant lymph nodal groups is considered as poor prognostic factor[30].

Extranodal extension beyond lymph node capsule indicates poor prognosis and thus considered as N3b stage in UICC/AJCC eighth edition (Table 5). Invasion of adjacent soft tissue, skin, nerve and involvement of underlying muscle or adjacent

structures are considered as extranodal extension. Pathological N staging system is based on histological assessment which takes into account total number of nodes in neck dissection specimen[30].

| N category | Criteria |
|---|---|
| NX | Regional lymph nodes cannot be assessed |
| N0 | No regional lymph node metastasis |
| N1 | Metastasis in a single ipsilateral lymph node, 3 cm or smaller in greatest dimension and ENE-negative |
| N2a | Metastasis in a single ipsilateral lymph node larger than 3 cm but not larger than 6 cm in greatest dimension and ENE-negative |
| N2b | Metastasis in multiple ipsilateral lymph nodes, none larger than 6 cm in greatest dimension and ENE-negative |
| N2c | Metastasis in bilateral or contralateral lymph nodes, none larger than 6 cm in greatest dimension and ENE-negative |
| N3a | Metastasis in a lymph node larger than 6 cm in greatest dimension and ENE-negative |
| N3b | Metastasis in any node(s) and clinically overt ENE-positive |
| Note: Midline nodes are considered ipsilateral nodes. $ENE_c$ is defined as invasion of skin, infiltration of musculature, dense tethering or fixation of adjacent structures, or cranial nerve, brachial plexus, sympathetic trunk, or phrenic nerve invasion with dysfunction. | |
| Note: A designation of "U" or "L" may be used for any N category to indicated metastasis above the lower border of the cricoid (U) or below the lower border of the cricoid (L). Similarly, clinical and pathological ENE should be recorded as ENE negative or ENE positive. | |

Table 5: Clinical N staging: 8th edition of AJCC cancer staging[30]

## OCCULT NODAL DISEASE

Occult disease in cervical lymph nodes indicate presence of metastases in the neck nodes that cannot be identified either clinically or radiologically. Occult nodal disease can be further divided into two categories: occult metastases identified on light microscopy or micrometastases (less than 2 mm) identified on special histological techniques (immunohistochemistry/step serial sectioning/molecular analysis)[31].

## CERVICAL LYMPH NODE METASTASIS FROM UNKNOWN ORIGIN (MUO)

MUO is a disease entity characterized by the presence of pathology proven cervical lymph node metastasis in the absence of clinically or radiologically obvious primary tumor. In a true MUO primary tumor is never identified inspite of extensive clinical, radiological and pathological investigation. Whereas in occult disease, primary tumor is present but not detected on initial investigation[32].

Most common histotype in pathology proven malignant cervical lymph node is squamous cell carcinoma followed by adenocarcinoma, undifferentiated carcinoma and other malignancies. Management protocol, treatment guidelines and prognosis vary according to histopathological diagnosis[33].

Lymph from each part of the human body drains into specific group of lymph nodes, hence level or group of lymph node affected can give a clue to possible site of primary tumor (Table 6). Level II and level III groups are most commonly involved

as compared to lymph nodes of other neck levels. Head and neck region carcinoma tend to metastasize to upper and middle neck levels, whereas metastasis to level IV and supraclavicular nodes is usually from below the level of clavicle. Any malignancy from head and neck region, thorax, abdomen and pelvis (including lung, breast, esophageal, gastric, pancreatic, cervix, and prostate cancers) can present with metastasis to supraclavicular lymph nodes[33].

| **Level of lymph node** | | **Primary drainage site** |
|---|---|---|
| Level I | Submental (IA) and submandibular (IB) | Oral cavity, oropharynx |
| Level II | Upper jugular | Oral cavity, oropharynx, larynx, nose, hypopharynx, parotid, nasopharynx |
| Level III | Middle jugular | Oral cavity, oropharynx, larynx, hypopharynx, thyroid, nasopharynx |
| Level IV | Lower jugular | Larynx, thyroid, hypopharynx, oesophagus |
| Level V | Posterior compartment | Nasopharynx, hypopharynx, thyroid, oropharynx |
| Level VI | Anterior compartment | Thyroid, larynx, hypopharynx, cervical oesophagus |

Table 6: First echelon lymph nodes for various primary sites[34]

## EVALUATION OF CERVICAL METASTASIS FROM UNKNOWN ORIGIN

### I. HISTORY & CLINICAL EXAMINATION

Metastatic cervical lymph nodes should be evaluated in a systematic structured manner, starting with thorough history taking (ex: history of alcohol consumption and smoking). Clinical examination of the nasal cavity, nasopharynx, oral cavity, oropharynx, larynx and hypopharynx should be done under direct vision and also using rigid and flexible endoscopes wherever possible. Narrow band imaging (NBI) is a modification of the standard white light endoscope, which can identify neoplasm in an earlier stage as compared to conventional endoscopy. If no obvious primary is found at the end of clinical examination, then the case is labelled as cervical metastasis from a clinically unknown primary[32,34].

### II. HISTOPATHOLOGY:

Ultrasound guided FNAC or core biopsy can be performed from suspected lymph nodes to confirm histology. Histopathology along with immunohistochemistry helps in differentiating between SCC (most common), thyroid, salivary, breast or bronchial origins. Identification of Human papilloma virus (HPV) and Epstein-Barr virus (EBV) suggests possible primary site in oropharynx and nasopharynx respectively. Targeted biopsy can be planned accordingly for further analysis[34].

`

## III. CROSS-SECTIONAL IMAGING:

### A. COMPUTED TOMOGRAPHY

All patients will undergo CT scan from skull base to diaphragm. Contrast enhanced CT helps in identifying primary tumor, to assess extent of cervical lymphadenopathy, extranodal extension, presence/absence of contralateral lymph nodes and to identify any other metastasis (ex: lungs, bone)[34].

Metastatic nodes are usually enlarged; however small nodes can also harbour metastatic deposit and should be evaluated with respect to other CT features. Metastatic deposit can alter morphology of the lymph node resulting in loss of fatty hila or necrosis/ cystic degeneration or calcification within the lymph node[35].

Presence of nodal necrosis has high specificity (95-100%) for metastatic involvement in patients with primary as biopsy proven squamous cell carcinoma. Necrosed nodes show central hypoattenuation on CT with peripheral enhancement on post-contrast study. Central necrosis is due to obstruction of lymphatic flow. Presence of necrosis helps in differentiating lymphoma from metastatic node[35].

Cystic lymph nodes have central fluid attenuation with thin wall. They are feature of metastasis from papillary thyroid cancer and oropharyngeal SCC. Papillary and medullary thyroid carcinomas are frequently associated with calcified lymph nodes. Calcified cervical lymph nodes are also found in mucinous adenocarcinoma, post-radiotherapy cases of lymphoma and tuberculosis[35].

Metastatic deposit in lymph node changes shape of lymph node from oval to round. Eventually extracapsular extension occurs especially in large lymph nodes (> 3 cm). Imaging features of extranodal extension include irregular margin of lymph node, adjacent fat stranding, and loss of fat planes with adjacent structures (sternocleidomastoid muscle, IJV or carotid artery)[35].

**B. MRI (Magnetic Resonance Imaging):**

MRI is not generally advocated for all cases of nodal metastasis. However, for patients with metastatic lymph nodes in level II and III, MRI of the oropharynx can help in identification of previously occult primary (especially in base of tongue and tonsillar region). MRI features of metastatic lymph node include: spiculated and indistinct borders on fat-suppressed T2-weighted images, heterogeneous signal intensity on T2-weighted images and heterogeneous enhancement on post-contrast study[34,36].

**C. 18-FLUORODEOXYGLUCOSE POSITRON EMISSION TOMOGRAPHY (FDG-PET)/ COMPUTED TOMOGRAPHY (CT)**

MRI and CT can detect pathology when there is an anatomical abnormality or when it shows abnormal contrast enhancement. Hence, small lesions and non-enhancing lesions are missed in conventional cross-sectional imaging studies. FDG-PET/CT scanning is an important whole-body imaging modality for evaluation of the unknown primary with sensitivity better than CT and MRI[37].

High lesion-to-background contrast increases sensitivity in detection of FDG avid lesions. It can even detect other metastasis and thus help in accurate staging of

the disease. Post-biopsy inflammatory changes can lead to increase in uptake of the FDG tracer giving false positive result. Hence, FDG-PET should always be done before the biopsies[32,37].

## IV. PANENDOSCOPY, BILATERAL TONSILLECTOMY, TONGUE BASE MUCOSECTOMY:

Panendoscopy and directed biopsy should be done under general anaesthesia based on the potential primary sites identified on cross-sectional imaging. If both cross-sectional imaging and panendoscopy fail to identify primary lesion, random biopsies can be taken from post-nasal space, tongue base or pyriform fossa and also bilateral tonsillectomy. Inspite of all the investigations if the primary tumor is not identified, diagnosis will be 'true' unknown primary and the treatment is given based on N staging and histopathology of the lymph node[32,34].

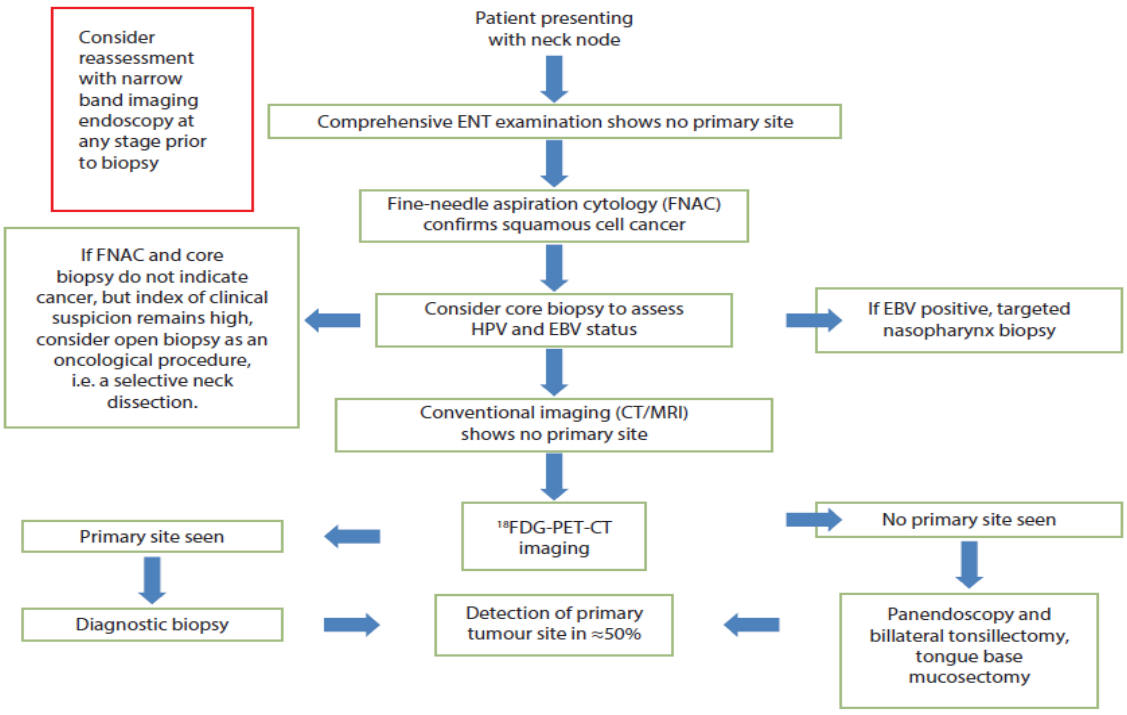


Figure 8: Algorithm for the management of MUO

# ULTRASOUND (USG)

Ultrasound is usually the first imaging modality used to assess cervical lymph nodes. Ultrasound is widely accessible, cheaper, no effects of radiation and can even be used for guided FNAC of suspicious lymph nodes[38].

Normal lymph node has ovoid shape on USG and appears hypoechoic with a central echogenic hilum (figure 9). Ultrasound evaluation is based on various B-mode features and colour Doppler evaluation. B-mode parameters usually employed in nodal assessment are size, shape, echogenicity, border, hilum, matting and calcifications[38].

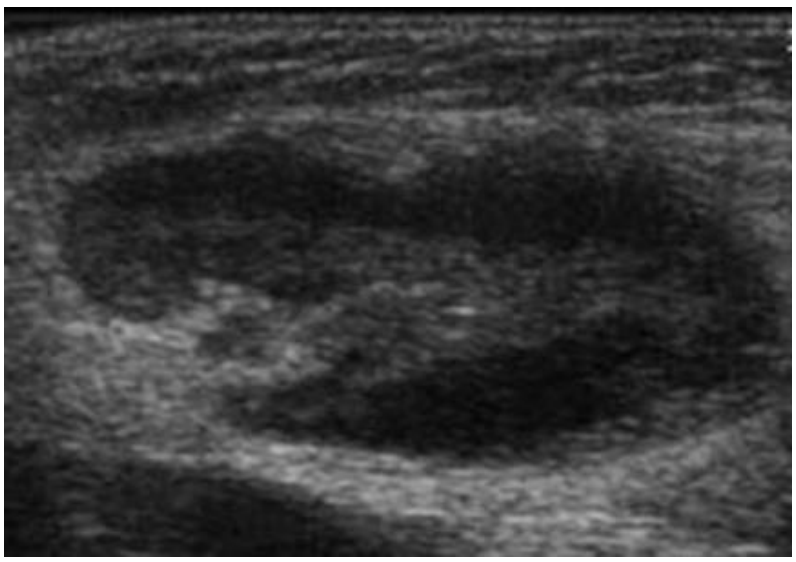

Figure 9: Ultrasound appearance of normal cervical lymph node

## SIZE (SHORT-AXIS DIAMETER)

Size of cervical lymph nodes varies with the level of lymph node. Those in the upper neck levels (submandibular and upper jugular) tend to be larger than those in other neck levels. Size of the lymph node also varies with the age. Intranodal fatty infiltration occurs in old age with resultant increase in size of the normal cervical lymph nodes in older age group. Various common cut-off values are evaluated, of which short-axis diameter of 8 mm showed better sensitivity[39].

## SHAPE

Shape of the malignant node changes from oval to round secondary to malignancy or metastasis. However, even normal submandibular and parotid lymph nodes can be round in shape. Shape is assessed by short-to-long axis ratio (S/L ratio) of lymph node. Commonly used cut-off for S/L ratio is 0.6. Focal metastatic deposit can cause eccentric cortical hypertrophy in affected lymph nodes[2,39.]

## HILUM

Hilum is seen as echogenic line within the lymph node. Echogenicity of hilum is secondary to presence of medullary lymphatic sinus and fat. Hilum is preserved in case of reactive and benign lymphadenopathy. Absence of fatty hila is seen in tubercular, metastatic and lymphomatous lymph nodes. However, hilum can be seen in metastatic lymph node in early stages[38,39].

## ECHOGENICTY OF LYMPH NODE

Echogenicity of the lymph node is compared with adjacent muscle. Malignant (metastatic and lymphomatous) lymph nodes are predominantly hypoechoic.

However, metastasis from papillary carcinoma of thyroid appear hyperechoic, likely secondary to thyroglobulin present in the metastatic deposits. Reactive and tubercular lymph nodes can also be hypoechoic[40].

**BORDER**

Sharp borders are seen in metastatic lymph nodes, whereas benign lymph nodes usually have unsharp borders. Tubercular lymph nodes can also show unsharp borders due to either edema or inflammation of surrounding tissues. Metastatic lymph nodes in advanced cases show ill-defined borders secondary to extranodal spread of disease[39].

**ANCILLIARY FINDINGS**

Tubercular lymph nodes have other ancillary features like adjacent soft tissue edema and matting secondary to perinodal inflammation. Adjacent soft tissue edema is also seen in metastatic lymph nodes likely due to extranodal extension into surrounding soft tissue. Soft tissue edema is also a finding in post-radiotherapy cases. Reactive and lymphomatous nodes are not associated with soft tissue edema or matting[38,41].

Papillary thyroid carcinoma metastasis is the most common etiology of intranodal calcifications and are seen as fine or punctate peripherally located hyperechoic foci with thin posterior acoustic shadowing. Lymph node necrosis is seen in advanced stage. There are two types of intranodal necrosis: cystic or coagulation necrosis. Cystic necrosis is most common and appears as ill-defined cystic areas within the lymph node. It is seen in papillary thyroid carcinoma, SCC metastasis and

in tuberculous nodes. Coagulation necrosis appears as intranodal echogenic area and can be seen in both malignant and infective nodes[41].

**COLOUR DOPPLER IMAGING (CDI)**

Normal lymph nodes on CDI show hilar vascularity or appear avascular. Reactive lymph nodes also usually have hilar vascularity. Malignant lymph nodes have either mixed (peripheral and hilar) or peripheral vascularity. Development of peripheral vascularity in malignant lymph nodes is due to tumor angiogenesis and proliferation of capsular vessels[41].

Role of Doppler indices like, resistivity index (RI) and pulsatility index (PI) in differentiating malignant from benign nodes is still controversial. Doppler indices of malignant lymph nodes usually have higher value than benign and/ or normal lymph nodes. When tumor cells grow, they replace a large portion of the lymph node and compress intranodal blood vessels. This results in increase in vascular resistance and hence high RI and PI values in malignant lymph nodes. Studies have shown that Doppler indices have poor diagnostic accuracy in discriminating benign from malignant lymph nodes[38,41].

# ELASTOGRAPHY

Palpation is an age-old method used by clinicians to assess soft tissue and detect abnormality based on difference in elasticity of the tissues. This is based on the fact that abnormal tissues (malignant) tend to be harder than the normal tissue[42].

Elasticity is the ability of the material to resume its original size and shape after applying a deforming force or stress. Pathological changes in the tissue lead to change in elasticity. Elastography is an imaging modality which can qualitatively and quantitatively assess the changes in elasticity of the tissue due to pathological process.

Assuming that a material is entirely elastic, elasticity can be described by Hooke's Law as:

$$\sigma=\Gamma\cdot\varepsilon$$

$\sigma$: stress (force per unit area with units kilopascals i.e. $N/m^2$)

$\varepsilon$: strain (expansion per unit length)

$\Gamma$: elastic modulus (three types: Young's modulus (E), shear modulus (G), and bulk modulus (K)).

Since its inception, concept of elastography is constantly evolving and is being used to assess liver, breast, thyroid, kidney, prostate and lymph nodes[43].

Ultrasound elastography techniques are classified based on the measured physical quantity. They are strain and shear wave elastography (SWE) techniques. Strain imaging is a semi-qualitative technique which can assess the relative stiffness

of lesion as compared to normal tissue. It can be further subdivided into strain elastography and acoustic radiation force impulse (ARFI). SWE is a quantitative method to measure the tissue stiffness[43,44].

## STRAIN IMAGING

### A. STRAIN ELASTOGRAPHY

Strain elastography is one of the earliest elastography technique used with ultrasound. There are two excitation methods to induce tissue displacement. In first method, manual compression is applied by the operator using ultrasound transducer. This is usually used for superficial structures like lymph nodes, thyroid and breast. For deep seated organs like liver, ultrasound transducer is held steady and the displacement is produced by internal physiologic motion (ex: respiration, cardiac pulsations). This method is non-operator dependent and the results are easily reproducible as compared to first method[43].

In strain elastography, the amount of displacement produced in the lesion by transducer or the physiological movement of the patient is compared to that in normal surrounding tissue and is displayed as elastograms. Elastograms are colour maps laid on B-mode images. Low strain or hard tissue is displayed in blue colour, whereas high strain or softer tissue is displayed in red colour. Five patterns are described on elastograms for characterizing the lymph nodes based on the distribution and percentage of blue area (hard area)[4].

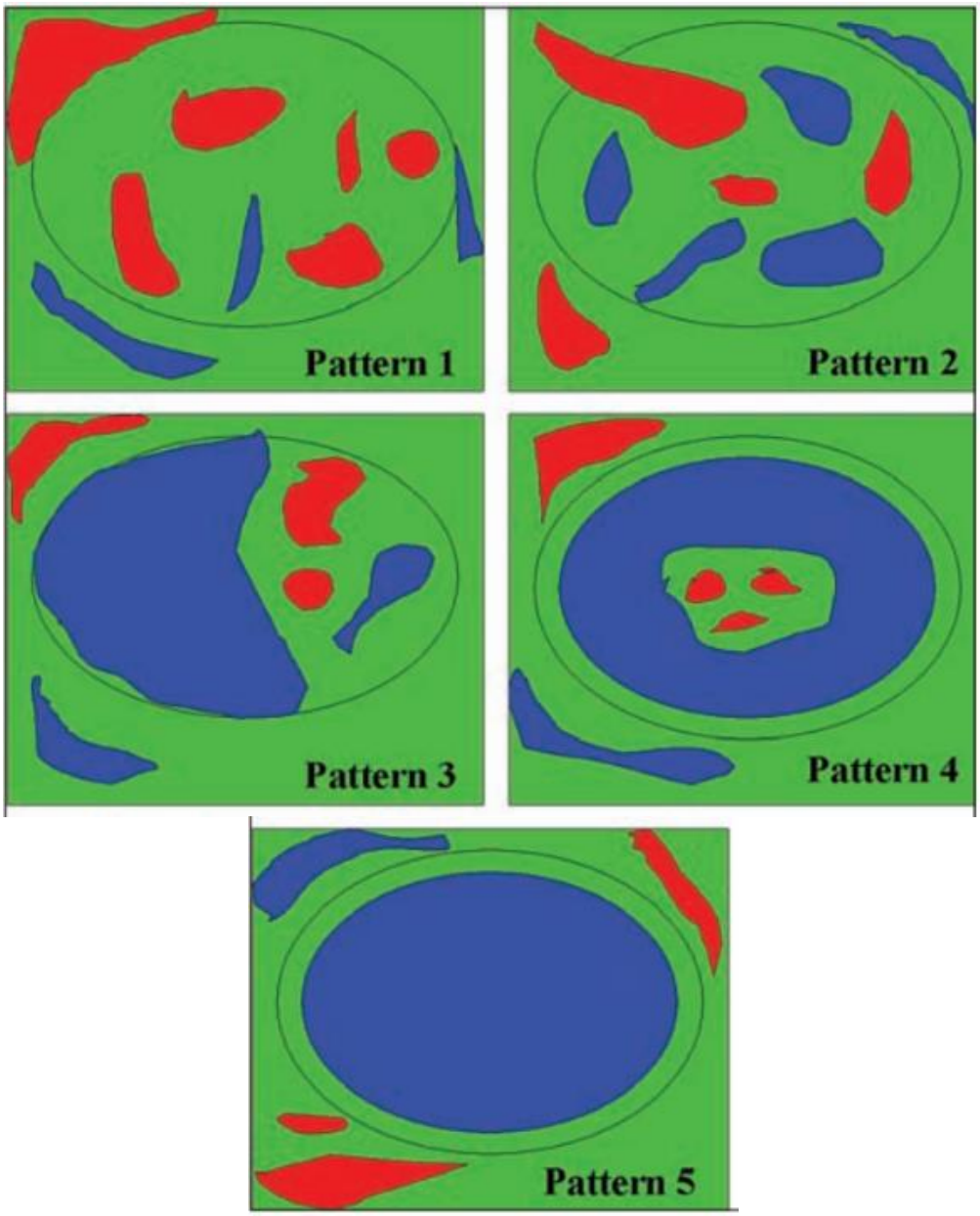


Figure 10: Elastogram patterns of lymph node on strain elastography

Five patterns on elastogram for lymph node characterisation[4]

| | |
|---|---|
| Pattern 1 | Absent or very small blue (hard) area(s). |
| Pattern 2 | Small scattered blue (hard) areas, blue area < 45%. |

| | |
|---|---|
| Pattern 3 | Large blue area(s), total blue area >45%. |
| Pattern 4 | Peripheral blue area and central green area, suggesting central necrosis. |
| Pattern 5 | Blue area occupying entire lymph node with or without a green (soft) rim. |

Strain ratio is a semi-quantitative method to measure tissue stiffness. It is a ratio of strain measured in the ROI in the lesion and the strain within the ROI in adjacent normal tissue. Low strain ratio indicates that the lesion is more easily compressible and hence are considered to be benign. Whereas, malignant lesions are less compressible and have high strain ratio. Cut-off value varies depending on the tissue assessed[5].

**B. ACOUSTIC RADIATION FORCE IMPULSE (ARFI) STRAIN IMAGING**

ARFI is a relatively new elastography technique used to measure strain. In ARFI strain imaging, short duration, high-intensity acoustic pulses produced by ultrasound transducer are used to displace tissue. Virtual touch tissue imaging (VTI) qualitatively assess the displacement of the tissue within a specified ROI and it can be displayed as an elastogram similar to strain elastography. Softer tissues have larger displacement and produce brighter image as compared to harder tissues which have smaller displacement and produce darker image. VTI images are graded (6 grades) depending on the proportion of dark and bright areas in the lymph node[45].

## SHEAR-WAVE ELASTOGRAPHY

Shear wave elastography (also called as dynamic elastography) is a newer technique which gives quantitative assessment of the elasticity of the tissue. Shear waves generated using focused acoustic radiation force from a linear US array, are used to cause local displacement in the tissue. Tissue displacement is used to calculate shear wave velocity (expressed in kPa or $m/sec^2$) (quantitative measure of elasticity of the tissue). Shear waves propagate faster in stiffer tissues and have higher velocity. Hence, malignant lymph nodes have higher shear wave velocity as compared to benign lymph nodes[46].

SWE is non-operator dependent and hence is reproducible and has less inter-observer variability. It provides quantitative measurements of tissue elasticity and is therefore considered superior to strain elastography[46].

## COMPUTED TOMOGRAPHY (CT)

CT is done to assess level of lymph node involved, extent of lymph nodal disease, spread to adjacent structures and to identify primary pathology in case of metastatic disease. CT is also frequently used for follow-up of nodal status. Most of the parameters used in CT are same as those used in ultrasound like, size, shape (short/ long axis ratio), border, presence of intranodal necrosis / cystic components or intranodal calcification[35].

CT scan is also used to predict the prognosis of the disease. Extranodal spread of lymph nodal disease and invasion into adjacent structures indicates poor prognosis.

Lymph nodal mass can invade adjacent structures like, muscle, bone and neurovascular structures[35].


Figure 11: Vascular invasion from SCC nodal metastasis. CECT neck axial section shows necrosed right level IIA node (asterix) with extracapsular spread. There is >180° encasement of right common carotid artery (arrow) and invasion of sternocleidomastoid muscle (arrowhead). A = common carotid artery, IJV = internal jugular vein.

Presence of arterial invasion can lead to several complications like occlusion of vessel, pseudoaneurysm formation or carotid blowout. Loss of fat planes with adjacent artery is considered to be the most sensitive sign of arterial invasion, whereas narrowing or irregularity of the arterial wall is the most specific sign. Circumferential encasement (>180–270$^0$) of carotid artery can indicate adventitial invasion and is not operable[35].

Dual energy CT combines both morphological and functional changes in lymph nodes thus helps in better evaluation. Studies have shown that dual energy CT

can characterize metastatic cervical lymphadenopathy based on qualitative analysis (monochromatic data) and quantitative analysis (iodine concentration and the slope of the spectral HU curve)[47].

CT perfusion imaging (CTP) is a functional imaging technique which can quantitatively and qualitatively assess the enhancement in the lymph node. Blood flow (BF), blood volume (BV), and mean transit time (MTT) will be calculated and depicted in a color-coded display. Metastatic lymph nodes have higher BF and BV and lower MTT as compared to benign lymph nodes[48].

## MAGNETIC RESONANCE IMAGING (MRI)

MRI has high intrinsic soft-tissue discrimination and thus is preferred for evaluating the head and neck soft tissues. Morphological features assessed in conventional MRI are similar to those in CT and ultrasound and include size, shape, border, vascularity, extranodal extension and other ancillary findings like presence of calcifications, necrosis or cystic components, extranodal spread of tumor and involvement of carotid artery. Presence of homogenous signal intensity on contrast-enhanced T1 and T2 weighted images favors benign etiology[49].

Diffusion weighted imaging (DWI) is a functional technique which is based on analysis of motion of water molecule in the lymph nodes. Restriction diffusion on DWI is seen in malignant lymph nodes and they have low apparent diffusion coefficient (ADC) values, whereas benign lymph nodes have low ADC values and do not show restricted diffusion. Cut-off ADC value of $0.93\times10^{-3}$ $mm^2/s$ yielded 97.6% sensitivity and 100% specificity. Infective nodes can show false positive result[49].

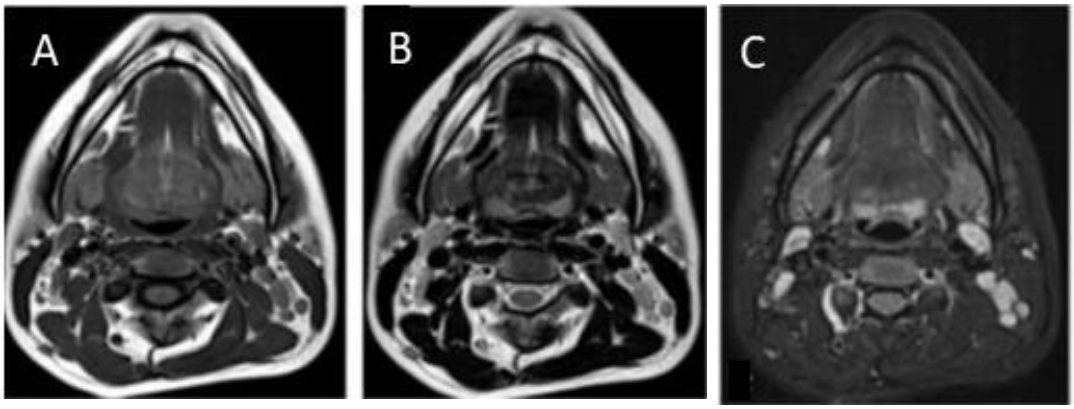


Figure 12: Benign lymph nodes: Oval shaped lymph nodes at bilateral level II, III and IV. Benign lymph nodes appear iso-intense on T1WI (A), homogenously hyperintense on T2WI (B) and STIR (C) images.

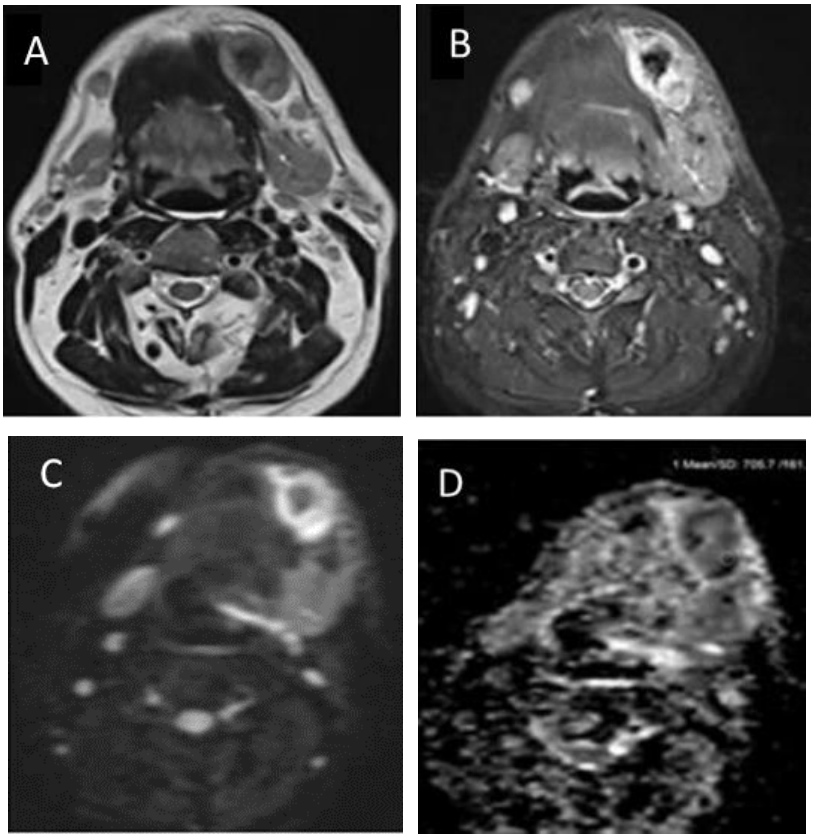


Figure 13: Metastatic lymph node: Well-defined enlarged necrotic lymph node in left level Ib. It appears heterogeneously hyperintense on T2WI (A) & STIR (B) images and shows diffusion restriction with corresponding low ADC values on DWI (C & D).

FDG-PET/CT

PET scan is a functional imaging technique used to identify metabolic changes in the tissue and can detect changes earlier than the other imaging methods. PET scan is found to have better diagnostic accuracy in differentiating cervical lymph nodes with sensitivity of 89% and specificity of 98%. It is used for tumor staging (including N staging), treatment response assessment, and to look for recurrence. PET- CT provides better anatomical localization of the lymph nodes[50].

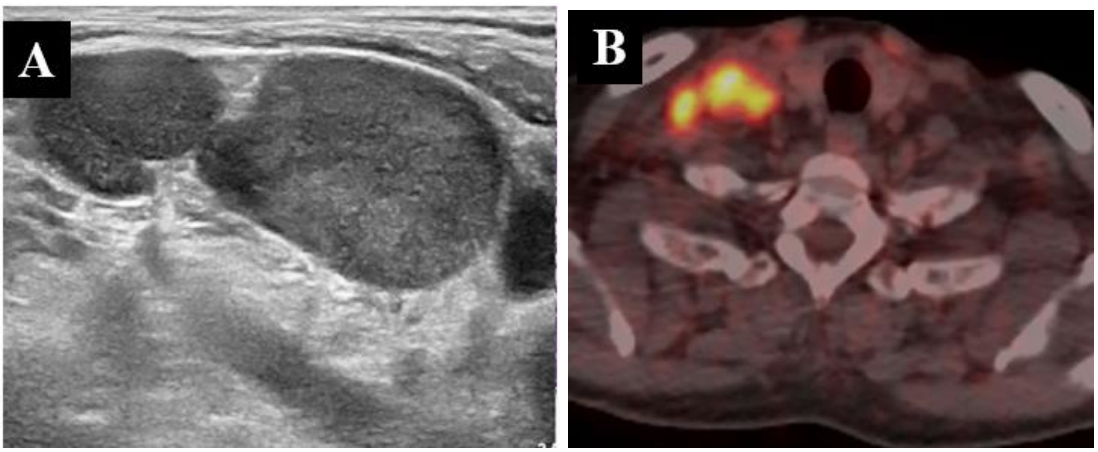


Figure 14: Ultrasound of a patient with carcinoma lung shows enlarged right supraclavicular lymph nodes with loss of fatty hila and coarse heterogeneous echotexture (A). Avid FDG uptake in right supraclavicular region confirming metastasis to supraclavicular lymph nodes (B).

# CLINICAL STUDIES

B-mode ultrasonography has been the cornerstone in the evaluation of cervical lymph nodes. Studies have used various criteria like size, shape, border, lymph node hilum and echogenicity. In an Indian study done in 2017, on 50 patients, only border and lymph node hilum were found to have diagnostic accuracy of more than 70% when compared with FNAC/biopsy findings[2].

Alam F et al conducted a prospective study which included 37 patients. They found that short axis diameter and hilum are more accurate than other B-mode parameters. However, the study states that common cut-off values for short axis diameter cannot be used for different levels of lymph nodes[4].

Elzawawy et al conducted study on 40 patients with cervical lymphadenopathy to evaluate vascular pattern and resistive index of intranodal vessels. They observed that the hilar pattern of vascularity was predominant in benign lymph nodes, whereas the peripheral pattern was predominant in malignant lymph nodes. Resistive index (cut-off value of 0.7) was found to have poor sensitivity (50%)[51].

Teng DK et al stated that ultrasound elastography is an important adjunct to conventional ultrasonography in differentiating benign from malignant lymph nodes, thus can aid in reducing unnecessary FNAC/biopsy. Characterization of lymph nodes on elastography is done based on two methods: Elastography color scoring and strain index[52].

Strain index is a measure of muscle to lymph node strain ratio. It compares elasticity of the lymph node with adjacent neck muscles. Various studies have used different strain index cut-off values. Lyshchik A et al, included 43 patients in their study and compared diagnostic accuracy of B-mode ultrasonography, color Doppler and elastography with histopathology as standard. They concluded that, diagnostic accuracy of strain index is better than any other B-mode or color Doppler criteria. Strain index was found to have diagnostic accuracy of 92% when 1.5 is used as cut-off. However, the study included patients with nodal metastasis secondary to only thyroid or hypopharyngeal carcinoma[3].

Elastography patterns were described based on percentage of blue (hard) area. Some studies have divided elastography patterns into 4 patterns (pattern 1 and 2 considered as benign, pattern 3 and 4 considered as malignant). However, majority of the studies have used 5 elastography patterns, where patterns 1 & 2 are considered as benign and patterns 3 to 5 are considered as malignant patterns[1,2,5,24].

In an Indian study done in 2017 on 50 patients, to evaluate diagnostic potential of elastography in comparison with B-mode and color Doppler found that elastography pattern in lymph node evaluation had sensitivity of 90%, specificity of 89% and accuracy of 90%[2].

Ghajarzadeh M et al conducted systematic review and meta-analysis on role of elastography in diagnosis of cervical lymph nodes. They included a total of 936 cervical lymph nodes (502 malignant and 434 benign) and stated that strain ratio

(semi-quantitative measure of lymph node elasticity) had better sensitivity, specificity and diagnostic accuracy than elastography colour patterns (qualitative method)[53].

A prospective study done on 37 patients reported a sensitivity of 92%, accuracy of 93% and specificity of 94% when B-mode ultrasonography and elastography are combined together[54].

An Indian study published in 2016, compared ultrasonography and elastography with histopathology. They found that tuberculosis and chronic granulomatous lymph nodes were over diagnosed on elastography as malignant lymph nodes. Also, lymphomatous lymph nodes were found to have benign features on elastography thus giving false negative results on elastography. They concluded that combination of conventional ultrasonography with elastography improves diagnostic accuracy and decreases false negative results[55].

# MATERIALS AND METHODS

## Source of data

The study was conducted over a period of eighteen months from January 2019 to June 2020 on 78 patients with enlarged cervical lymph nodes referred for ultrasonography at Department of Radio-Diagnosis, R.L. Jalappa Hospital and Research Center attached to Sri Devaraj Urs Medical College, Tamaka, Kolar. Informed consent was taken from the patients prior to inclusion in the study.

**Study design**: Prospective observational study

**Sample Size:**

Sample was calculated based on sensitivity of elastography as 90% in a study by Gupta R et al, with 95% confidence interval and absolute error of 8%[2].

Formula used –

$$\text{Sample size} = \frac{Z_{1-\alpha/2}{}^2 \, p(1-p)}{d^2}$$

Z1-α/2 = 1.96 at 5 % error alpha. As in majority of studies p values are considered significant below 0.05 hence 1.96 is used in formula.

p = Expected proportion in population based on previous studies or pilot studies.

d = Absolute error or precision – Has to be decided by researcher.

- p = 90 or 0.9
- 1 – p = 10 or 0.1
- d = 8%

Using the above values at 95% confidence level a sample size calculated was 54 subjects with enlarged cervical lymph nodes. Considering 10% nonresponsive, a sample size of 54 + 5.4 ≈ 60 subjects were planned to be included in the study. A total of 78 patients were included in the final analysis.

The patients were included in the study if they fulfilled the inclusion/exclusion criteria listed below:

**Inclusion criteria:**

All the patients with enlarged cervical lymph nodes who are referred for ultrasonography.

**Exclusion criteria:**

• Patients who have received radiotherapy/chemotherapy.

• Patients who underwent recent lymph node FNAC/biopsy.

## Method of collection of data:

Informed consent was taken from all the patients before inclusion in the study. Baseline data was collected along with pertinent clinical history, relevant lab investigations and pathology reports.

Individuals with cervical lymph nodes first underwent ultrasonography and color Doppler followed by elastography by using 5-12 MHz linear array transducer (PHILIPS EPIQ 5G Ultrasound Machine).

Lymph node morphology was defined on ultrasonography and vascularity on color Doppler. B-mode parameters that were evaluated include short axis dimension (cut-off value: 8 mm), short-to-long axis ratio (cut-off value: 0.6), fatty hilum (presence or absence of hilum), echogenicity (homogenous or heterogenous) and lymph node margin (regular or irregular). Based on the vascularity on colour Doppler imaging lymph nodes are divided into three patterns: Pattern I (hilar vascularity or no flow), Pattern II (peripheral vascularity) and pattern III (mixed vascularity). Patterns I and II were considered as benign patterns and pattern III was considered as malignant pattern.

Lymph nodes on elastography were evaluated based on two criteria: elastography pattern and strain index. During strain elastography linear probe was placed perpendicularly and gentle compression (> 50%) was applied to generate elastograms (colour maps). Elastography pattern was assessed based on percentage of blue and red area in the lymph node. Blue indicates hard area, red indicates soft area and green indicates intermediate tissue hardness. Cervical lymph nodes with patterns 1 and 2 were considered as benign and lymph nodes with patterns 3, 4 and 5 were labelled as malignant lymph nodes.

Strain index is the ratio of hardness of the lymph node with adjacent normal tissue. First region of interest (ROI 1) was placed in the lymph node and the second region of interest (ROI 2) was placed in the adjacent muscle at the same level. The strain index was calculated as ratio of ROI 1 to ROI 2 and values were generated. The cut off strain index used was 2.0. The cut off value of 2.0 was taken based on our initial experience, which showed a good correlation for differentiating benign from

malignant nodes. Cervical lymph nodes with strain index less than 2 were considered as benign and those with strain index more than 2 were considered as malignant.

Both ultrasonography and elastography findings were recorded and interpreted. Patient underwent pathological investigation, either ultrasound guided FNAC or biopsy. Elastography and ultrasonography findings were compared with pathology findings.

## Data analysis

The data were entered in Microsoft excel sheet. The measurable variables were analyzed and interpreted between them by the student's t test and the ordinal and categorical variables between them were interpreted by Chi-square ($\chi 2$) test. The predictive value of strain elastography for differentiating benign and malignant nodes was estimated. The statistical procedures were performed with the help of an SPSS statistical package (ver 21) and OpenEpi ver 3.01. P value less than 0.05 ($p<0.05$) was considered as statistically significant.

Figure 15. Philips EPIQ 5G premium ultrasound machine.

# RESULTS

## Demographics

Total of 78 patients were included in our study which was conducted from January 2019 to June 2020. Out of which, benign lymph nodes were 46 and malignant lymph nodes were 32.

## Age distribution

Mean age in our study was 38 ± 12.8 years with range of 4-75 years. Commonest age group was 30-59 years (n = 36; 46%) (Graph 1). Most of the lymph nodes in <30 years age group were benign and in older age group (> 60 years) were malignant. There was near equal distribution of benign and malignant lymph nodes in the middle age group (30-60 years) (Graph 2).

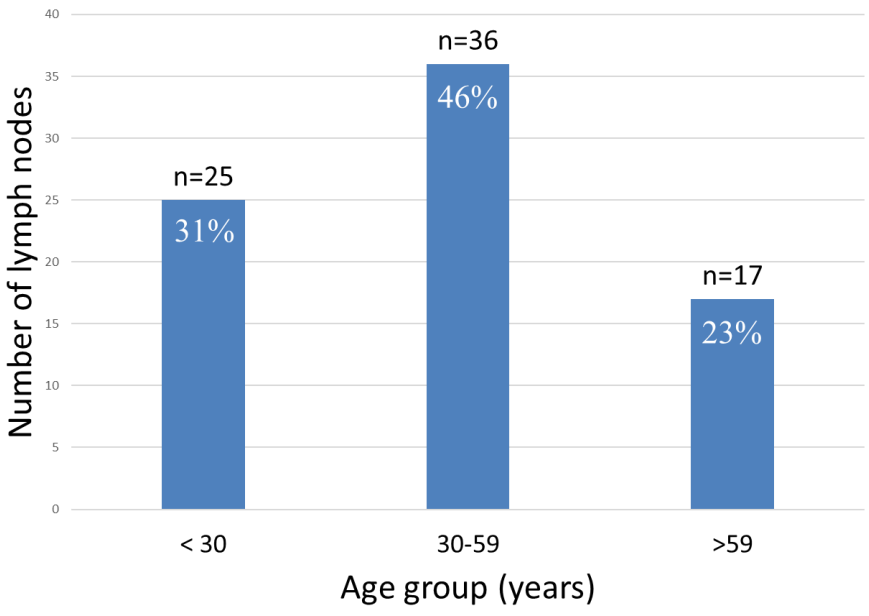


(Graph 1- Age group distribution)

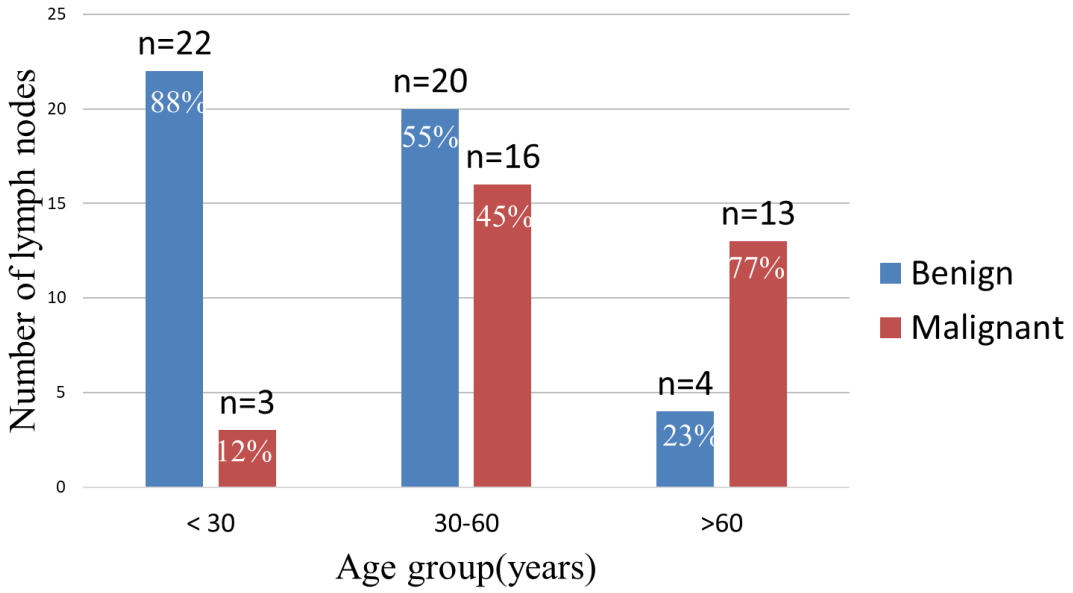


Graph 2- Age group wise distribution of cervical lymph nodes

**Gender distribution**

In our study group, there were total of 43 female (55%) and 35 male (45%) patents (Graph 3).

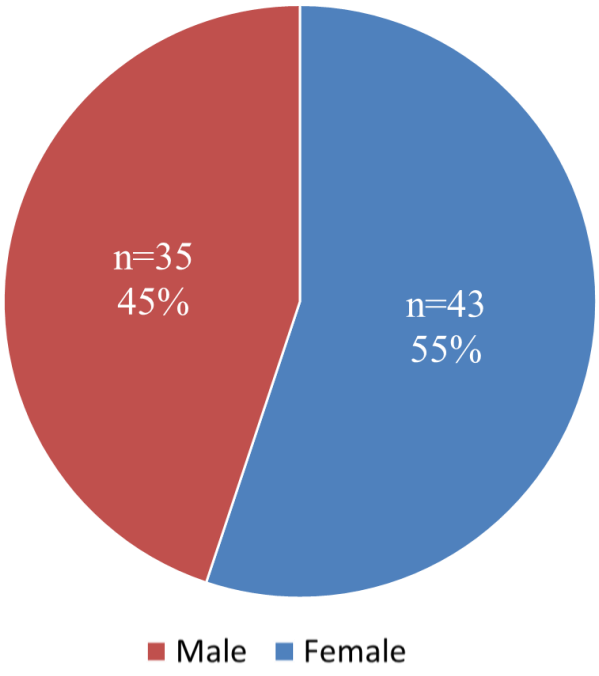


(Graph 3- Sex wise distribution)

There was near equal distribution of cervical lymph nodes in male and female patients. 60% of female and 57% of male patients had benign lymph nodes and 40% of female and 43% of male patients had malignant lymph nodes.

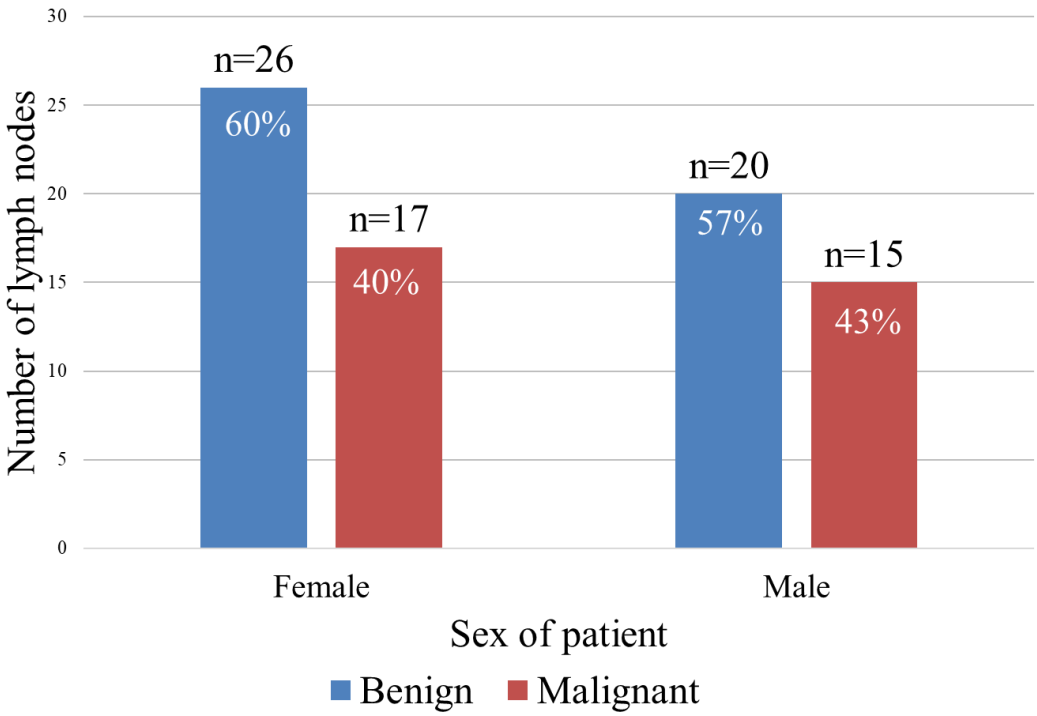


Graph 4- Sex wise distribution

**Distribution of cervical lymph nodes**

Greater proportion of the study population had bilateral enlarged cervical lymph nodes (50%), followed by left neck levels (27%) and right neck levels (23%). Majority of the cervical lymph nodes with bilateral distribution were benign (77%), whereas majority of cervical lymph nodes with unilateral distribution were malignant (60%).

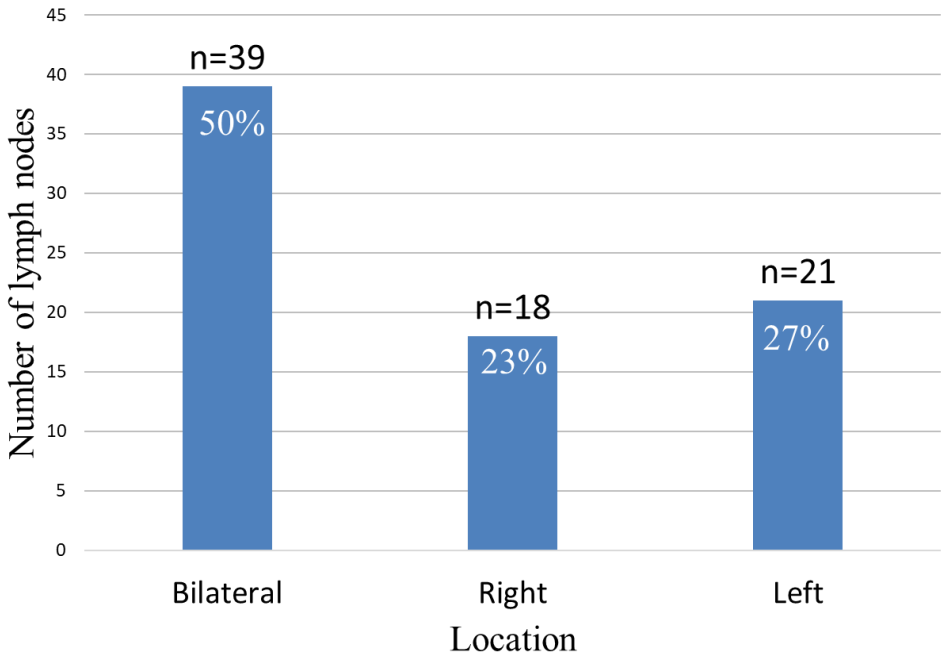


Graph 5: Cervical lymph node distribution

## B-MODE ULTRASONOGRAPHY FINDINGS

### Short axis dimension

Short axis dimension cut-off value used was 8 mm. Large number of lymph nodes with < 8 mm short axis dimension were benign. However, out of 63 cervical lymph nodes which had > 8 mm of short axis dimension, 32 were proven as benign and 31 were proven as malignant. Hence, though this parameter has high specificity and statistical significance (p = 0.0026), it has low sensitivity and accuracy.

| | Benign | Malignant | Sensitivity | Specificity | PPV | NPV | Accuracy |
|---|---|---|---|---|---|---|---|
| < 8 mm | 14 | 1 | 30 % | 97 % | 93 | 49 | 58 % |
| > 8 mm | 32 | 31 | | | | | |

Table 7: Short axis dimension

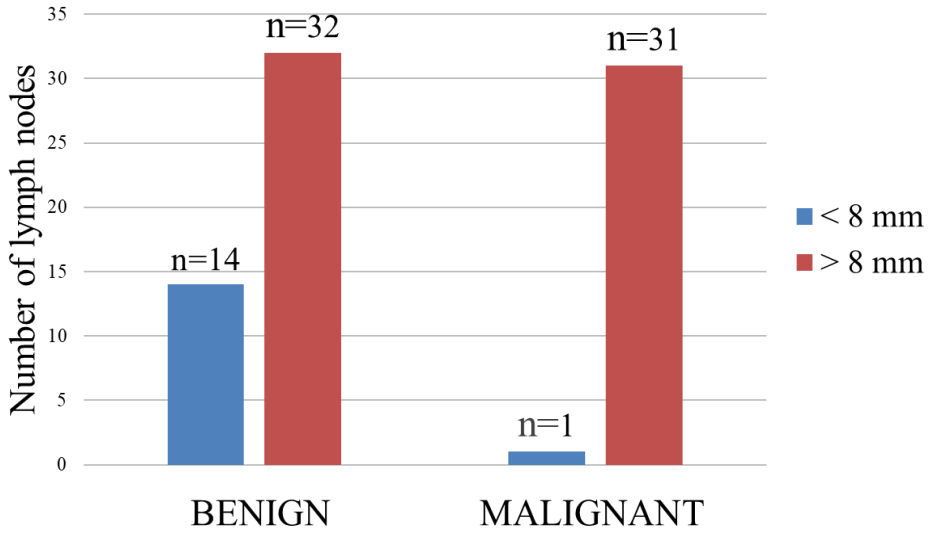


Graph 6: Short axis dimension

## Short/long axis ratio (S/L ratio)

Cut-off value in our study for short/long axis ratio was of 0.6. S/L ratio of less than 0.6 was found in majority of the benign cervical lymph nodes (87%). However, large number of malignant lymph nodes (63%) also had S/L ratio less than 0.6. Though S/L axis ratio was statistically significant (p value = 0.0116) and had sensitivity of 87%, specificity was low (38%).

| | Benign | Malignant | Sensitivity | Specificity | PPV | NPV | Accuracy |
|---|---|---|---|---|---|---|---|
| < 0.6 | 40 | 20 | 87% | 38% | 67 | 67 | 67% |
| > 0.6 | 6 | 12 | | | | | |

Table 8: Short/long axis ratio

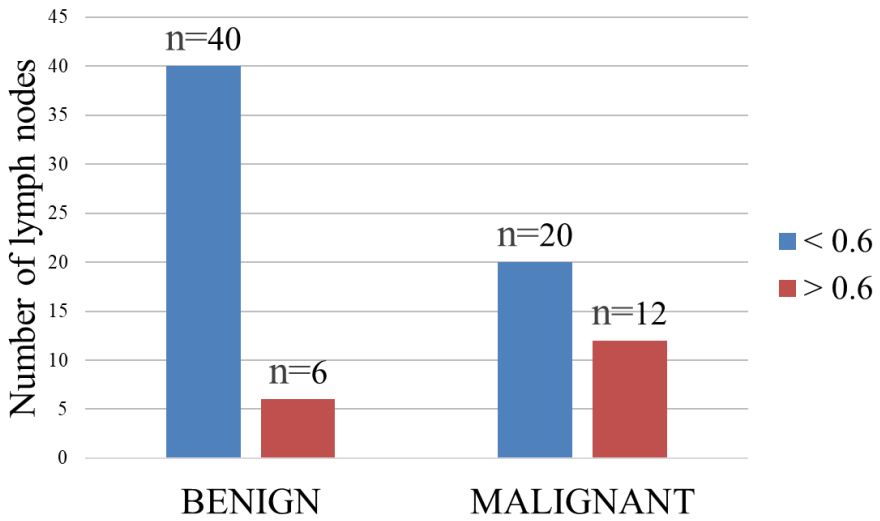


Graph 7: Short/long axis ratio

## Lymph node margin

Large number (46%) of benign lymph nodes had regular margin. Among benign cervical lymph nodes, suppurative and tubercular etiology nodes were found to have an irregular margin secondary to adjacent inflammation and edema. Out of 32 malignant cervical nodes, 22 nodes showed regular margin and 10 showed irregular margin. Hence, lymph node margin had poor specificity and was also found to be statistically insignificant (p value = 0.152).

| | Benign | Malignant | Sensitivity | Specificity | PPV | NPV | Accuracy |
|---|---|---|---|---|---|---|---|
| Regular | 38 | 22 | 83% | 31% | 63 | 56 | 62% |
| Irregular | 8 | 10 | | | | | |

Table 9: Lymph node margin

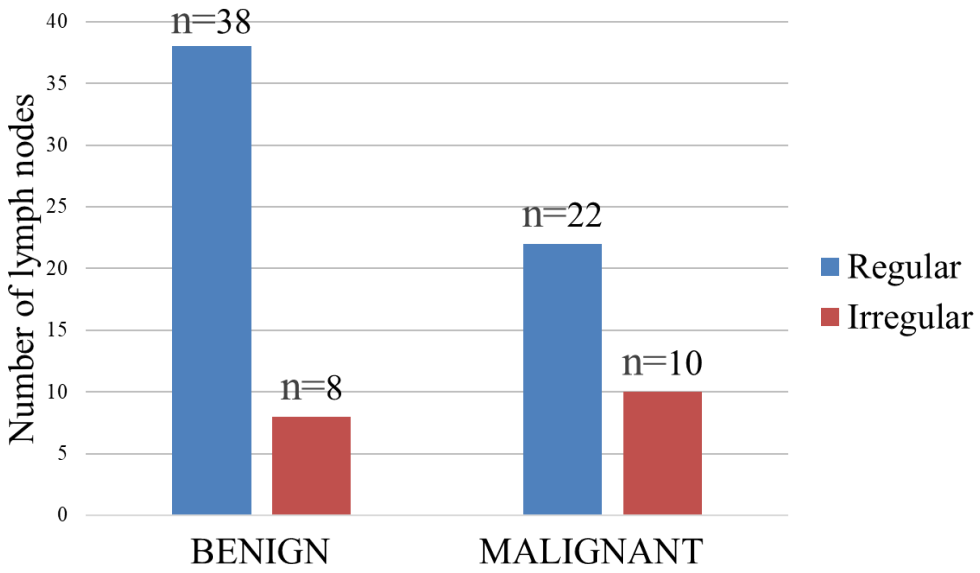


Graph 8: Lymph node margin

## Echogenicity

Benign lymph nodes predominantly showed homogenous echotexture (35 out of 46). However, malignant lymph nodes either showed homogenous (47%) or heterogeneous echogenicity (53%). Statistically significant difference was found in echogenicity of the lymph nodes of benign and malignant etiology (p value = 0.0081).

| | Benign | Malignant | Sensitivity | Specificity | PPV | NPV | Accuracy |
|---|---|---|---|---|---|---|---|
| Homogenous | 35 | 15 | 76% | 53% | 70 | 60 | 67% |
| Heterogenous | 11 | 17 | | | | | |

Table 10: Lymph node echogenicity

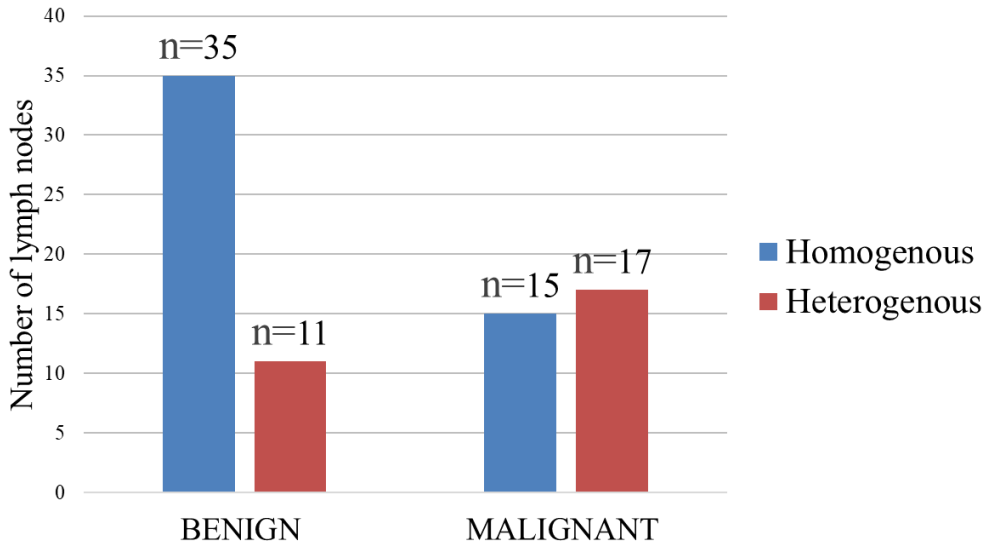


Graph 9: Lymph node echogenicity

## Fatty hilum

67% of benign lymph nodes had preserved fatty hila. In majority (81%) of the malignant lymph nodes, fatty hilum was absent. Among all B-mode parameters, fatty hilum showed high diagnostic accuracy (73%) and p value of < 0.0001 (high statistical significance).

| | Benign | Malignant | Sensitivity | Specificity | PPV | NPV | Accuracy |
|---|---|---|---|---|---|---|---|
| Present | 31 | 6 | 67% | 81% | 84 | 63 | 73% |
| Absent | 15 | 26 | | | | | |

Table 11: Fatty hilum

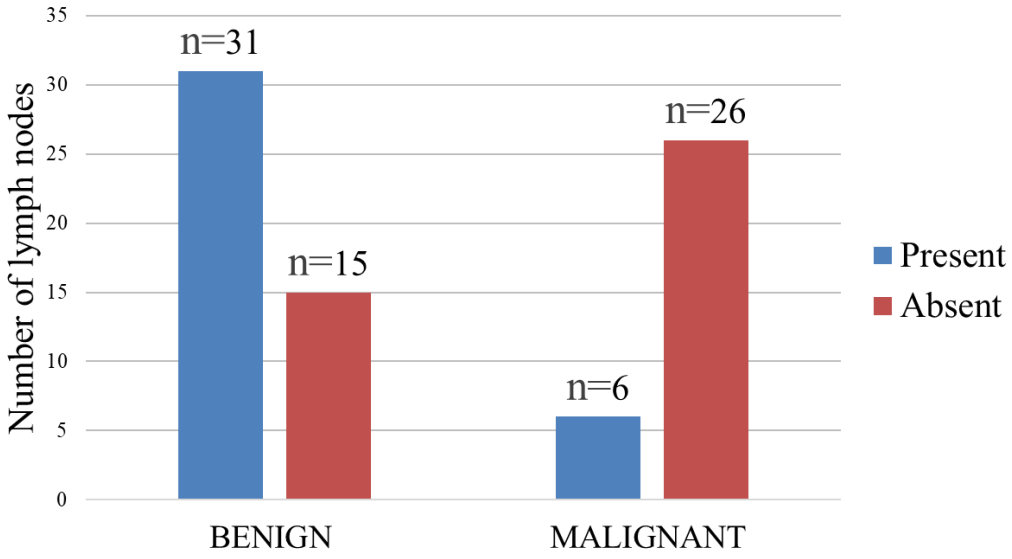


Graph 10: Fatty hilum

## Vascularity on color Doppler imaging

71% of benign cervical lymph nodes (33 out of 46 benign lymph nodes) showed vascularity pattern I (hilar vascularity or no flow) on CDI, whereas 69% of malignant cervical lymph nodes (22 out of 32 malignant lymph nodes) showed either pattern II (peripheral) or pattern III (mixed vascularity) on CDI. Vascularity pattern was statistically significant (p value=.0004) parameter.

| | Benign | Malignant | Sensitivity | Specificity | PPV | NPV | Accuracy |
|---|---|---|---|---|---|---|---|
| Benign Pattern (I) | 33 | 10 | 71% | 68% | 76 | 62 | 70% |
| Malignant Pattern (II,III) | 13 | 22 | | | | | |

Table 12: Vascularity pattern

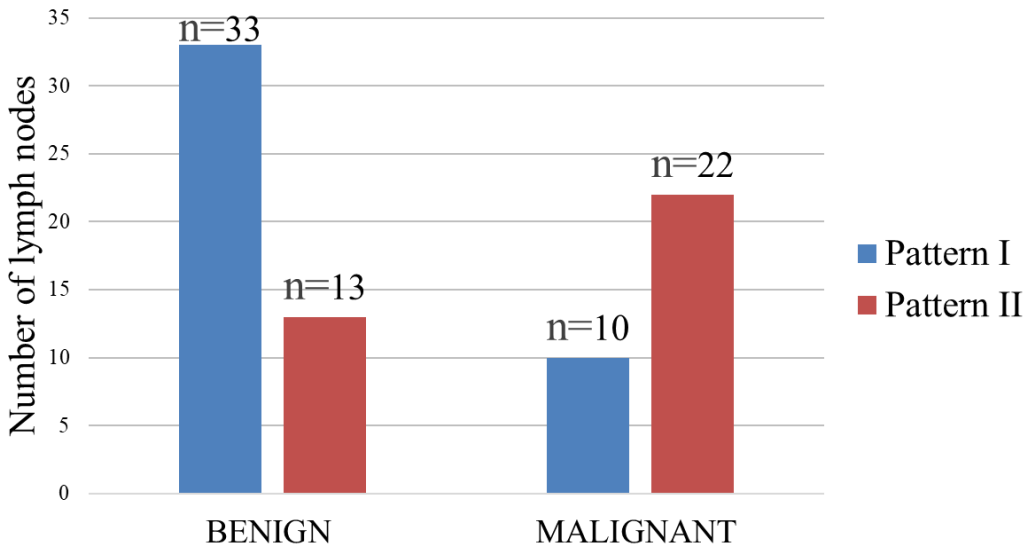


Graph 11: Vascularity pattern

## Elastography

On elastography, cervical lymph nodes were assessed based on elastography pattern and strain index.

## Elastography pattern

Maximum number of lymph nodes had pattern 2 on elastography (35 cervical lymph nodes), followed by pattern 3 (18 cervical lymph nodes) and pattern 4 (16 cervical lymph nodes). A total of 39 lymph nodes had benign pattern on elastography (4 lymph nodes with pattern 1 and 35 lymph nodes with pattern 2). All 4 cervical lymph nodes with pattern 1 on elastography were confirmed to be benign on pathology. Of the 35 cervical lymph nodes with pattern 2, 34 lymph nodes were benign and one lymph node was malignant on pathology.

There were total 39 cervical lymph nodes which showed malignant pattern. Out of these, 8 nodes (5 lymph nodes with pattern 3 and 3 lymph nodes with pattern 4) were proven to be of benign etiology and 31 nodes showed malignant features on pathology. All pattern 5 cervical lymph nodes were proven as malignant on pathology. We found a significant difference between elastography pattern of benign and malignant cervical lymph nodes ($p < .00001$).

| | Total | Benign | Malignant |
|---|---|---|---|
| Pattern 1 | 4 | 4 | 0 |
| Pattern 2 | 35 | 34 | 1 |
| Pattern 3 | 18 | 5 | 13 |
| Pattern 4 | 16 | 3 | 13 |
| Pattern 5 | 5 | 0 | 5 |

Table 13: Distribution of cervical lymph nodes according to elastography pattern

| | Benign | Malignant | Sensitivity | Specificity | PPV | NPV | Accuracy |
|---|---|---|---|---|---|---|---|
| Benign pattern | 38 | 1 | 83% | 97% | 97 | 80 | 89% |
| Malignant pattern | 8 | 31 | | | | | |

Table 14: Elastography pattern of cervical lymph nodes

## Elastography strain index

We used a mean strain index cut-off of 2, which yielded a diagnostic accuracy of 94% and showed statistical significance ($p < .00001$). Among a total of 78 cervical lymph nodes, 44 had strain index less than 2, suggestive of benign etiology and 34 lymph nodes had strain index more than 2, suggestive of malignant etiology. Mean strain index for benign cervical lymph node was $1.45 \pm 0.306$ (mean ± SD), and the mean strain index for malignant cervical lymph node was $3.01 \pm 0.690$ (mean ± SD). One malignant lymph node showed strain index of less than 2, whereas 3 benign nodes had strain index of more than 2.

| | Benign | Malignant | Sensitivity | Specificity | PPV | NPV | Accuracy |
|---|---|---|---|---|---|---|---|
| Benign (<2) | 43 | 1 | 93% | 96% | 97 | 91 | 94% |
| Malignant (>2) | 3 | 31 | | | | | |

Table 15: Distribution of cervical lymph nodes according to elastography pattern

## Pathology diagnosis of cervical lymph nodes

Following ultrasonography and elastography patient underwent FNAC or biopsy of the lymph node. On final diagnosis, 46 out of 78 patients (60%) had benign lymph nodes and 32 (40%) patients had malignant lymph nodes. Among benign cervical lymph nodes, reactive lymphadenitis (59%) was found to be most common followed by granulomatous lymphadenitis (26%).

Among malignant cervical lymph nodes, metastatic lymph nodes accounted for 78% and lymphoma cases accounted for 22%. Metastasis from SCC of head and neck region (50%) is most common followed by metastasis from adenocarcinoma (13%). There were 4 patients of Non-Hodgkin's lymphoma and 3 patients of Hodgkin's lymphoma (Graph 12 & 13).

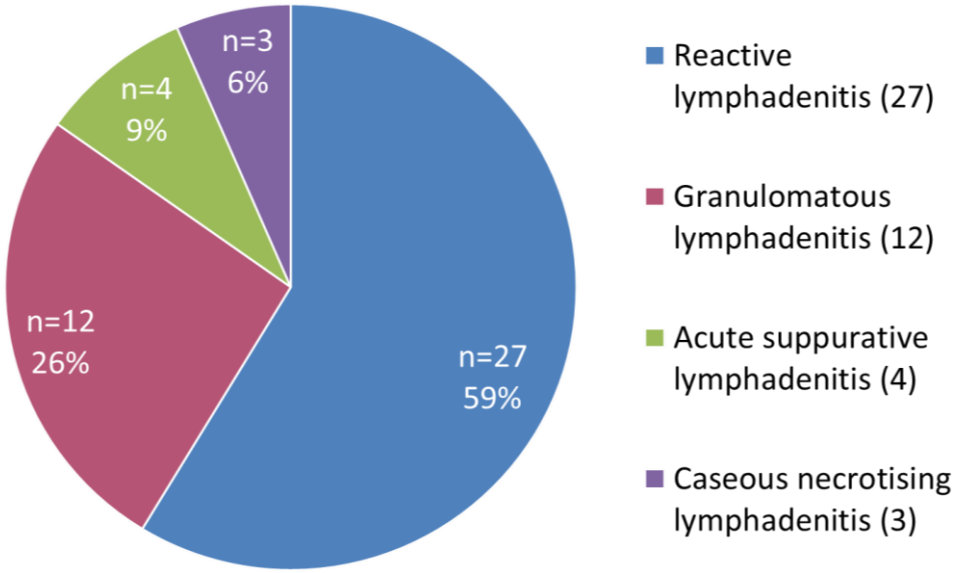


Graph 12: Benign cervical lymph node

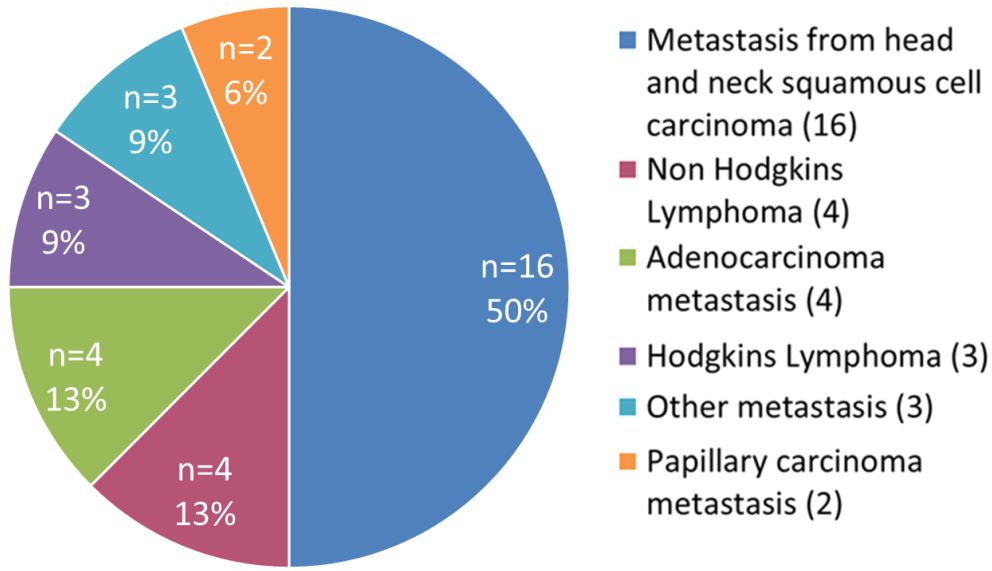


Graph 13: Malignant cervical lymph node

## Comparison of various parameters in B-mode, colour Doppler imaging and elastography findings:

All B-mode and CDI parameters except lymph node margin were statistically significant. Among them, fatty hilum and vascularity pattern were found to have high statistical significance and highest accuracy in differentiating benign from malignant cervical lymph nodes.

Both elastography parameters were statistically significant (p value < 0.00001) in differentiating cervical lymph nodes. Diagnostic accuracy of strain index (94%) was marginally better than that of elastography pattern (89%).

| | SENSITIVY (%) | SPECIFICITY (%) | ACCURACY (%) | p value |
|---|---|---|---|---|
| Short axis dimension | 30 | 97 | 58 | 0.0026 |
| Short/long axis dimension | 87 | 38 | 67 | 0.0116 |
| Echogenicity | 76 | 53 | 67 | 0.0081 |
| Margin | 83 | 31 | 62 | 0.1520 |
| Fatty hilum | 67 | 81 | 73 | 0.00002 |
| Color Doppler vascularity | 71 | 68 | 70 | 0.0004 |
| Elastography pattern | 83 | 97 | 89 | <0.00001 |
| Strain index | 93 | 96 | 94 | <0.00001 |

Table 16: Comparison of various parameters in B-mode, CDI and elastography.

## Correlation of ultrasonography & elastography with pathological diagnosis:

Our study had 46 benign and 32 malignant lymph nodes diagnosed on pathology. Diagnosis on ultrasound was based on all b-mode parameters and vascularity pattern of the lymph node. Elastography diagnosis was based on both elastography pattern and strain index.

When ultrasonography and elastography were used separately, 41 lymph nodes on ultrasonography and 43 lymph nodes on elastography were accurately diagnosed as benign. 28 lymph nodes on ultrasonography and 30 lymph nodes on elastography were correctly diagnosed as malignant. When both the findings were combined 44 lymph nodes were accurately diagnosed as benign and 30 lymph nodes were accurately diagnosed as malignant. Combined use of elastography and ultrasonography had augmented diagnostic accuracy (95%) than individual modality.

Four malignant cervical lymph nodes were misdiagnosed by ultrasonography as benign; one was a case of Hodgkin's lymphoma and other three were metastasis. Ultrasound incorrectly diagnosed five benign lymph nodes as malignant. It includes, two cases of granulomatous lymphadenitis, two cases of reactive lymphadenitis and one case of acute suppurative lymphadenitis. Elastography underdiagnosed two malignant cases as benign (Hodgkin's lymphoma and metastasis) and overdiagnosed three benign cases as malignant (one reactive lymphadenitis and two granulomatous lymphadenitis cases). Combination of elastography and ultrasound findings incorrectly diagnosed two benign cases (granulomatous lymphadenitis and reactive

lymphadenitis) as malignant and two malignant cases (Hodgkin's lymphoma and SCC metastasis) as benign.

| | | Pathology Diagnosis | | Sensitivity (%) | Specificity (%) | Accuracy (%) |
|---|---|---|---|---|---|---|
| | | Benign | Malignant | | | |
| USG | Benign | 41 | 4 | 90% | 88% | 89% |
| | Malignant | 5 | 28 | | | |
| Elastography | Benign | 43 | 2 | 93% | 94% | 94% |
| | Malignant | 3 | 30 | | | |
| Combined USG + Elastography | Benign | 44 | 2 | 96% | 94% | 95% |
| | Malignant | 2 | 30 | | | |

Table 17: Correlation of USG & Elastography with pathological diagnosis.

# IMAGES

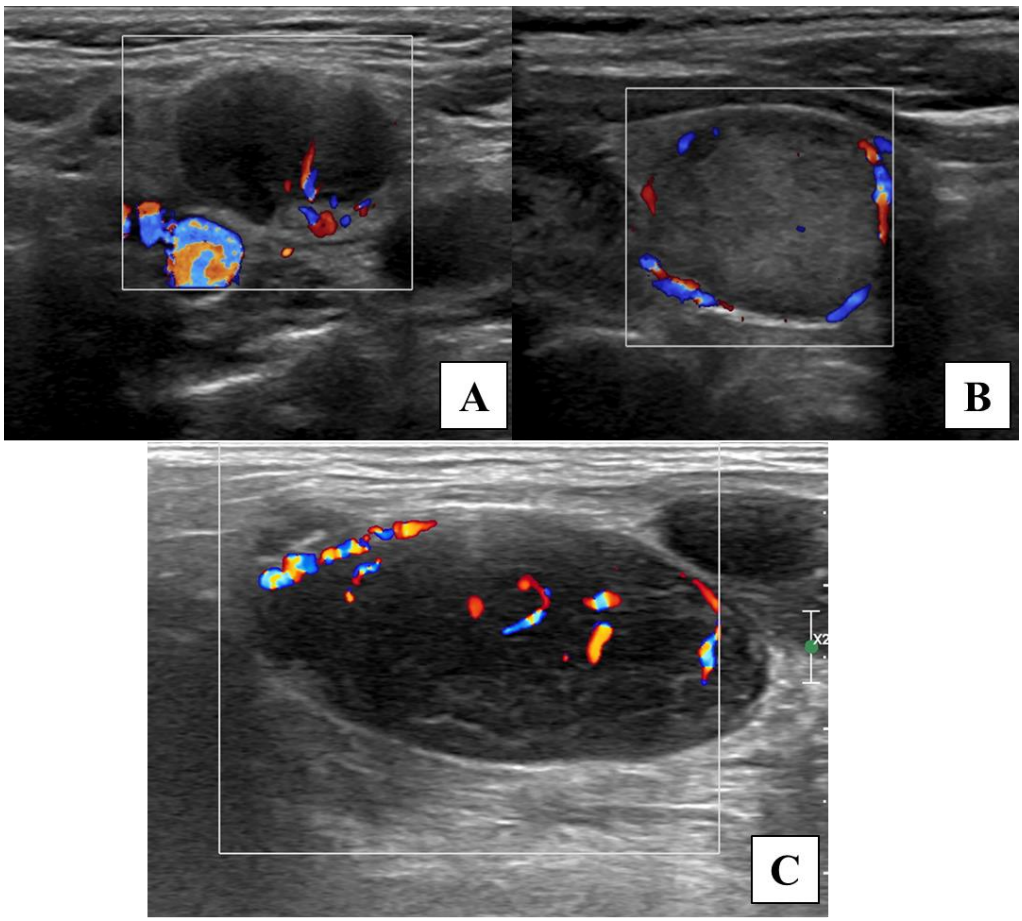


Figure 16: Vascular patterns on color Doppler imaging. Pattern I: Hilar vascularity (A). Pattern II: Peripheral vascularity (B). Pattern III: Mixed vascularity (C). Pattern I is a benign pattern and pattern II and III are malignant patterns.

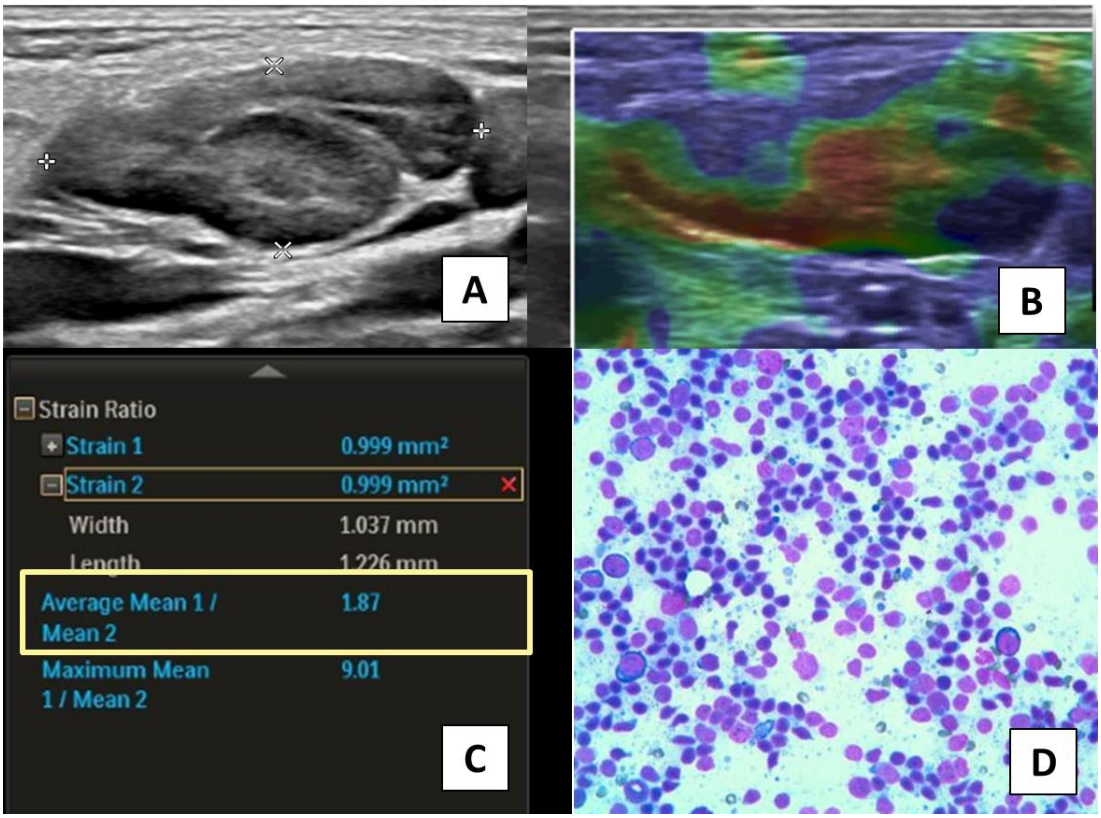


Figure 17: 4-year-old male patient presented with cervical lymphadenopathy. On USG, lymph nodes were oval in shape with preserved fatty hila (Figure A). On elastography, lymph node had elastography pattern II and strain index of 1.87 (Figure B and C). Ultrasonography and elastography findings are suggestive of benign etiology. FNAC of the lymph node showed reactive cervical lymphadenitis (Figure D).

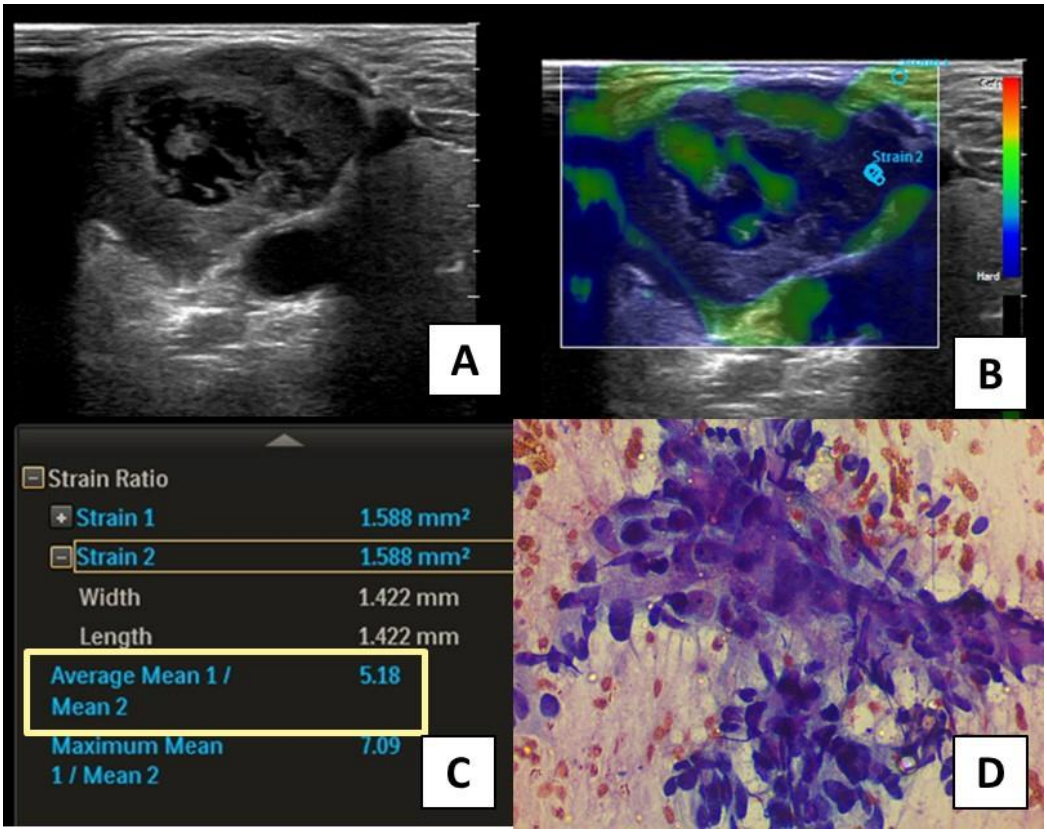


Figure 18: Ultrasonography of 70-year-old male showed enlarged cervical lymph node in right level II with loss of fatty hila, heterogeneous echotexture and central necrosis (Figure A). On elastography, lymph node had elastography pattern III with strain index of 5.18 (Figure B and C). Ultrasonography and elastography findings are suggestive of malignant etiology and FNAC showed features of metastatic adenocarcinoma (Figure D).

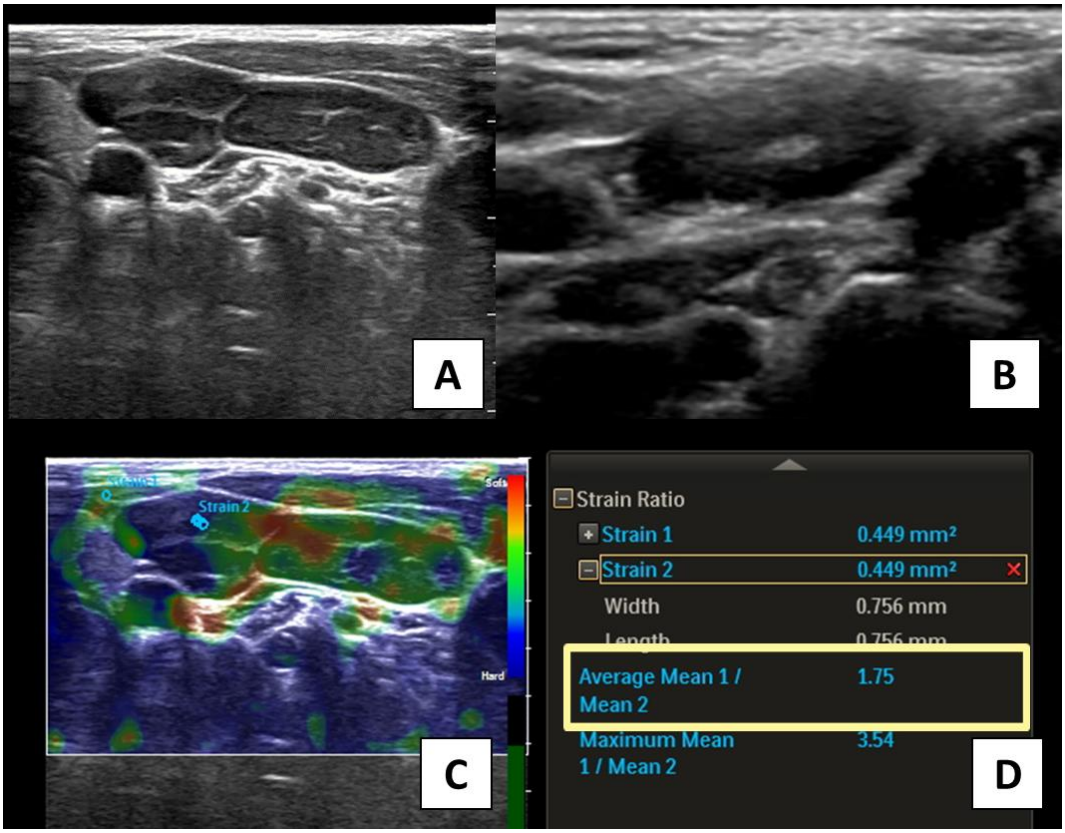


Figure 19: Ultrasound neck of 9-year-old female showed multiple cervical lymph nodes with short axis dimension of less than 8 mm, oval shape and maintained fatty hila (Figure A & B). Lymph nodes had elastography pattern II on elastogram with strain index of 1.75 (Figure C and D). Ultrasonography and elastography findings were suggestive of benign etiology, however FNAC features were suggestive of Hodgkin's lymphoma.

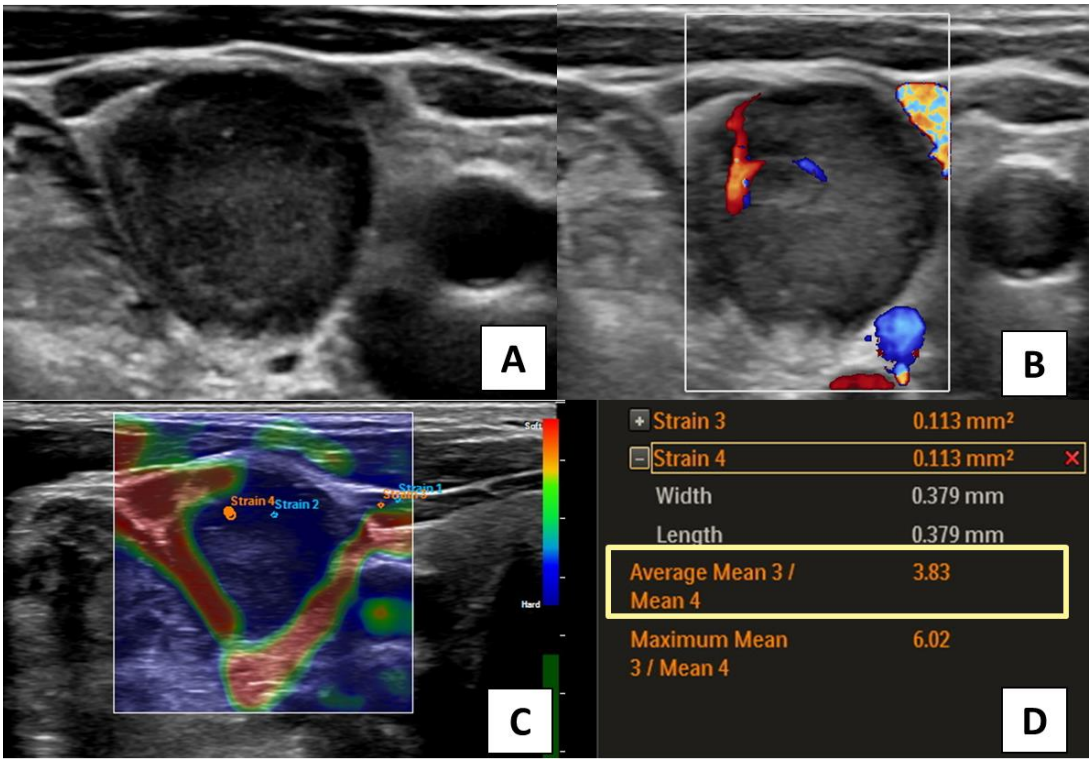


Figure 20: Ultrasonography of 52-year-old male showed enlarged lymph node in left supraclavicular region with loss of fatty hila, S/L ratio of > 0.6 (round) and central vascularity on CDI (malignant pattern) (Figure A & B). On elastography, lymph node had strain index of 3.8 and showed elastography pattern V (Figure C and D). Both ultrasound and elastography findings were suggestive of malignant etiology, however FNAC diagnosis was reactive lymphadenitis.

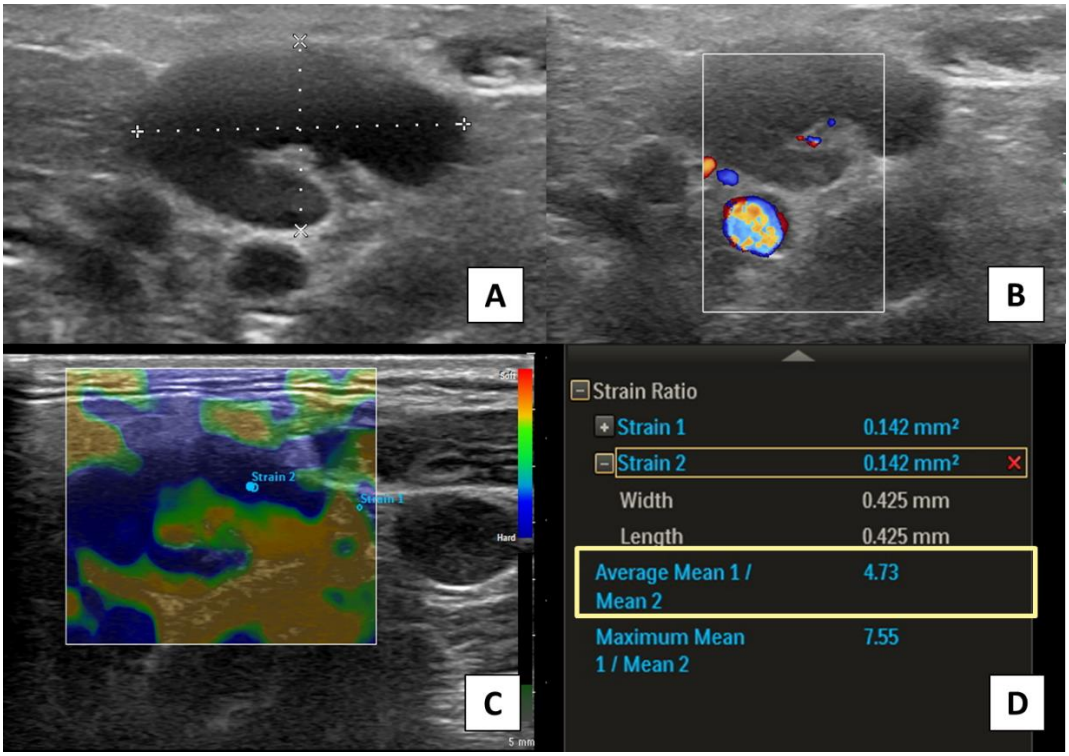


Figure 21: Ultrasonography of 51-year-old male showed enlarged lymph node in right level II with maintained fatty hila, S/L ratio of < 0.6 and hilar vascularity on CDI (Figure A & B). On elastography, lymph node showed elastography pattern IV and strain index of 4.73 (Figure C and D). Lymph node had benign features on ultrasonography, however it showed malignant features on elastography which was consistent with FNAC findings (metastasis).

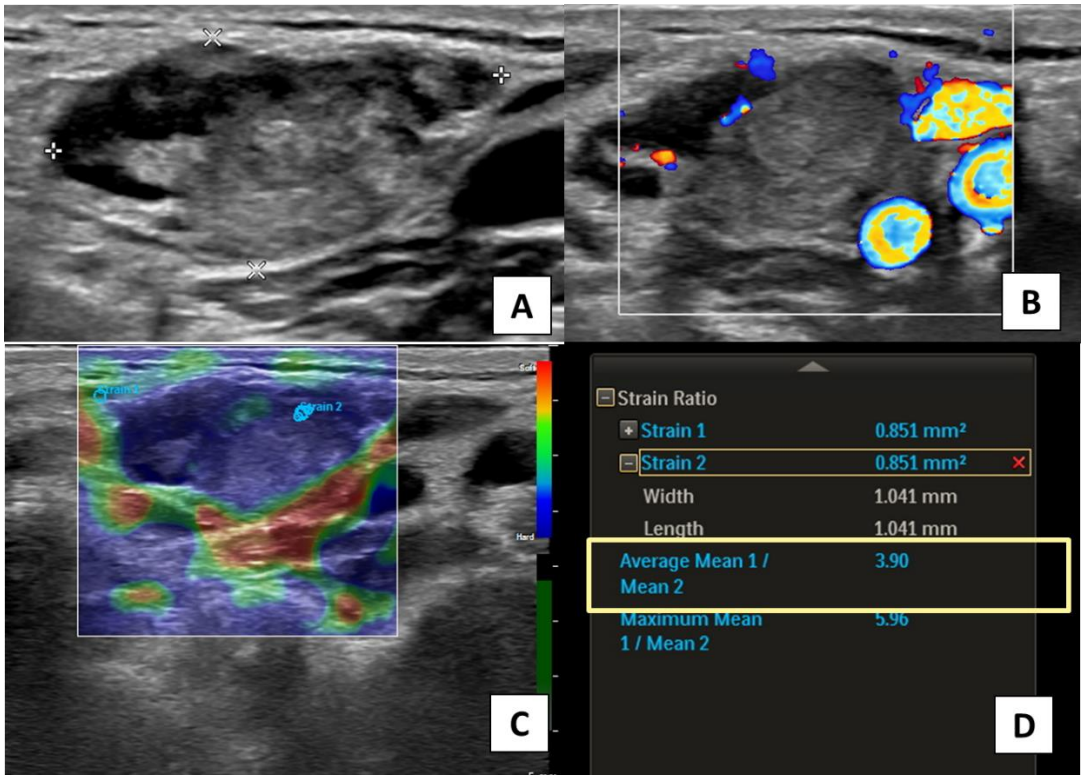


Figure 22: Ultrasonography of 69-year-old male showed enlarged and heterogenous cervical lymph node in left level IB with peripheral and central vascularity (Figure A & B), elastography pattern V and strain index of 3.9 (Figure C and D). Ultrasonography and elastography findings were suggestive of malignant etiology which correlated with pathology findings (metastasis).

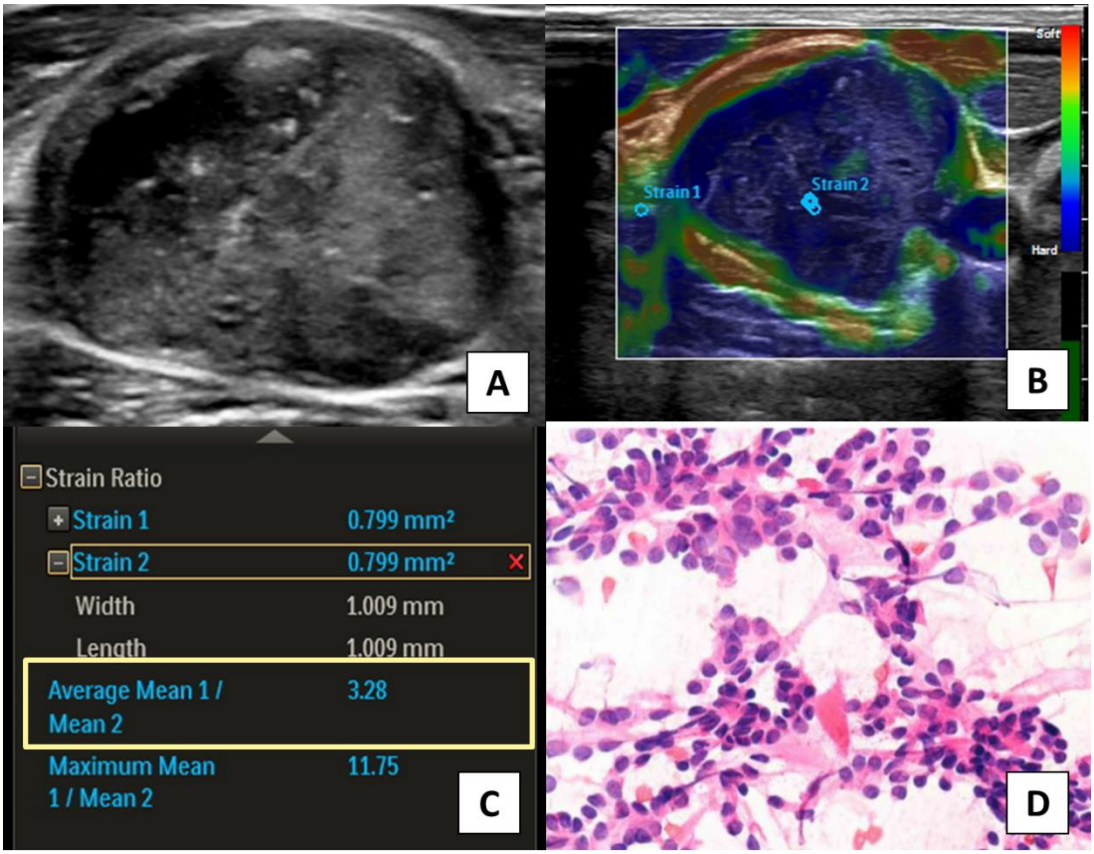


Figure 23: Ultrasound neck of 40-year-old male showed TIRADS V lesion in right lobe of thyroid and ipsilateral cervical lymphadenopathy. Lymph nodes had multiple intranodal calcifications with heterogenous echotexture (Figure A). On elastography, lymph node showed pattern V with strain index of 3.28 (Figure B & C). Lymph nodes were diagnosed as malignant based on ultrasonography and elastography findings. FNAC of right thyroid lesion and ipsilateral cervical lymph node (level IV) showed papillary thyroid carcinoma with ipsilateral cervical nodal metastasis (Figure D).

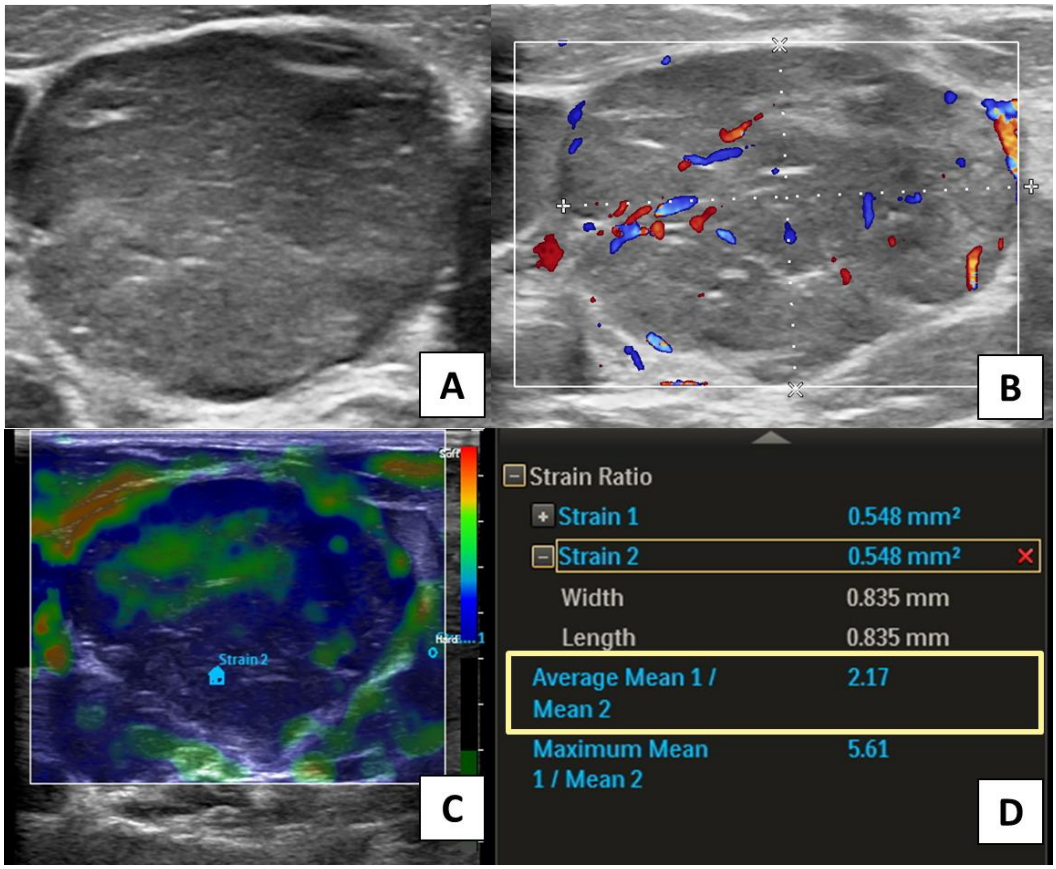


Figure 24: 18-year-old male presented with generalised lymphadenopathy. Cervical lymph node showed homogenous echotexture with loss of fatty hila and mixed vascularity on CDI (Figure A & B). Lymph node showed malignant features on elastography (pattern IV on elastogram and strain index of 2.17) (Figure C and D). Based on ultrasonography and elastography findings possibility of lymphoma was considered. FNAC of cervical lymph nodes showed features consistent with Hodgkin's lymphoma.

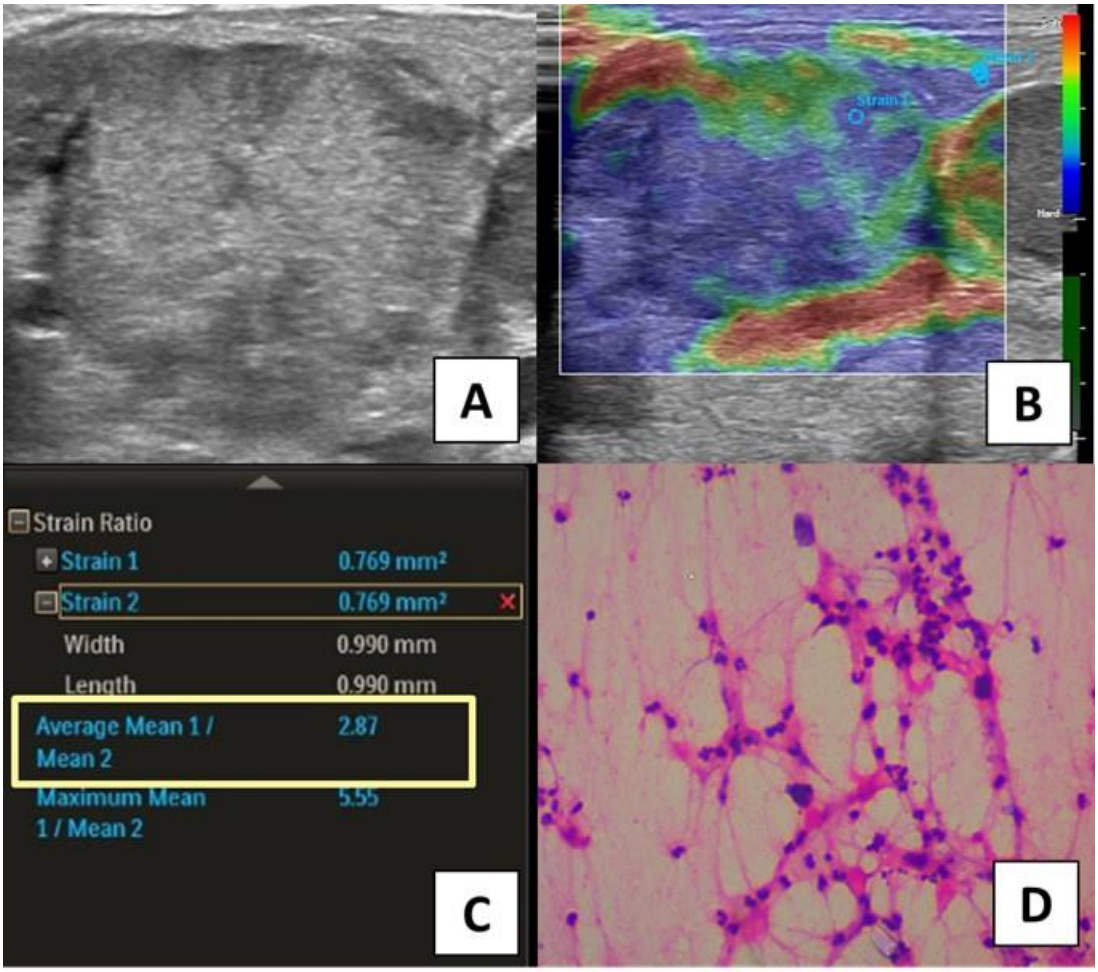


Figure 26: 69-year-old male with carcinoma right buccal mucosa presented with enlarged right cervical lymph nodes. Lymph nodes had homogenous echotexture with loss of fatty hila, S/L ratio of > 0.6 (Figure A) and mixed vascularity (central and peripheral) on CDI. On elastography, they had pattern IV on elastogram and strain index of 2.87 (Figure B & C). Lymph nodes showed features of malignant etiology on ultrasonography and elastography. FNAC confirmed the diagnosis as squamous cell carcinoma metastasis (Figure D).

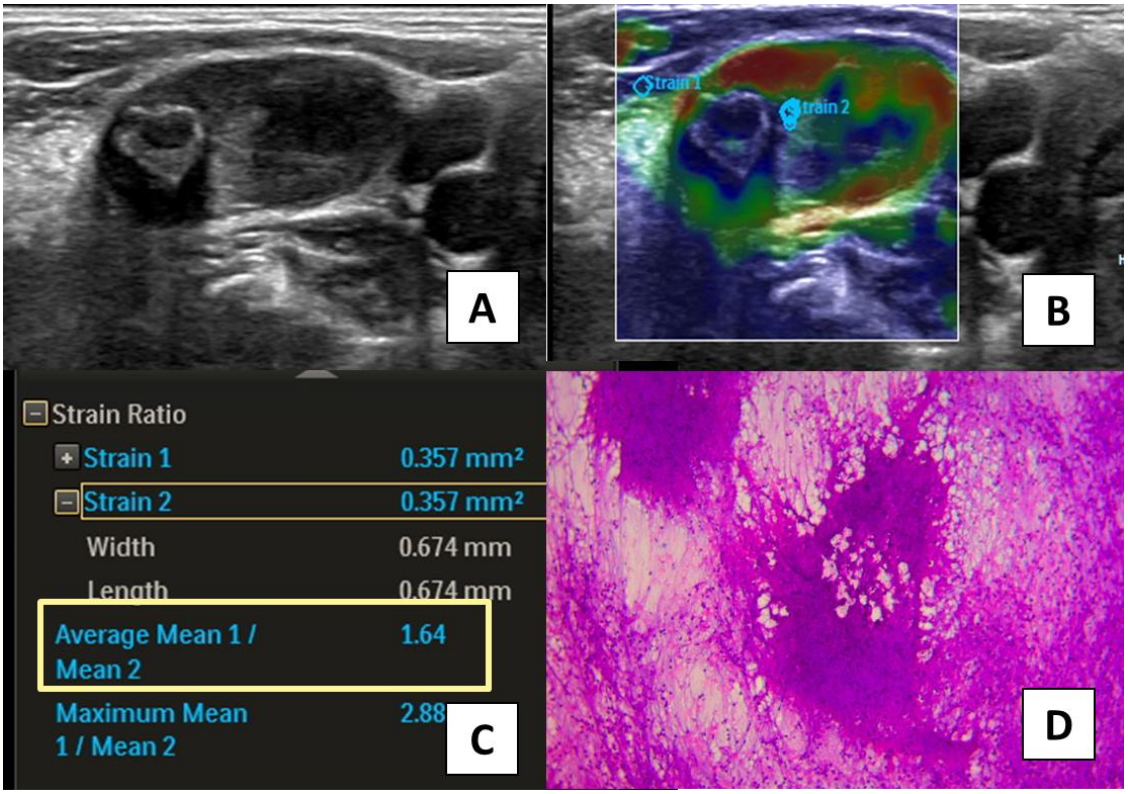


Figure 25: 11-year-old female presented with enlarged cervical lymph node with homogenous echotexture, loss of fatty hila, S/L ratio of > 0.6 and intranodal calcifications with posterior acoustic shadowing (Figure A). Lymph node had pattern II on elastogram and strain index of 1.64 (Figure B & C). Lymph node was diagnosed as benign based on combined ultrasonography and elastography findings. Pathology diagnosis on FNAC was caseous granulomatous lymphadenitis (Figure D).

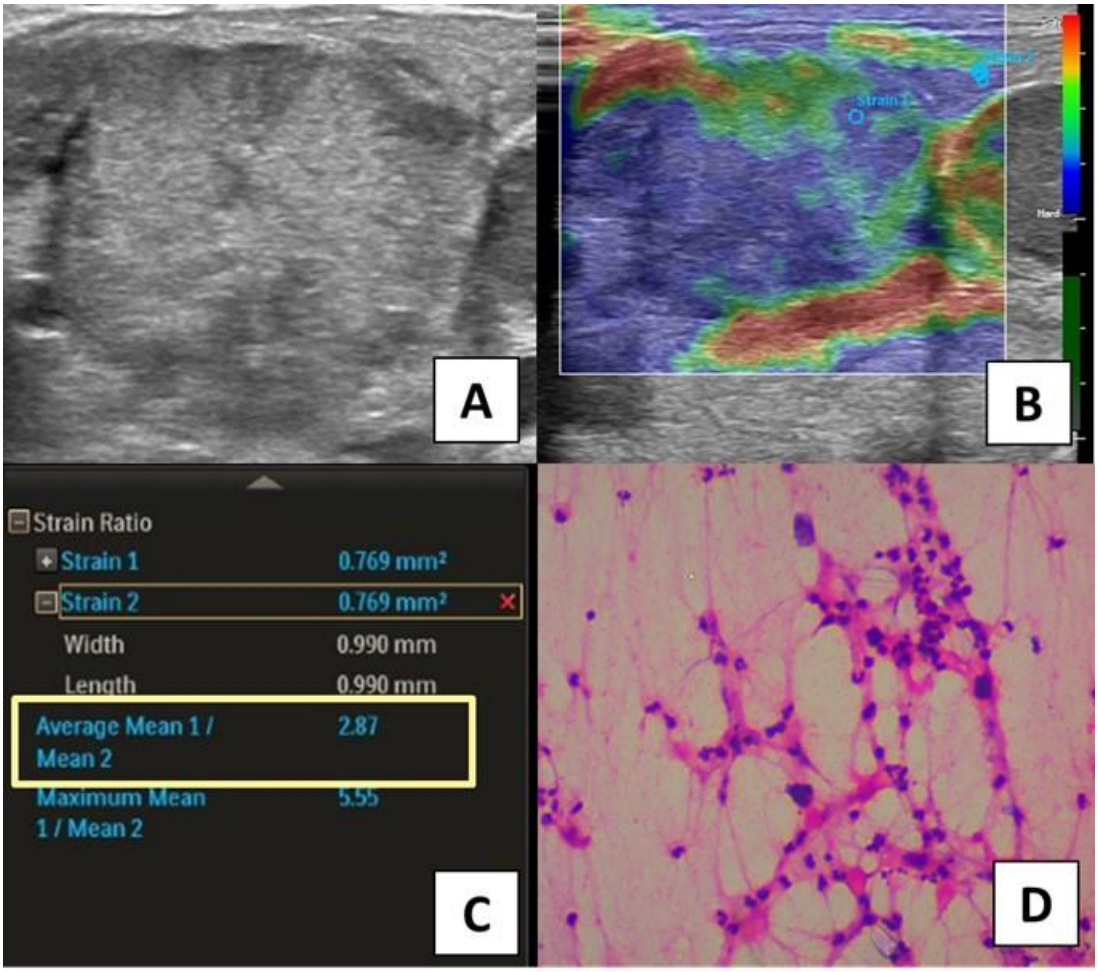


Figure 26: 69-year-old male with carcinoma right buccal mucosa presented with enlarged right cervical lymph nodes. Lymph nodes had homogenous echotexture with loss of fatty hila, S/L ratio of > 0.6 (Figure A) and mixed vascularity (central and peripheral) on CDI. On elastography, they had pattern IV on elastogram and strain index of 2.87 (Figure B & C). Lymph nodes showed features of malignant etiology on ultrasonography and elastography. FNAC confirmed the diagnosis as squamous cell carcinoma metastasis (Figure D).

# DISCUSSION

Ultrasonography is frequently used as initial imaging tool for evaluation of lymphadenopathy. Various etiologies of cervical lymphadenopathy have overlapping imaging features on ultrasonography. Pathology is gold standard for diagnosing the cause, however it is an invasive procedure. Biopsy/FNAC can be avoided in benign cases, especially in pediatric population. Elastography can improve the diagnostic efficacy of ultrasonography and can aid in decreasing unnecessary FNAC/ biopsy.

In our study, we compared ultrasonography and elastography findings in 78 cervical lymph nodes. Commonest age group was 30-60 years (46%), followed by < 30 years (31%). Mean age of the patients was 38 ± 10 years and range was 4-75 years. There was increase in number of malignant lymph nodes with increase in age group, 77% in > 60-year age group as opposed to 12% in < 30-year age group. Similar observation was also made by Sharadamani GS in a study conducted in rural population[56].

We recognized that there was higher lymphoma: metastatic lymph node ratio in < 30 years age group as compared to middle and older age groups. All malignant lymph nodes (100%) in younger age group (<30 years) were lymphoma cases. 93% of the malignant nodes in middle age group (30-60 years) and 77% in elderly age group were metastatic. This observation was consistent with study by Cunnane M et al. They also observed that, lymphoma cases were predominantly found in younger age

group as opposed to middle and elderly age groups, which showed predominantly metastatic lymph nodes[57].

Our study population had 43 female and 35 male patients. The ratio of cervical lymph nodes of benign and malignant etiology among female and male patients was 6:4 and 4:3 respectively. We did not find any statistically significant association between etiology of the lymph node and gender of the patient. This was in concordance with a study conducted by Cunnane M et al on 184 patients with cervical lymphadenopathy. Among malignant cervical lymph nodes, both Hodgkin's lymphoma (HL) and Non-Hodgkin's lymphoma (NHL) showed male predominance. An Indian study conducted by Moddal SK et al on 455 patients with lymphoma observed that, male:female ratio was 3.1:1 and NHL: HL ratio was 3.2:1[58].

Short-axis dimension is the most frequently employed B-mode parameter. Various cut-off values are proposed depending on the location of lymph node in the neck. However, common cut-off value (8 mm) was used by various studies[2,3,59]. In a study conducted by Acu L et al using a fixed cut-off diameter of 8 mm, the accuracy of the short-axis diameter was 54.5%, which was similar to our study (51.8%)[59]. Alam F et al used separate cut-off values for lymph nodes in different neck levels and the diagnostic accuracy was 84%, better than other studies which used common cut-off value[4].

Shape of the lymph node was assessed based on short/long axis ratio. S/L ratio less than 0.6 (oval shape) was considered as benign feature and ratio more than 0.6 was considered as a malignant feature. Tumor deposit in the lymph node changes the

shape from oval to round with resultant increase in S/L ratio. In our study, S/L ratio showed statistically significant difference between benign and malignant cervical lymph nodes with diagnostic accuracy, sensitivity and specificity of 67%, 87% and 38% respectively. A similar observation was made by Lakshmi CR et al, who reported a sensitivity of 86.6%, however had better specificity than our study[60].

Lymph node margin had p value > 0.05 (statistically insignificant) and showed poor diagnostic accuracy (62%). An Indian study conducted by Pattanayak S et al, concluded that lymph node margin has no statistical significance in differentiating tubercular and metastatic lymph nodes. Irregular nodal border in malignant cases is secondary to extracapsular extension[38].

In our study, lymph nodal echogenicity had diagnostic accuracy of 67%. Similar results were obtained in a study by Acu L et al[59]. Benign lymph nodes (tuberculous and reactive lymphadenitis) tend to have homogenously hypoechoic echopattern. However, lymphomatous and metastatic cervical lymph nodes can also show hypoechoic echopattern. Hyperechoic lymph nodes are feature of papillary carcinoma metastasis secondary to intranodal deposition of thyroglobulin. Presence of necrosis in benign lymph node is responsible for heterogenous echotexture. We observed that necrosis was prevalent in large number of metastatic lymph nodes with squamous cell carcinoma as primary. Apart from necrosis, metastatic nodal deposit itself can alter the echotexture of the node[61,62].

Fatty hilum is one of the commonly used parameter to differentiate benign and malignant cervical lymph node. In our study, fatty hilum had highest diagnostic

accuracy (73%) when compared to other B-mode parameters and showed high statistical significance (p value <0.0001). Sensitivity was 67% and specificity was 81%, which is similar to study conducted by Sathyanarayan V et al (75% sensitivity and 84.5% specificity)[63]. Normal and reactive cervical lymph nodes show central echogenic hilum which is seen in continuity with the perinodal fat. Both metastatic and lymphomatous lymph nodes tend to show loss of fatty hila due to replacement of hila by malignant cells. However, in our study we found that 33% of benign lymph nodes (predominantly tubercular and suppurative lymph nodes) also showed loss of fatty hila and 23% of malignant lymph nodes showed presence of fatty hilum[62].

Three patterns of vascularity are defined on colour Doppler imaging. Normal and reactive cervical lymph nodes may show hilar vascularity or no vascularity (Pattern I). Increase in hilar vessel diameter and increase in blood flow in inflammatory conditions accounts for hilar vascularity. Peripheral vascularity (Pattern II) is considered as malignant feature. In malignant lymph nodes, hilum along with hilar vessels are infiltrated by malignant cells, resulting in increased vascular supply from perinodal vessels. Mixed vascularity (Pattern III) of the lymph node is due to tumor angiogenesis resulting in central and peripheral vascularity[64]. In our study, color Doppler vascularity showed sensitivity of 71%, diagnostic accuracy of 70% and specificity of 68%. An Indian study conducted in 2017, on 50 patients also showed results similar to present study[2]. An Egyptian study by Elzawawy MS et al, also concluded that hilar vascularity is benign pattern whereas peripheral and mixed vascularity are malignant patterns[51].

Apart from vascularity pattern of the lymph node, various studies have also used spectral Doppler parameters like resistive index (RI) and pulsatality index (PI). The results of previous studies using RI and PI values were contradicting and controversial. We did not include spectral Doppler parameters in the present study. Naik RM et al, observed that malignant lymph nodes showed high RI value. Rapid replication of tumor cells cause compression of the intranodal vessels, thereby increasing vascular resistance and RI[65]. Other studies are concordant with this theory. However, Chang DB et al, observed that malignant lymph nodes have low vascular resistance (low RI value) secondary to presence of arteriovenous shunting and lack of a muscular layer in intranodal vessels in malignant lymph nodes[66]. When RI cut-off value is 0.7 was used, all nodes with RI value > 0.7 were malignant; however among lymph nodes with low RI value (< 0.7), 43% were malignant and 57% were benign. Thus, they concluded that resistive index has poor sensitivity[51].

We combined B-mode and colour Doppler imaging findings in the present study. Four cases that were diagnosed as benign on ultrasonography were proven as malignant on pathology and five lymph nodes diagnosed as malignant on ultrasonography were diagnosed as benign on pathology. Specificity, sensitivity and diagnostic accuracy was 88%, 90% and 89% respectively, which is significantly better than any individual B-mode or colour Doppler parameters.

A study conducted in Japan in 2008 proposed a scoring system combining all B-mode parameters. Ultrasound diagnosis was based on the sum of scores for B-mode parameters (short-axis diameter, shape, border, echogenicity, and hilum). Benign features were given score of 1 and score of 2 was given for malignant

features. Lymph nodes with combined score of less than 7 are labelled as benign and those with score of 7-10 are labelled as malignant. Sensitivity of 98%, specificity of 54% and diagnostic accuracy of 84% was achieved for the combined ultrasonography diagnosis[4].

Strain elastography assessment of cervical lymph node includes both quantitative and qualitative measurement of the hardness of the lymph node. Elastography pattern is a qualitative assessment based on the percentage of hard area or blue area. In the current study, we used five elastography patterns to characterise lymph nodes on elastogram. Elastography pattern showed 83% sensitivity, 97% specificity and 89% diagnostic accuracy. Alam F et al, were one of the initial researchers to use five-point scale for elastography pattern and they achieved diagnostic accuracy of 89%[4]. An Egyptian study conducted in 2017 also used similar elastography pattern scoring and found sensitivity, specificity, PPV, NPV and diagnostic accuracy of 86%, 100%, 100%, 78.1%, 90.6% respectively[67].

Four-point scale for elastography pattern was also used in many studies. Lyshchik et al proposed four-point elastography scoring system based on lymph node morphology on elastogram, they are, visualisation of lymph node, relative brightness, margin regularity and margin definition on elastography images. They observed that maximum diagnostic accuracy achieved was 82%, which was less than the diagnostic accuracy (89%) achieved in the current study. Other studies described four pattern elastography scoring based on percentage of blue or hard area, similar to five pattern elastography score. Patterns 1 and 2 are considered as benign patterns and patterns 3 and 4 are considered as malignant patterns[68,69,70]. Zhang Y et al, achieved sensitivity,

specificity and accuracy of 74.7%, 97.1%, and 84.5% respectively using four pattern elastography scoring[68].

In this study mean strain index of 2 was taken as a cut off value. Among 46 benign cervical lymph nodes, 43 of them showed strain index of < 2 and 3 lymph nodes showed strain index > 2. Out of 32 malignant lymph nodes diagnosed on pathology, 31 had high strain index (>2) and only one malignant lymph node had low strain index (<2). Difference in the mean strain index for benign (1.45 ± 0.306) and malignant (3.01 ± 0.690) cervical lymph nodes was found to be statistically significant. Elastography strain index showed higher sensitivity (93%) as compared to elastography pattern (sensitivity of 83%). Specificity (96%) was marginally less than elastography pattern (97%). However, overall diagnostic accuracy of strain index (94%) was better than that of elastography pattern (89%) and all other ultrasound parameters. This observation was consistent with several other studies which compared elastography with B-mode and colour Doppler parameters[1,2,4.]

Using 1.5 as cut-off, strain index achieved 98% specificity, 85% sensitivity, and 92% overall accuracy[3]. Another study obtained a cut-off value of 1.78 and sensitivity and diagnostic accuracy were 98% and 84% respectively[52]. Zhang et al used higher cut-off value of 2.3 and obtained 78.4% sensitivity and 98.5% specificity[68]. The variation in cut off strain ratios can partly be explained by different demographic regions, difference in scanners and elastography procedure. Strain index is a measure of displacement of the tissue secondary to external compression. We observed that amount of compression applied can alter the elastography parameters. Inadequate or overcompression may result in reduced or increased strain ratio. The

ultrasound machine used in our study shows amount of compression applied using a colour bar. For measurement of elastography strain index and pattern, uniform compression was applied and static images were obtained at the central phase of compression. Images acquired at the beginning and near the end of compression tend to give inaccurate values. This technique minimizes interobserver variability and gives better reproducibility.

Elastography pattern and strain index together had 93% sensitivity, 94% specificity and 94% diagnostic accuracy. Combined use of elastography and ultrasonography gave sensitivity of 96%, specificity of 94% and diagnostic accuracy of 95%. Several previous studies which compared diagnostic potential of elastography and ultrasonography reported similar observations[4,68.]

| Author | Publication year | Elastography pattern | Diagnostic accuracy | Strain index cut-off | Diagnostic accuracy |
|---|---|---|---|---|---|
| Lyshchik A et al[3] | 2007 | 4 pattern | 82% | 1.5 | 92% |
| Alam F et al[4] | 2008 | 5 pattern | 89% | - | - |
| Zhang Y et al[68] | 2009 | 5 pattern | 84% | 2.39 | 98% |
| Teng DK et al[52] | 2013 | 4 pattern | 66% | 1.78 | 84% |
| Gupta R et al[2] | 2017 | 5 pattern | 90% | 2 | 94% |
| Moharram MA et al[67] | 2017 | 5 pattern | 90% | 1.5 | 88% |
| Current study | 2020 | 5 pattern | 89% | 2 | 94% |

Table 18: Comparison of diagnostic accuracy of strain index and elastography pattern in various studies

Strain elastography has certain limitations. It can have interobserver and intraobserver variations. We did not evaluate these variations in our study. However, use of standardized procedure for elastography has improved the reproducibility and diagnostic performance in the current study. Lymphoma lymph nodes tend to be softer and can give low strain index. Correlation with B-mode and vascularity pattern can avoid false negative results.

# CONCLUSION

In our study, all B-mode parameters (except lymph node margin) and colour Doppler vascularity showed statistically significant difference between benign and malignant cervical lymph nodes. Among them, fatty hilum was found to have highest diagnostic accuracy (73%), followed by colour Doppler vascularity (70%). Combined use of all ultrasonography parameters yielded better sensitivity (90%), specificity (88%) and diagnostic accuracy (89%) than individual parameters.

In the current study, five scale elastography pattern had diagnostic accuracy of 89%, sensitivity of 83% and specificity of 97%. Strain index cut-off of 2 showed sensitivity of 93%, specificity of 96% and diagnostic accuracy of 94%. Elastography pattern and strain index together had sensitivity of 93%, specificity of 94% and diagnostic accuracy of 94%.

Combined ultrasonography and elastography achieved sensitivity of 96%, specificity of 94% and diagnostic accuracy of 95%. We concluded that elastography can be a useful adjunct to ultrasonography. Use of elastography pattern and cut-off strain index of 2 along with ultrasonography can effectively differentiate benign and malignant cervical lymph nodes, thereby reducing unnecessary invasive procedures and interventions.

# SUMMARY

Cervical lymph node enlargement is secondary to numerous causes, which can be broadly divided into benign or malignant etiology. Cervical lymph nodes evaluation will give a clue to underlying etiology and aid in appropriate treatment planning. Ultrasonography is easily available and is also cost effective, therefore is usually employed for diagnostic work-up of cervical lymphadenopathy. Elastography is the recent addition to ultrasonography, which characterizes lymph node depending on its hardness/stiffness. Elastography has the potential to improve diagnostic accuracy of ultrasonography.

The aims and objectives of the study were to perform B-mode ultrasonography, color Doppler imaging and elastography of the cervical lymph nodes. To correlate B-mode ultrasonography, color Doppler imaging and elastography findings with pathological findings and to calculate sensitivity, specificity and diagnostic accuracy of ultrasonography and elastography.

This is a prospective observational study which was conducted over a period of eighteen months from January 2019 to June 2020 on 78 patients with clinically diagnosed cervical lymphadenopathy referred for ultrasonography at Department of Radio-Diagnosis, R.L. Jalappa Hospital and Research Center attached to Sri Devaraj Urs Medical College, Tamaka, Kolar. Informed consent was taken from the patients before inclusion in the study. The inclusion criterion was all the patients with clinically suspected cervical lymphadenopathy and exclusion criterion was recent

FNAC/biopsy of the lymph node and patient who has received radiotherapy/chemotherapy.

Baseline data was collected along with pertinent clinical history, relevant lab investigations and pathology reports. Individuals with cervical lymph nodes first underwent ultrasonography and color Doppler imaging followed by elastography by using 5-12 MHz linear array transducer (PHILIPS EPIQ 5G Ultrasound Machine). Lymph node morphology was defined on ultrasonography and vascularity on color Doppler. B-mode parameters that are evaluated to characterize cervical lymph nodes are short axis dimension (cut-off value: 8 mm), short-to-long axis ratio (cut-off value: 0.6), fatty hilum (presence or absence of hilum), echogenicity (homogenous or heterogenous) and lymph node margin (regular or irregular). Based on the vascularity on colour Doppler imaging lymph nodes are divided into three patterns: Pattern I (hilar vascularity or no flow), Pattern II (peripheral vascularity) and pattern III (mixed vascularity). Patterns I and II were considered as benign patterns and pattern III was considered as malignant pattern.

Elastography pattern and strain index determine the nature of lymph node on elastography. During strain elastography linear probe was placed perpendicularly on the lymph node and gentle compression (> 50%) was applied to generate elastograms (colour maps). Elastography pattern was assessed based on percentage of blue, green and red areas in the elastogram. Blue indicates hard area, red indicates soft area and green indicates intermediate tissue hardness. Lymph nodes with patterns 1 and 2 were identified as benign and lymph nodes with patterns 3, 4 and 5 were categorized as malignant lymph nodes.

Strain index was calculated by placing two regions of interest (ROIs), one within the lymph node and the second one in the adjacent normal tissue at the same level. The strain index was calculated as ratio of ROI 1 to ROI 2 and values were generated. In the current study, cut off value for strain index was taken as 2.0. Cervical lymph nodes with mean strain index value lower than 2 were considered as benign and those with higher strain index were considered as malignant.

Both ultrasonography and elastography findings were recorded and interpreted. Patient underwent pathological investigation, either FNAC or biopsy. Elastography and ultrasonography findings were compared with pathological findings.

The data were entered in Microsoft excel sheet. The measurable variables were analyzed and interpreted between them by the student's t test and the ordinal and categorical variables between them were interpreted by Chi- square ($\chi 2$) test. For statistical procedures we used SPSS statistical package (ver 21) and OpenEpi ver 3.01. P value $< 0.05$ was considered as statistically significant.

Total of 78 patients were included in the present study. Out of which, 46 lymph nodes were diagnosed as benign and 32 lymph nodes were diagnosed as malignant on pathology. In our study, $38 \pm 12.8$ years was the mean age and range was 4-75 years. 81% of lymph nodes in younger age group were benign whereas 77% of lymph nodes in older age group (> 60 years) were malignant. Out of 78 patients, there were total 43 females (55%) and 35 males (45%). Gender of the patient was not statistically significant in distinguishing cervical lymph nodes.

Cut-off of 8 mm for short axis dimension gave high specificity of 97%, however had low sensitivity of 30% and diagnostic accuracy of 58%. Short/long axis ratio (cut-off 0.6) and echogenicity were statistically significant (p value < 0.05), however both had low specificity (38% for S/L ratio and 53% for echogenicity). Margin of the lymph node was statistically insignificant (p value = 0.152) and had poor specificity (31%). Fatty hilum showed highest diagnostic accuracy among all B-mode parameters (73%).

71% of benign cervical lymph nodes (33 out of 46 benign lymph nodes) showed benign vascularity (pattern I) on CDI whereas 69% of malignant cervical lymph nodes (22 out of 32 malignant lymph nodes) showed malignant vascularity pattern (either pattern II or pattern III) on CDI. Vascularity pattern was found to be statistically significant (p value=.0004).

In our study, lymph nodes were divided into five elastography patterns. Maximum number of lymph nodes showed pattern 2 on elastography (35 cervical lymph nodes). 39 cervical lymph nodes were found to have benign pattern (4 lymph nodes had pattern 1 and 35 lymph nodes had pattern 2) on elastography. All 4 cervical lymph nodes showing pattern 1 on elastography were confirmed to be benign on pathology. Of the 35 cervical lymph nodes with pattern 2, 34 lymph nodes were benign and 1 was malignant on pathology. There were total 39 cervical lymph nodes which showed malignant pattern. Out of these, 8 cervical lymph nodes which showed malignant pattern (5 in pattern 3 and 3 in pattern 4) were diagnosed as benign on pathology. All 5 cervical lymph nodes with pattern 5 were proven as malignant.

We employed a cut off value of 2 for strain index in our study. Among a total of 78 cervical lymph nodes included in the study, 44 lymph nodes had strain index <2, suggesting a benign etiology and 34 lymph nodes had strain ratio >2, suggestive of malignant etiology. Mean strain index for cervical lymph node of benign and malignant was 1.45 ± 0.306 (mean ± SD) and 3.01 ± 0.690 (mean ± SD) respectively. Both elastography parameters were statistically significant in differentiating between benign and malignant etiology (p value < 0.00001). Strain index achieved better sensitivity (93%) and diagnostic accuracy (94%) as compared to elastography pattern (sensitivity of 83% and diagnostic accuracy of 89%).

On pathology diagnosis, 46 patients (60%) had benign lymph nodes and 32 patients (40%) had malignant lymph nodes. Among benign cervical lymph nodes, reactive lymphadenitis (59%) was found to be more common followed by granulomatous lymphadenitis (26%). Among malignant lymph nodes SCC metastasis (50%) is most common, followed by Non-Hodgkin's lymphoma (13%).

For final ultrasound diagnosis all B-mode and color Doppler findings were combined. Four lymph nodes of malignant etiology were misdiagnosed by ultrasonography as benign, one patient had Hodgkin's lymphoma and other three patients had SCC metastasis. Ultrasound incorrectly diagnosed five benign lymph nodes as malignant which includes, two cases each of granulomatous lymphadenitis and reactive lymphadenitis and one case of acute suppurative lymphadenitis. Elastography and ultrasound together misdiagnosed two benign cases (granulomatous lymphadenitis and reactive lymphadenitis) as malignant and two malignant cases (metastasis from SCC and Hodgkin's lymphoma) as benign.

When ultrasonography and elastography were used separately, 41 lymph nodes on ultrasonography and 43 lymph nodes on elastography were accurately diagnosed as benign. 28 lymph nodes on ultrasonography and 30 lymph nodes on elastography were correctly diagnosed as malignant. When both the findings were combined 44 lymph nodes were accurately diagnosed as benign and 30 lymph nodes were accurately diagnosed as malignant. Combined use of elastography and ultrasonography had augmented diagnostic accuracy (95%) than individual modality.

Combined use of all ultrasonography parameters yielded better sensitivity (90%), specificity (88%) and diagnostic accuracy (89%) than any other individual parameter. Five scale elastography pattern had sensitivity of 83%, specificity of 97% and diagnostic accuracy of 89%. Strain index cut-off of 2 showed sensitivity of 93%, specificity of 96% and diagnostic accuracy of 94%. Both elastography parameters together achieved 93% sensitivity, 94% specificity and 94% diagnostic accuracy.

We concluded that elastography can improve diagnostic potential of ultrasonography. It plays a major role in differentiating benign from malignant cervical lymph nodes and can avoid unnecessary intervention for lymph nodes of benign etiology. Together ultrasonography (B-mode and colour Doppler imaging) and elastography (elastography pattern and cut-off strain index of 2) achieved sensitivity of 96%, specificity of 94% and diagnostic accuracy of 95%.

# BIBLIOGRAPHY


1. Ahuja AT, Ying M. Sonographic evaluation of cervical lymph nodes. AJR Am J Roentgenol 2005;184:1691-9.

2. Gupta R, Mittal P, Kaur T, Kaur H, Aamir M, Malik R. Ultrasound elastography for differentiating benign from malignant cervical lymphadenopathy: Comparison with B-mode and color Doppler findings. J Clin Diagn Res 2017;11:5-8.

3. Lyshchik A, Higashi T, Asato R, Tanaka S, Ito J, Hiraoka M et al. Cervical lymph node metastases: Diagnosis at sonoelastography-initial experience. Radiology 2007;243:258-67.

4. Alam F, Naito K, Horiguchi J, Fukuda H, Tachikake T, Ito K. Accuracy of sonographic elastography in the differential diagnosis of enlarged cervical lymph nodes: Comparison with conventional B-mode sonography. AJR Am J Roentgenol 2008;191:604-10.

5. Lo WC, Cheng PW, Wang CT, Liao LJ. Real-time ultrasound elastography: an assessment of enlarged cervical lymph nodes. Eur Radiol 2013;23:2351-7.

6. Blum KS, Pabst R. Keystones in lymph node development. J Anat 2006;209:585-95.

7. Dubey A, Jethani SL, Mehrotra N, Singh D. Development of the Human Lymph Nodes- A Histological Study. J Clin Diagn Res 2012;6:1155-7.

8. Singh I. Cardiovascular System. In: Devi VS, editor. Inderbir Singh's Human embryology. Chapter 15. 11th edition. Jaypee. 2018: Pg 59-60.

9. Sadler TW. Cardiovascular system. Medical embryology. Chapter 13. 14th edition. Wolters Kluwer. 2019: Pg 219.

10. Singh V. Development of blood vessels. Textbook of clinical embryology. Chapter 19. 2nd edition. Elsevier Limited. 2017: Pg 228-9.

11. George AJT. Blood, lymphoid tissues and haemopoiesis. In: Standring S, editor. Gray's Anatomy: The Anatomical Basis of Clinical Practice. Chapter 4. 41st edition. Elsevier Limited. 2016: Pg 68-81.

12. Young B, O'Dowd G, Woodford P. Immune system. Wheater's functional histology: a text and colour atlas. Chapter 11. 6th edition. Elsevier 2013: Pg 209-10.

13. Bujoreanu I, Gupta V. Anatomy, Lymph Nodes. [Updated 2020 Aug 10]. In: StatPearls [Internet]. Treasure Island (FL): StatPearls Publishing; 2020 Jan. Available from: https://www.ncbi.nlm.nih.gov/books/NBK557717/.

14. Singh I. Lymphatics and Lymphoid Tissue. In: Vasudeva N, Mishra S, editor. Inderbir Singh's Textbook of Human Histology. Chapter 9. 7th edition. Jaypee Brothers. 2014: Pg 127-34.

15. Choi I, Lee S, Hong YK. The New Era of the Lymphatic System: No Longer Secondary to the Blood Vascular System. Cold Spring Harb Perspect Med 2012;2:a006445.

16. Moore MG, Cognetti D, Lin DT, Smith RV. Definition of Lymph Node Groups. Quick Reference Guide to TNM Staging of Head and Neck Cancer and Neck Dissection Classification. Chapter IV. 5th edition. American Academy of Otolaryngology- Head and Neck Surgery Foundation. 2018: Pg 33-6.

17. Dhingra PL, Dhingra S. Clinical methods in ENT. Diseases of Ear, Nose and Throat & Head and Neck Surgery. Chapter 76. 7th edition. 2018. Pg 374-90.

18. Banjar FK, Wilson AM. Anatomy, Head and Neck, Supraclavicular Lymph Node. StatPearls Publishing 2019.

19. Corbridge RJ. The neck. Essential ENT. Chapter 8. 2nd edition. Hodder Arnold. 2011. Pg 83-92.

20. Lang S, Kansy B. Cervical lymph node diseases in children. GMS Curr Top Otorhinolaryngol Head Neck Surg 2014;13:1-27.

21. Nag D, Dey S, Nandi A, Bandyopadhyay R, Roychowdhury D, Roy R. Etiological study of lymphadenopathy in HIV-infected patients in a tertiary care hospital. J Cytol 2016;33:66-70.

22. Ludwig BJ, Wang J, Nadgir RN, Saito N, Aragon IC, Sakai O. Imaging of Cervical Lymphadenopathy in Children and Young Adults. AJR Am J Roentgenol 2012;199:1105-33.

23. Gupta KB, Kumar A, Sen R, Sen J, Vermas M. Role of ultrasonography and computed tomography in complicated cases of tuberculous cervical lymphadenitis. Indian J Tuberc 2007;54:71-8.

24. Nwawka OK, Nadgir R, Fujita A, Sakai O. Granulomatous disease in the head and neck: developing a differential diagnosis. Radiographics 2014;34:1240-56.

25. Knopf A, Bas M, Chaker A, Strassen U, Pickhard A, Stark T et al. Rheumatic disorders affecting the head and neck: underestimated diseases. Rheumatology 2011;50:2029-34.

26. Ludwig BJ, Wang J, Nadgir RN, Saito N, Castro-Aragon I, Sakai O. Imaging of cervical lymphadenopathy in children and young adults. AJR Am J Roentgenol 2012;199:1105-13.

27. Radhakrishnan R, Kline-Fath BM. The Pediatric Head and Neck. Diagnostic ultrasound. Chapter 48. 5th edition. Elsevier. 2018. Pg 1628-71.

28. Lee YY, Tassel PV, Nauert C, North LB, Jing BS. Lymphomas of the head and neck: CT findings at initial presentation. AJR Am J Roentgenol 1987;149:575-81.

29. Arora N, Singh J, Davessar JL. Evaluation of Cervical Lymph Node Metastasis in Head and Neck Cancers. J Otolaryngol ENT Res 2017;7:00219.

30. Roland NJ. Staging of head and neck cancer. In: Watkinson JC, Clarke RW, editors. Scott-Brown's Otorhinolaryngology Head and Neck Surgery. Chapter 4. 8th edition. CRC Press. 2019. Pg 35-47.

31. Paleri V, O'Hara J. Metastatic neck disease. Scott-Brown's Otorhinolaryngology Head and Neck Surgery. In: Watkinson JC, Clarke RW, editors. Chapter 18. 8th edition. CRC Press. 2019. Pg 305-35.

32. Simo R, Jeannon JP, Urbano MTG. Neck metastasis from an unknown primary. In: Watkinson JC, Clarke RW, editors. Scott-Brown's Otorhinolaryngology Head and Neck Surgery. Chapter 17. 8th edition. CRC Press. 2019. Pg 295-304.

33. Calabrese L, Jereczek-Fossa BA, Jassem J, Rocca A, Bruschini R, Orecchia R et al. Diagnosis and management of neck metastases from an unknown primary. Acta Otorhinolaryngol Ital 2005;25:2-12.

34. Mackenzie K, Watson M, Jankowska P, Bhide S, Simo R. Investigation and management of the unknown primary with metastatic neck disease: United Kingdom National Multidisciplinary Guidelines. J Laryngol Otol 2016;130:170-5.

35. Hoang JK, Vanka J, Ludwig BJ, Glastonbury CM, Benjamin J. Evaluation of Cervical Lymph Nodes in Head and Neck Cancer with CT and MRI: Tips, Traps, and a Systematic Approach. AJR 2013;200:17–25.

36. De Bondt RB, Nelemans PJ, Bakers F, Casselman JW, Peutz-Kootstra C, Kremer B et al. Morphological MRI criteria improve the detection of lymph node metastases in head and neck squamous cell carcinoma: multivariate logistic regression analysis of MRI features of cervical lymph nodes. Eur Radiol 2009;19:626-33.

37. Kwee TC, Basu S, Alavi A. PET and PET/CT for unknown primary tumors. Methods Mol Biol 2011;727:317-33.

38. Pattanayak S, Chatterjee S, Ravikumar R, Nijhawan VS, Sharma V, Debnath J. Ultrasound evaluation of cervical lymphadenopathy: Can it reduce the need of histopathology/cytopathology? Med J Armed Forces India 2018;74:227-34.

39. Ying M, Ahuja A. Sonography of neck lymph nodes. Part I: normal lymph nodes. Clin Radiol 2003;58:351-8.

40. Ahuja AT, Ying M, Ho SY, Antonio G, Lee YP, King AD et al. Ultrasound of malignant cervical lymph nodes. Cancer Imaging 2008;8:48-56.

41. Ahuja A, Ying M. Sonography of neck lymph nodes. Part II: abnormal lymph nodes. Clin Radiol 2003;58:359-66.

42. Wells PN, Liang HD. Medical ultrasound: imaging of soft tissue strain and elasticity. J R Soc Interface 2011;8:1521-49.

43. Sigrist RMS, Liau J, Kaffas AE, Chammas MC, Willmann JK. Ultrasound Elastography: Review of Techniques and Clinical Applications. Theranostics 2017;7:1303-29.

44. Dietrich CF, Barr RG, Farrokh A, Dighe M, Hocke M, Jenssen C et al. Strain elastography- How to do it? Ultrasound Int Open 2017;3:e13-49.

45. Zhang F, Zhao X, Ji X, Han R, Li P, Du M. Diagnostic value of acoustic radiation force impulse imaging for assessing superficial lymph nodes. Medicine (Baltimore) 2017;96:e8125.

46. Taljanovic MS, Gimber LH, Becker GW, Latt LD, Klauser AS, Melville DM et al. Shear-Wave Elastography: Basic Physics and Musculoskeletal Applications. Radiographics 2017;37:855–70.

47. Yang L, Luo D, Li L, Zhao Y, Lin M, Guo W et al. Differentiation of malignant cervical lymphadenopathy by dual-energy CT: a preliminary analysis. Sci Rep 2016;6:31020.

48. Zhong J, Lu Z, Xu L, Dong L, Qiao H, Hua R et al. The diagnostic value of cervical lymph node metastasis in head and neck squamous carcinoma by using diffusion-weighted magnetic resonance imaging and computed tomography perfusion. Biomed Res Int 2014;2014:260859.

49. Choure AA, Khaladkar SM, Jain S. Differentiation of benign and malignant cervical lymph nodes on MRI with special emphasis on DWI. Int J Radiol Diagn Imaging 2019;2:96-105.

50. Çaylakl F, Yılmaz S, Özer C, Reyhan M. The Role of PET-CT in Evaluation of Cervical Lymph Node Metastases in Oral Cavity Squamous Cell Carcinomas. Turk Arch Otorhinolaryngol 2015;53:67-72.

51. Elzawawy MS, Azab SM, Elshiekh RM. Role of color Doppler ultrasonography in differentiating benign and malignant cervical lymphadenopathy. Menoufia Med J 2018;31:1030-5.

52. Teng DK, Wang H, Lin YQ, Sui GQ, Guo F, Sun LN. Value of ultrasound elastography in assessment of enlarged cervical lymph nodes. Asian Pac J Cancer Prev 2012;13:2081-5.

53. Ghajarzadeh M, Mohammadifar M, Azarkhish K, Emami-Razavi SH. Sono-elastography for Differentiating Benign and Malignant Cervical Lymph Nodes: A Systematic Review and Meta-Analysis. Int J Prev Med 2014;5:1521–8.

54. Hefeda MM, Badawy ME. Can ultrasound elastography distinguish metastatic from reactive lymph nodes in patients with primary head and neck cancers? Egypt J Radiol Nuclear Med 2014;45:715-22.

55. Roselin P, Aravind N. Sensitivity and Specificity of B Mode Ultrasonography, Ultrasound Elastography Vs Histopathology in Differentiation of Benign & Malignant Cervical Lymph Node. Indian J Appl Res 2016;6:234-6.

56. Sharadamani GS. Prevalence of various causes of lymphadenopathy in a rural setting in India. Indian J Pathol Oncol 2017;4:462-4.

57. Cunnane M, Cheung L, Moore A, di Palma S, McCombe A, Pitkin L. Level 5 Lymphadenopathy Warrants Heightened Suspicion for Clinically Significant Pathology. Head Neck Pathol 2016;10:509-12.

58. Mondal SK, Mandal PK, Samanta TK, Chakaborty S, Roy SD, Roy S. Malignant lymphoma in Eastern India: A retrospective analysis of 455 cases according to World Health Organization classification. Indian J Med Paediatr Oncol 2013;34:242-6.

59. Acu L, Oktar SÖ, Acu R, Yücel C, Cebeci S. Value of Ultrasound Elastography in the Differential Diagnosis of Cervical Lymph Nodes: A Comparative Study With B-mode and Color Doppler Sonography. J Ultrasound Med 2016;3:2491-9.

60. Lakshmi CR, Rao MS, Ravikiran A, Sathish S, Bhavana SM. Evaluation of Reliability of Ultrasonographic Parameters in Differentiating Benign and Metastatic Cervical Group of Lymph Nodes. Int Sch Res Notices 2014;238740:7.

61. Abdelgawad EA, Abu-samra MF, Abdelhay NM, Abdel-Azeem HM. B-mode ultrasound, color Doppler, and sonoelastography in differentiation between

benign and malignant cervical lymph nodes with special emphasis on sonoelastography. Egypt J Radiol Nucl Med 2020;51:157.

62. Dudea SM, Lenghel M, Botar-Jid C, Vasilescu D, Duma M. Ultrasonography of superficial lymph nodes: benign vs. malignant. Med Ultrason 2012;14:294-306.

63. Sathyanarayan V, Bharani SK. Enlarged lymph nodes in head and neck cancer: Analysis with triplex ultrasonography. Ann Maxillofac Surg 2013;3:35-9.

64. Misra D, Panjwani S, Rai S, Misra A, Prabhat M, Gupta P et al. Diagnostic efficacy of color Doppler ultrasound in evaluation of cervical lymphadenopathy. Dent Res J 2016;13:217–24.

65. Naik RM, Pai A, Guruprasad Y, Singh R. Efficacy of colour Doppler ultrasound in diagnosis of cervical lymphadenopathy. J Maxillofac Oral Surg 2013;12:123-9.

66. Chang DB, Yuan A, Yu CJ, Luh KT, Kuo SH, Yang PC. Differentiation of benign and malignant cervical lymph nodes with color Doppler sonography. Am J Roentgenol 1994;162:965–8.

67. Moharram MA, Abd-ElMaboud NM, Ahmed HA. Evaluation of the role of sono-elastography in diagnosis of enlarged cervical lymph nodes. Egypt J Radiol Nucl Med 2017;48:381–91.

68. Zhang Y, Lv Q, Yin Y, Xie M, Xiang F, Lu C et al. The value of ultrasound elastography in differential diagnosis of superficial lymph nodes. Front Med China 2009;3:368–74.

69. Bhatia KS, Cho CC, Tong CS, Yuen EH, Ahuja AT. Shear wave elasticity imaging of cervical lymph nodes. Ultrasound Med Biol 2012;38:195–201.

70. Rubaltelli L, Stramare R, Tregnaghi A, Scagliori E, Cecchelero E, Mannucci M et al. The role of sonoelastography in the differential diagnosis of neck nodules. J Ultrasound 2009;12:93–100.

# ANNEXURE I

# PROFORMA

**Demographic details:**

Name:

Age:

UHID number:

Address:

**Clinical History:**

**Local examination:**

Size of the lymph node:

Location of the lymph node:

Overlying skin changes:

Palpation (Local rise of temperature/ tenderness/ consistency/ matting):

**Clinical diagnosis:**

**USG Findings:**

| | |
|---|---|
| Location of lymph node | |
| Size (short axis dimension in mm) | |
| Short /long axis ratio | |

| | |
|---|---|
| Lymph node echogenicity | |
| Lymph node margin | |
| Fatty hilum | |
| Ancillary findings | |
| Vascularity pattern on CDI | |

**Ultrasound diagnosis:**

**Elastography Findings:**

| | |
|---|---|
| Elastography pattern | |
| Mean strain index | |

**Elastography diagnosis:**

**Combined ultrasonography and elastography diagnosis:**

**Pathology Diagnosis:**

# ANNEXURE II

## INFORMED CONSENT

STUDY TITLE: Role of sonoelastography in differentiating benign from malignant cervical lymph nodes and correlating with pathology.

**Chief researcher/ PG guide's name:** Dr. ANIL KUMAR SAKALECHA

**Principal investigator**: Dr. E. VINEELA

Name of the patient:

Age :

Gender:

1. I have been informed in my own language that this study involves ultrasonography and elastography as part of procedure. I have been explained thoroughly and understand the procedure.
2. I understand that the medical information produced by this study will become part of institutional record and will be kept confidential by the said institute.
3. I understand that my participation is voluntary and I may refuse to participate or may withdraw my consent and discontinue participation at any time without prejudice to my present or future care at this institution.
4. I agree not to restrict the use of any data or results that arise from this study provided such a use is only for scientific purpose(s).

5. I confirm that Dr. E. VINEELA / Dr. ANIL KUMAR SAKALECHA (chief researcher/ name of PG guide) has explained to me the purpose of research and the study procedure that I will undergo and the possible risks and discomforts that I may experience, in my own language. I hereby agree to give valid consent to participate as a subject in this research project.

Participant's signature/thumb impression

Signature of the witness: Date:

1)

2)

I have explained to _____ (subject) the purpose of the research, the possible risk and benefits to the best of my ability.

Chief Researcher/ Guide signature

# ಸಮ್ಮತಿ ಪತ್ರ:

ಈ ಕೆಳಗೆ ಸಹಿ ಮಾಡಿರುವ ---------- ಆದ ನಾನು ಈ ಅಧ್ಯಯನದಲ್ಲಿ ಪಾಲ್ಗೊಳ್ಳುವ ಸಲುವಾಗಿ ವೈದ್ಯಕೀಯ ಪರೀಕ್ಷೆಗೆ ಒಳಪಡಲು ನನ್ನ ವೈಯ್ಯಕ್ತಿಕ ವಿವರಗಳನ್ನು ನೀಡಲು ಸಮ್ಮತಿಸಿರುತ್ತೇನೆ.

ಈ ಅಧ್ಯಯನದ ಉದ್ದೇಶ, ಅಧ್ಯಯನದ ಸಂದರ್ಭದಲ್ಲಿ ನೀಡುವ ಮತ್ತು ಸಂಗ್ರಹಿಸುವ ಮಾಹಿತಿಯಗೋಪ್ಯತೆಯ ಬಗ್ಗೆ ನನಗೆ ನನ್ನ ಸ್ಥಳೀಯ ಭಾಷೆಯಲ್ಲಿ ಓದಿ ಹೇಳಲಾಗಿದೆ/ವಿವರಿಸಲಾಗಿದೆ ಮತ್ತು ನಾನು ಇದನ್ನು ಅರ್ಥ ಮಾಡಿಕೊಂಡಿರುತೇನೆ. ಈ ಅಧ್ಯಯನದ ವಿವಿಧ ಅಂಶಗಳ ಬಗ್ಗೆ ಪ್ರಶ್ನೆಗಳನ್ನು ಕೇಳುವ ಅವಕಾಶವನ್ನು ನನಗೆ ನೀಡಲಾಗಿದೆ ಮತ್ತು ನನ್ನ ಪ್ರಶ್ನೆಗಳಿಗೆ ತೃಪ್ತಿಕರವಾದ ಉತ್ತರಗಳು ದೊರೆತಿರುತವೆ. ಈ ಅಧ್ಯಯನದ ಮೂಲಕ ಸಂಗ್ರಹಿಸಿರುವ ಮಾಹಿತಿಯನ್ನು ಸಂಶೋಧನೆಯ ಉದ್ದೇಶಕ್ಕೆ ಮಾತ್ರ ಬಳಸತಕ್ಕದ್ದು.

ಈ ಅಧ್ಯಯನದಿಂದ ಯಾವುದೇ ಸಂದರ್ಭದಲ್ಲಿ ಹಿಂದೆ ಸರಿಯುವ ಸ್ವಾತಂತ್ರ್ಯ ನನಗಿದೆ ಎಂಬುದನ್ನೂ, ಈ ಅಧ್ಯಯನದಲ್ಲಿ ಪಾಲ್ಗೊಳ್ಳುವುದರಿಂದ ನನಗೆ ಯಾವುದೇ ಹೆಚ್ಚುವರಿ ವೆಚ್ಚ ತಗಲುವುದಿಲ್ಲವೆಂಬುದನ್ನು ತಿಳಿದಿರುತ್ತೇನೆ.

ರೋಗಿಯ ಸಹಿ:

ಹೆಸರು:

ಸಾಕ್ಷಿಯ ಸಹಿ:

ಹೆಸರು:

ಪ್ರಧಾನ ಪರೀಕ್ಷಕರ ಹೆಸರು ಮತ್ತು ಸಹಿ

ದಿನಾಂಕ:

# PATIENT INFORMATION SHEET

STUDY TITLE: Role of sonoelastography in differentiating benign from malignant cervical lymph nodes and correlating with pathology.

Principal Investigator: Dr. E.VINEELA / Dr. ANIL KUMAR SAKALECHA

I, Dr.E.Vineela, post-graduate student in Department of Radio-Diagnosis at Sri Devaraj Urs Medical College. I will be conducting a study titled "Role of sonoelastography in differentiating benign from malignant cervical lymph nodes and correlating with pathology" for my dissertation under the guidance of Dr. Anil Kumar Sakalecha, Professor, Department of Radiodiagnosis. In this study, we will assess the role of elastography in differentiating benign from malignant cervical lymph nodes. You would have to undergo ultrasonography before entering the study. You will not be paid any financial compensation for participating in this research project.

All of your personal data will be kept confidential and will be used only for research purpose by this institution. You are free to participate in the study. You can also withdraw from the study at any point of time without giving any reasons whatsoever. Your refusal to participate will not prejudice you to any present or future care at this institution.

Name and Signature of the Principal Investigator

Mobile number: 8762180520

Date

# ರೋಗಿಯ ಮಾಹಿತಿ ಪತ್ರ

ಮುಖ್ಯ ಸಂಶೋಧಕರು: ಡಾ|| ಈ. ವಿನೀಲ / ಡಾ|| ಅನಿಲ್ ಕುಮಾರ್ ಸಕಲೇಚ

ನಾನು ಡಾ|| ಈ ವಿನೀಲ, ಶ್ರೀ ದೇವರಾಜ್ ಅರಸು ಮೆಡಿಕಲ್ ಕಾಲೇಜಿನ ರೇಡಿಯೊಡಯಾಗ್ನೋಸಿಸ್ ವಿಭಾಗಲ್ಲಿನ ಸ್ನಾತಕೋತ್ತರ ವಿದ್ಯಾರ್ಥಿನಿ. ನಾನು " ದುಗ್ಧರಸ ಗ್ರಂಥಿಯ ಮೌಲ್ಯಮಾಪನದಲ್ಲಿ ಸೊನೊಲಾಸ್ಟೊಗ್ರಫಿ ಪಾತ್ರ" ನನ್ನ ಪ್ರಬಂಧಕ್ಕಾಗಿ ಡಾ|| ಅನಿಲ್ ಕುಮಾರ್ ಸಕಲೇಚ, ಪ್ರೊಫೆಸರ್, ರೇಡಿಯೊಡಯಾಗ್ನೋಸಿಸ್ ವಿಭಾಗ ಅವರ ಮಾರ್ಗದರ್ಶನದಲ್ಲಿ ಮಾಡುತ್ತೇನೆ.

ನೀವು ಈ ಅಧ್ಯಯನದ ಭಾಗವಾಗಲು ಒಪ್ಪಿಗೆ ಹೊಂದಿಲ್ಲದಿದ್ದರೆ ಅಥವಾ ಭಯಭೀತರಾಗುತಿದ್ದರೆ ನೀವು ಯಾವಾಗ ಬೇಕಾದರೂ ಅಧ್ಯಯನದಿಂದ ಹೊರಗುಳಿಯಲು ಮುಕ್ತರಾಗಿದ್ದೀರಿ. ನೀವು ಅಧ್ಯಯನದ ಭಾಗವಾಗಲು ನಿರಾಕರಿಸಿದರೆ ನಿಮ್ಮ ಚಿಕಿತ್ಸೆ ಮತ್ತು ಕಾಳಜಿಗೆ ಧಕ್ಕೆಯಾಗುವುದಿಲ್ಲ. ನೀವು ಅಧ್ಯಯನದ ಭಾಗವಾಗಿದ್ದರೆ ಅಧ್ಯಯನವು ನಿಮಗೆ ಯಾವುದೇ ಅಪಾಯ ಅಥವಾ ಆರ್ಥಿಕ ಹೊರೆಯಾಗುವುದಿಲ್ಲ.

ನಿಮ್ಮ ಗುರುತು ಮತ್ತು ವೈದ್ಯಕೀಯ ವಿವರಗಳು ಗೌಪ್ಯವಾಗಿರುತ್ತದೆ. ಅಧ್ಯಯನದ ಭಾಗವಾಗಿರುವುದರಿಂದ ನೀವು ಯಾವುದೇ ಆರ್ಥಿಕ ಲಾಭವನ್ನು ಪಡೆಯುವುದಿಲ್ಲ. ನೀವು ಹೊಂದಿರುವ ಯಾವುದೇ ಅನುಮಾನ ಅಥವಾ ಸ್ಪಷ್ಟೀಕರಣಕ್ಕಾಗಿ ನೀವು ಡಾ|| ಈ ವಿನೀಲ ಅಥವಾ ಮೇಲಿನ ಸಂಶೋಧನಾ ತಂಡದ ಯಾವುದೇ ಸದಸ್ಯರನ್ನು ಸಂಪರ್ಕಿಸಬಹುದು.

ಸಂಪರ್ಕ ವಿವರಗಳು:
ಡಾ|| ಈ. ವಿನೀಲ. ದೂರವಾಣಿ: 8762180520
ಡಾ|| ಅನಿಲ್ ಕುಮಾರ್ ಸಕಲೇಚ

# ANNEXURE III

## MASTER CHART

| Sl.no | Trail ID No | Age | Sex | Short axis dimension (cm) | S/L ratio | Margin | Echogenicity | Fatty hilum | Vascularity pattern | Elastography pattern | Strain index | Ultrasound Diagnosis | Elastography diagnosis | Ultrasound + Elastography diagnosis | Pathology diagnosis | Pathology Diagnosis |
|---|---|---|---|---|---|---|---|---|---|---|---|---|---|---|---|---|
| 1 | 516203 | 39 | F | 1.05 | 0.6 | R | HO | Absent | M | 4 | 2.34 | M | M | M | M | Non-Hodgkin's lymphoma |
| 2 | 770551 | 50 | F | 1.1 | 0.8 | R | HE | Absent | M | 3 | 0.94 | B | B | B | B | Granulomatous lymphadenitis |
| 3 | 787836 | 15 | F | 1.4 | 0.5 | R | HO | Present | B | 1 | 1.26 | B | B | B | B | Reactive lymphadenitis |
| 4 | 798654 | 45 | F | 2 | 0.6 | R | HO | Present | B | 2 | 0.8 | B | B | B | B | Granulomatous lymphadenitis |
| 5 | 127654 | 25 | M | 1.7 | 0.7 | R | HO | Present | B | 1 | 1.73 | B | B | B | B | Reactive lymphadenitis |
| 6 | 564790 | 16 | M | 0.7 | 0.3 | R | HO | Present | B | 3 | 1.1 | B | B | B | B | Reactive lymphadenitis |
| 7 | 899076 | 22 | F | 2 | 0.5 | IR | HE | Absent | M | 2 | 1.28 | B | B | B | B | Caseous necrotizing lymphadenitis |
| 8 | 546789 | 34 | F | 0.7 | 0.4 | R | HO | Present | B | 2 | 1.34 | B | B | B | B | Granulomatous lymphadenitis |
| 9 | 894037 | 67 | F | 0.9 | 0.7 | R | HO | Absent | B | 3 | 3.6 | M | M | M | M | Squamous cell carcinoma metastasis |
| 10 | 478390 | 45 | F | 1.2 | 0.9 | R | HE | Absent | M | 4 | 3.9 | M | M | M | M | Squamous cell carcinoma metastasis |
| 11 | 748390 | 20 | F | 1.2 | 0.6 | R | HO | Present | B | 1 | 1.79 | B | B | B | B | Reactive lymphadenitis |
| 12 | 345647 | 65 | F | 1.9 | 0.8 | IR | HE | Absent | M | 4 | 2.6 | M | M | M | M | Squamous cell carcinoma metastasis |
| 13 | 267489 | 9 | F | 1.2 | 0.4 | R | HO | Present | B | 3 | 1.7 | B | B | B | M | Classical Hodgkin's lymphoma- Mixed cellularity |
| 14 | 748493 | 35 | F | 0.7 | 0.3 | R | HO | Present | B | 1 | 1.6 | B | B | B | B | Granulomatous lymphadenitis |
| 15 | 659302 | 31 | F | 1.6 | 0.6 | IR | HE | Absent | M | 3 | 2.6 | M | M | M | M | Adenocarcinoma |
| 16 | 126389 | 75 | F | 2 | 0.5 | R | HO | Absent | M | 3 | 3 | M | M | M | M | Non-Hodgkin's lymphoma |
| 17 | 748592 | 75 | M | 3.1 | 0.7 | IR | HE | Absent | M | 5 | 4 | M | M | M | M | Squamous cell carcinoma metastasis |
| 18 | 657489 | 62 | F | 1.6 | 0.53 | R | HO | Absent | M | 3 | 2.5 | M | M | M | M | Non-Hodgkin's lymphoma |

Sex: F – Female, M- male. Margin: R- Regular, IR – Irregular. Echogenicity: HO- Homogenous, HE- Heterogenous. Diagnosis: B-Benign, M-Malignant.

# ANNEXURE III

## MASTER CHART

| Sl.no | Trail ID No | Age | Sex | Short axis dimension (cm) | S/L ratio | Margin | Echogenicity | Fatty hilum | CDI (Pattern) | Elastography pattern | Strain index | USG Diagnosis | Elastography diagnosis | USG+ Elastography diagnosis | Pathology diagnosis | Pathology Diagnosis |
|---|---|---|---|---|---|---|---|---|---|---|---|---|---|---|---|---|
| 19 | 630584 | 48 | M | 1.6 | 0.6 | R | HO | Absent | M | 3 | 3.6 | M | M | M | M | Squamous cell carcinoma metastasis |
| 20 | 748057 | 40 | M | 1.8 | 0.48 | IR | HE | Absent | B | 3 | 3.6 | M | M | M | M | Papillary carcinoma metastasis |
| 21 | 984750 | 55 | M | 1.8 | 0.48 | IR | HE | Absent | M | 5 | 3.6 | M | M | M | M | Squamous cell carcinoma metastasis |
| 22 | 948304 | 35 | F | 1.3 | 0.35 | R | HO | Absent | B | 4 | 3.3 | M | M | M | B | Granulomatous lymphadenitis |
| 23 | 658390 | 4 | M | 0.9 | 0.3 | R | HO | Present | B | 2 | 0.7 | B | B | B | B | Reactive lymphadenitis |
| 24 | 354748 | 8 | F | 0.79 | 0.28 | R | HO | Present | B | 2 | 1.6 | B | B | B | B | Granulomatous lymphadenitis |
| 25 | 657394 | 24 | F | 2 | 0.5 | R | HE | Present | B | 4 | 4.2 | M | M | M | M | Hodgkin’s lymphoma |
| 26 | 758390 | 9 | M | 1.3 | 0.4 | R | HO | Present | B | 2 | 1.7 | B | B | B | B | Reactive lymphadenitis |
| 27 | 546478 | 70 | M | 2.9 | 0.9 | IR | HE | Absent | M | 4 | 5.18 | M | M | M | M | Adenocarcinoma metastasis |
| 28 | 846304 | 55 | M | 0.78 | 0.3 | R | HO | Present | B | 2 | 1.49 | B | B | B | B | Reactive lymphadenitis |
| 29 | 857390 | 50 | M | 0.5 | 0.3 | R | HO | Present | B | 2 | 1.6 | B | B | B | B | Reactive lymphadenitis |
| 30 | 846385 | 61 | F | 0.82 | 0.4 | R | HO | Present | B | 2 | 1.3 | B | B | B | B | Reactive lymphadenitis |
| 31 | 546389 | 18 | F | 1.2 | 0.5 | R | HE | Absent | B | 2 | 0.8 | B | B | B | B | Reactive lymphadenitis |
| 32 | 344689 | 8 | F | 0.9 | 0.3 | R | HO | Present | B | 2 | 1.6 | B | B | B | B | Granulomatous lymphadenitis |
| 33 | 233527 | 4 | F | 1.6 | 0.5 | IR | HE | Absent | M | 2 | 1.6 | B | B | B | B | Acute suppurative lymphadenitis |
| 34 | 324678 | 36 | M | 0.81 | 0.5 | R | HO | Present | B | 3 | 1.5 | B | B | B | B | Tuberculous lymphadenitis |
| 35 | 947735 | 28 | F | 1.2 | 0.6 | R | HO | Present | B | 2 | 1.4 | B | B | B | B | Granulomatous lymphadenitis |
| 36 | 646897 | 30 | M | 1.4 | 0.5 | R | HE | Absent | M | 2 | 1.4 | M | B | B | B | Acute suppurative lymphadenitis |
| 37 | 935647 | 4 | M | 1.7 | 0.3 | R | HO | Present | B | 2 | 1.7 | B | B | B | B | Reactive lymphadenitis |

Sex: F – Female, M- male. Margin: R- Regular, IR – Irregular. Echogenicity: HO- Homogenous, HE- Heterogenous. Diagnosis: B-Benign, M-Malignant.

# ANNEXURE III

## MASTER CHART

| Sl.no | Trail ID No | Age | Sex | Short axis dimension (cm) | S/L ratio | Margin | Echogenicity | Fatty hilum | CDI (Pattern) | Elastography pattern | Strain index | USG Diagnosis | Elastography diagnosis | USG+ Elastography diagnosis | Pathology diagnosis | Pathology Diagnosis |
|---|---|---|---|---|---|---|---|---|---|---|---|---|---|---|---|---|
| 38 | 326898 | 10 | F | 0.9 | 0.4 | R | HE | Absent | M | 2 | 1.5 | B | B | B | B | Acute suppurative lymphadenitis |
| 39 | 435578 | 6 | M | 0.4 | 0.2 | R | HO | Present | B | 2 | 1.8 | B | B | B | B | Reactive lymphadenitis |
| 40 | 122578 | 12 | M | 0.5 | 0.3 | R | HO | Present | B | 3 | 1.9 | B | B | B | B | Reactive lymphadenitis |
| 41 | 234167 | 18 | M | 2.9 | 0.7 | R | HO | Absent | M | 3 | 2.1 | M | M | M | M | Hodgkin’s lymphoma |
| 42 | 682956 | 63 | F | 1 | 0.6 | R | HE | Absent | M | 4 | 2.3 | B | M | M | M | Squamous cell carcinoma metastasis |
| 43 | 946673 | 35 | F | 1.3 | 0.5 | R | HO | Present | B | 2 | 1.6 | B | B | B | B | Reactive lymphadenitis |
| 44 | 325378 | 51 | M | 1.2 | 0.5 | R | HO | Present | B | 4 | 4.7 | B | M | M | M | Metastasis |
| 45 | 726894 | 52 | M | 1.5 | 0.9 | R | HO | Absent | M | 4 | 3.8 | M | M | M | B | Reactive lymphadenitis |
| 46 | 426638 | 54 | F | 0.6 | 0.5 | R | HO | Present | B | 2 | 2.7 | B | B | B | M | Metastasis |
| 47 | 253787 | 42 | F | 1.5 | 0.8 | R | HO | Present | B | 4 | 2.8 | B | M | B | B | Necrotising granulomatous lymphadenitis |
| 48 | 883774 | 65 | M | 1.9 | 0.8 | R | HO | Absent | M | 3 | 2.3 | M | M | M | M | Non-Hodgkin’s Lymphoma |
| 49 | 345378 | 50 | F | 1.2 | 0.6 | R | HE | Absent | M | 4 | 2.5 | M | M | M | M | Adenocarcinoma/ Anaplastic large cell carcinoma |
| 50 | 537907 | 49 | M | 0.6 | 0.4 | R | HO | Absent | M | 2 | 1.7 | B | B | B | B | Reactive lymphadenitis |
| 51 | 927884 | 55 | M | 1 | 0.7 | R | HO | Absent | M | 3 | 2.5 | M | M | M | M | Adenocarcinoma |
| 52 | 748950 | 8 | F | 0.7 | 0.4 | R | HO | Present | M | 2 | 1.6 | B | B | B | B | Reactive lymphadenitis |
| 53 | 436479 | 65 | M | 1.8 | 0.5 | R | HE | Absent | M | 2 | 1.7 | M | B | B | B | Reactive lymphadenitis |
| 54 | 729045 | 7 | F | 2 | 0.6 | IR | HE | Absent | M | 2 | 1.6 | B | B | B | B | Acute suppurative lesion |
| 55 | 537895 | 41 | M | 1.4 | 0.9 | R | HE | Absent | M | 2 | 1.2 | B | B | B | B | Reactive lymphadenitis |

Sex: F – Female, M- male. Margin: R- Regular, IR – Irregular. Echogenicity: HO- Homogenous, HE- Heterogenous. Diagnosis: B-Benign, M-Malignant.

# ANNEXURE III

## MASTER CHART

| Sl.no | Trail ID No | Age | Sex | Short axis dimension (cm) | S/L ratio | Margin | Echogenicity | Fatty hilum | CDI (Pattern) | Elastography pattern | Strain index | USG Diagnosis | Elastography diagnosis | USG+ Elastography diagnosis | Pathology diagnosis | Pathology Diagnosis |
|---|---|---|---|---|---|---|---|---|---|---|---|---|---|---|---|---|
| 56 | 979502 | 11 | M | 1.1 | 0.4 | R | HO | Absent | B | 2 | 1.8 | B | B | B | B | Granulomatous lymphadenitis |
| 57 | 152684 | 40 | M | 2.1 | 0.6 | R | HE | Absent | M | 5 | 3.2 | M | M | M | M | Papillary thyroid carcinoma |
| 58 | 253780 | 62 | M | 2.5 | 0.6 | IR | HE | Absent | M | 2 | 1.3 | B | B | B | B | Nonspecific Lymphadenitis |
| 59 | 738953 | 40 | M | 1.2 | 0.7 | R | HO | Present | B | 2 | 1.3 | B | B | B | B | Reactive lymphadenitis |
| 60 | 647895 | 45 | F | 1.2 | 0.5 | R | HO | Present | B | 2 | 1.8 | B | B | B | B | Granulomatous lymphadenitis |
| 61 | 937895 | 48 | F | 0.8 | 0.5 | R | HO | Present | B | 2 | 1.4 | B | B | B | B | Reactive lymphadenitis |
| 62 | 537859 | 65 | M | 2.6 | 0.6 | R | HE | Absent | M | 4 | 2.3 | M | M | M | M | Squamous cell carcinoma metastasis |
| 63 | 547829 | 45 | F | 1 | 0.5 | R | HO | Present | B | 2 | 1.8 | B | B | B | B | Reactive lymphadenopathy |
| 64 | 224688 | 39 | F | 1.1 | 0.5 | R | HO | Present | B | 2 | 1.6 | B | B | B | B | Reactive lymphadenopathy |
| 65 | 142783 | 63 | F | 0.8 | 0.4 | R | HO | Present | B | 2 | 1.6 | B | B | B | B | Reactive lymphadenopathy |
| 66 | 267894 | 28 | F | 1.3 | 0.6 | R | HO | Present | B | 2 | 1.5 | B | B | B | B | Granulomatous lymphadenitis |
| 67 | 523893 | 30 | F | 1.7 | 0.8 | R | HE | Absent | B | 3 | 2.1 | M | M | M | M | Squamous cell carcinoma metastasis |
| 68 | 926784 | 4 | M | 1 | 0.4 | R | HO | Present | B | 2 | 1.7 | B | B | B | B | Reactive lymphadenopathy |
| 69 | 436748 | 65 | F | 1.6 | 0.5 | R | HO | Absent | M | 4 | 2.7 | M | M | M | M | Squamous cell carcinoma metastasis |
| 70 | 162788 | 7 | M | 1.6 | 0.3 | R | HO | Present | B | 3 | 0.8 | B | B | B | B | Reactive lymphadenopathy |
| 71 | 263784 | 50 | F | 0.9 | 0.7 | R | HO | Absent | B | 3 | 2.7 | M | M | M | M | Squamous cell carcinoma metastasis |
| 72 | 826749 | 52 | M | 1.6 | 0.4 | IR | HO | Absent | B | 3 | 2.9 | M | M | M | M | Squamous cell carcinoma metastasis |
| 73 | 273894 | 39 | M | 1.47 | 0.4 | R | HE | Absent | M | 2 | 1 | M | B | B | B | Granulomatous lymphadenitis |
| 74 | 648959 | 69 | M | 2.6 | 0.8 | R | HE | Absent | M | 4 | 2.8 | M | M | M | M | Squamous cell carcinoma metastasis |

Sex: F – Female, M- male. Margin: R- Regular, IR – Irregular. Echogenicity: HO- Homogenous, HE- Heterogenous. Diagnosis: B-Benign, M-Malignant.

# ANNEXURE III

## MASTER CHART

| Sl.no | Trail ID No | Age | Sex | Short axis dimension (cm) | S/L ratio | Margin | Echogenicity | Fatty hilum | CDI (Pattern) | Elastography pattern | Strain index | USG Diagnosis | Elastography diagnosis | USG+ Elastography diagnosis | Pathology diagnosis | Pathology Diagnosis |
|---|---|---|---|---|---|---|---|---|---|---|---|---|---|---|---|---|
| 75 | 263789 | 45 | F | 0.9 | 0.6 | R | HO | Absent | B | 4 | 2.8 | M | M | M | M | Squamous cell carcinoma metastasis |
| 76 | 739579 | 69 | M | 1.4 | 0.5 | IR | HE | Absent | M | 5 | 3.9 | M | M | M | M | Metastasis |
| 77 | 437599 | 57 | F | 2.1 | 0.7 | R | HE | Absent | M | 4 | 2.3 | M | M | M | M | Squamous cell carcinoma metastasis |
| 78 | 327499 | 64 | M | 1 | 0.5 | R | HE | Absent | M | 5 | 2.4 | M | M | M | M | Squamous cell carcinoma metastasis |

Sex: F – Female, M- male. Margin: R- Regular, IR – Irregular. Echogenicity: HO- Homogenous, HE- Heterogenous. Diagnosis: B-Benign, M-Malignant.